University of Liege

Faculty of Medicine

GIGA-I^3

Laboratory of Immunoendocrinology – Pr Vincent Geenen

Reassessment of the impact of the GHRH/GH/IGF-1 somatotrope axis on developmental and functional immunology

Réévaluation de l'impact de l'axe somatotrope GHRH/GH/IGF-1 en immunologie développementale et fonctionnelle

Gwennaëlle BODART

Master in Biomedical Sciences

Promoter

Pr Vincent GEENEN

Co-promoter

Dr Henri MARTENS

Thesis submitted in fulfillment of the requirements for the Degree of Doctor in Biomedical and Pharmaceutical Sciences

Academic year 2016-2017

Reassessment of the impact of the GHRH/GH/IGF-1 somatotrope axis on developmental and functional immunology

Réévaluation de l'impact de l'axe somatotrope GHRH/GH/IGF-1 en immunologie développementale et fonctionnelle

Gwennaëlle Bodart

Abstract

It is now well acknowledged that a close relationship exists between neuroendocrine and immune systems. Within this field, the question of the physiological role of the GHRH/GH/IGF-1 axis on the immune system is still highly debated. The purpose of this thesis was to address this issue by investigating developmental and functional adaptive immunity in the *Ghrh*$^{-/-}$ mouse model of somatotrope deficiency. Analyses in basal conditions reveal that *Ghrh*$^{-/-}$ mice have functional B and T lymphopoiesis and exhibit decreased B/T ratio and increased naïve T cells in periphery compared to non-deficient mice, but no immunodeficiency was found. Immune aging was not aggravated in *Ghrh*$^{-/-}$ mice and short-term GH treatment had no impact on immune parameters of deficient or normal mice, despite its visible metabolic effect. Altogether, those results suggest that somatotrope axis is not required for immune system development, maintenance or aging. This finding is in accordance with the stress hypothesis, according which somatotrope hormones are important counter-regulators of stress-induced immunosuppressors. In an attempt to test this hypothesis, mice were injected with dexamethasone (DXM), a synthetic glucocorticoid inducing massive thymocyte apoptosis. Thymocyte distribution two days post-DXM treatment was less disturbed in *Ghrh*$^{-/-}$ than in normal mice, but ensuing recovery was slower, even though both mice present full recovery of thymic parameters 10 days after DXM injection. Also in the line of the stress hypothesis, study of infectious stress seems more relevant, as suggested by preliminary results obtained with *Streptococcus pneumoniae* (*S.pneum*) infection. In conclusion, this thesis brings new evidence of the non-essential role played by the GHRH/GH/IGF-1 axis on adaptive immune system development and function. It also opens the way for further investigations regarding the role of this axis on innate immunity and immune response to infectious stress.

Résumé

Il est aujourd'hui bien admis qu'une relation étroite existe entre les systèmes neuroendocrinien et immunitaire. Parmi les connaissances dans ce domaine, la question du rôle physiologique exercé par l'axe GHRH/GH/IGF-1 sur le système immunitaire est toujours fortement débattue. L'objectif de cette thèse était d'étudier cette problématique, via l'étude du développement et de la fonction du système immunitaire de la souris *Ghrh*$^{-/-}$, un modèle murin de déficience de l'axe somatotrope. A l'état basal, les analyses ont montré que les souris *Ghrh*$^{-/-}$ avaient une lymphopoïèse B et T fonctionnelle, et présentaient une diminution du rapport B/T et une augmentation des cellules T naïves en périphérie. Cependant, aucune immunodéficience n'a été détectée chez ces souris. Le vieillissement du système immunitaire n'était pas aggravé chez les souris *Ghrh*$^{-/-}$ et un traitement à court terme par GH s'est révélé sans impact sur les paramètres immunitaires des souris déficientes ou normales. Pris ensemble, ces résultats suggèrent que l'axe somatotrope n'est pas nécessaire pour le développement, la maintenance ou le vieillissement du système immunitaire. Cette conclusion est en accord avec l'hypothèse du stress, selon laquelle les hormones somatotropes seraient d'importants contre-régulateurs des facteurs immunosuppresseurs induits en cas de stress. Pour tester cette hypothèse, les souris ont été injectées avec de la dexaméthasone, un glucocorticoïde de synthèse connu pour induire une atrophie massive des thymocytes. La distribution des thymocytes deux jours après le traitement DXM était moins perturbée chez les souris *Ghrh*$^{-/-}$ que chez les souris normales, mais la récupération qui s'ensuit semblait retardée, bien que chez les deux types de souris un rétablissement complet des paramètres thymique était obtenu en 10 jours. Egalement en rapport avec l'hypothèse du stress, il semblerait que l'étude du stress infectieux soit mieux adaptée, au vu des résultats préliminaires obtenus avec des infections par *Streptococcus Pneumoniae*. En conclusion, cette thèse apporte de nouvelles preuves du rôle non essentiel que joue l'axe GHRH/GH/IGF-1 sur le développement et la fonction du système immunitaire et elle ouvre la voie vers de futures études concernant le rôle de l'axe somatotrope sur l'immunité innée et la réponse au stress infectieux.

Acknowledgements

At the end of this work, I would like to thank all the people that participated to this project, directly or indirectly.

First I would like to warmly thank my promoter, Pr Vincent Geenen, who gave me the opportunity to realize my thesis in his laboratory. During all those years, his support and trust were precious. He showed me the way to become the scientist I am today.

I also sincerely thank my co-promoter, Dr Henri Martens, for his priceless help and advice in all aspects of my research work. Besides his extensive scientific knowledge, I have also greatly appreciated his kindness and sympathy.

I want to express my gratitude to the members of my thesis committee, Pr Michel Moutschen, Pr Catherine Sadzot, Pr Albert Beckers and Pr Alain Vanderplasschen, for their useful and pertinent advice. I also profusely thank the members of my jury, Pr Philippe Touraine and Pr Pierre Coulie, for the time they spent to evaluate and comment this manuscript.

I could not perform all this work without the inestimable help of Chantal Renard. Her experience, efficacy and knowledge of various techniques were as useful as her assistance and friendship.

What would have been those 5 years without the support, friendship and good mood of my dear colleagues, Virginie Gridelet, Barbara Polese, Khalil Farhat, Hélène Michaux and also the former ones Lindsay Goffinet, Marie Mottet, Alisson Beckers and Philippe Ruggeri? You were one of the reasons I was happy to get up and go to work in the morning. I am so grateful to have met such amazing people.

I should also acknowledge all the people who helped me or collaborated with me to make this work a success: Pr Roberto Salvatori for kindly sending us Ghrh$^{-/-}$ mice and also providing advice and reviewing; Pr Didier Hober who welcomed me for an internship in his laboratory of virology; Pr Rémi Cheynier for his technical help to set up TREC quantification and providing corresponding plasmids; Dr Guillaume Becker and Pr Alain Pleneveaux for their collaboration and expertise with MRI acquisition; Pr Pierre Drion, Luc Duwez and Fabrice Olivier from the GIGA Animal Facility for their help with animal care and ethic; and Dr Sandra Ormanese and Rafaat Stefan from the Cell Imaging and Flow Cytometry GIGA Technological Platform for their help with flow cytometry experiments design and analyses.

I also warmly thank Tim and Françoise for the time they spent to correct English grammar and orthography in this manuscript.

Pour la suite, je souhaiterais adresser toute ma reconnaissance et ma gratitude envers ma famille : mes parents, mes grands-parents, mes frères, ma marraine et mon parrain. Ils ont toujours cru en moi, ils m'ont soutenue, aidée et encouragée dans tous les moments, bons ou mauvais, que j'ai pu traverser au cours de cette thèse et dans ma vie en générale.

Pour finir, j'aimerais remercier tout particulièrement mon fiancé, Julien Guillain. Il a vécu toute cette expérience à mes côtés, il était là à chaque moment pour partager mes joies, mes peines, mes doutes, mon enthousiasme et même, à quelques occasions, la tâche pénible de numérotation des tubes. Surtout, il a fait le sacrifice de quitter son travail, sa famille et son pays pour me permettre d'accomplir ma vocation. Je ne le remercierai jamais assez pour cela. Je souhaiterais lui dédier tout spécialement cette thèse.

Alors merci, à chacun d'entre vous, pour tout ce que vous m'avez apporté. C'est grâce à chacun d'entre vous que ce travail a été possible.

P.S. : Me voici dans la nécessité, près d'un mois après avoir écrit les lignes ci-dessus, de rajouter un paragraphe à ces remerciements. Il me tient à cœur de faire une mention spéciale à mon frère Quentin, décédé tragiquement en ce début d'année 2017. Il était fier de mon parcours, et il aurait été encore plus fier de pouvoir enfin m'appeler Dr Bodart. Je le remercie pour son soutien, je le remercie et l'admire pour le jeune homme bon, persévérant et inspirant qu'il était. Il restera à jamais un modèle pour moi, bien qu'il fût plus jeune. Dans cette étape importante de ma vie, j'aimerais lui rendre hommage en lui dédiant également cette thèse, ainsi que mon futur titre de Docteur.

This work was supported by grants from the "Fonds National de la Recherche Scientifique" (F.R.S-FNRS; Belgium), the Fonds Léon Fredericq (Belgium) and the Federation Wallonia-Brussels (ARC Somasthym) for financial support.

Summary

List of abbreviations

AC	adenylyl cyclase
APC	antigen-presenting cells
BCR, TCR	B-cell receptor, T-cell receptor
cAMP	cyclic 3',5'-adenosine monophosphate
CLP	common lymphoid progenitor
CMJ	cortico-medullary junction
CREB	cAMP response element bingind
DAG	diacylgycerol
DC	dendritic cell
DN, DP, SP	double negative, double positive, single positive
DXM	dexamethasone
EAE	experimental autoimmune encephalomyelitis
ERK	extracellular signal regulated kinase
ETP	early T-cell protenitor
FoxP3	forkhead box protein
GC	glucocorticoid
G-CSF	granulocyte colony-stimulating factor
GH, GHR, GHBP	growth hormone, GH receptor, GH binding protein
(A)GHD	(adult) growth hormone deficiency
GHS, GHSR	growth hormone secretagogue, GHS receptor
Grb2	growth factor receptor-bound protein 2
HPRT	hypoxyanthine-guanine phosphoribosyltransferase
HSC	hematopoietic stem cell
Ig, H, L	immunoglobulin, heavy and light chain
IGF-1, IGFR, IGFBP	insulin-like growth factor, IGF receptor, IGF binding protein
IL	interleukin
ILC	innate lymphoid cells
IP3	inositol triphosphate
IRS	insulin receptor substrate
JAK	janus kinase
KO	knock-out
lit/lit	little mouse
LN	lymph node
MAPK	Ras/mitogen activated protein kinase
MHC	major histocompatibility complex
MPP	multipotent protenitor
MOG	myelin oligodendrocyte glycoprotein
NK	natural killer
PBMC	peripheral blood mononuclear cell
(D)PBS	(Dubelcco's) phosphate buffered saline
PIP2	phosphatidylinositol 4,5-diphosphate
PKA, PKC	protein kinase A, C
PLC	phospholipase C

PMN	polymorpohnuclear cell
PRL, PRLR	prolactin, prolactin receptor
PROP-1	prophet of Pit-1
RAG	recombination-activating gene
ROS	reactive oxygen species
RTE	recent thymic emigrant
S.pneum	*Streptococcus pneumonaie*
SCF	stem cell factor
SCID	severe combined immunodeficiency
SCZ	sub-capsular zone
SH2, SHC	src homology 2, SH2 domain containing protein
SRIF/SS, SRIFR	somatotropin release-inhibiting factor/somatostatin, SRIF receptor
STAT	signal transducer and activator of transcription
Tc, Th, Treg	cytotoxic, helper, regulatory T-cell
TEC, cTEC, mTEC	thymic epithelial cell, cortical TEC, medullary TEC
TEM, TCM	T effector memory cell, T central memory cell
TNF	tumor necrosis factor
TREC	TCR rearrangement excision circle
TSH	thyroid-stimulating hormone
WT	wild-type

1 Introduction

It is now well acknowledged that a crosstalk exists between neuroendocrine and immune system. Both systems share common receptors and ligands: some cytokines, including interleukin (IL)-1 or IL-6 exert effects on endocrine cells and conversely neuroendocrine hormones may act on immune cells [1]. The physiological reality of this bidirectional link is still under the scope of many researches. The present work focuses on the interaction between the immune system and the neuroendocrine somatotrope axis. After a comprehensive description of the somatotrope axis and the immune system, this introduction will review the up-to-date knowledge in this field.

1.1 The somatotrope axis

The somatotrope axis is a hypothalamo-pituitary axis where growth hormone (GH) secretion by pituitary somatotroph cells is under the control of two hypothalamic factors; growth hormone releasing hormone (GHRH) which stimulates, and somatostatin (or somatotropin release-inhibiting factor – SRIF/SS) which inhibits GH secretion (**Figure 1.1**). In periphery, most of the GH actions are mediated by the insulin-like growth factor (IGF-1), a peptide produced mainly in the liver but also locally, so that it can acts in an endocrine, autocrine or paracrine way. IGF-1 exerts a negative feedback on the hypothalamus and pituitary to suppress GH production. Finally, ghrelin is another factor that regulates GH production. This orexigenic hormone, essentially produced in the stomach, induces GH release through GHRH stimulation. As indicated by their names, GH and IGF-1 stimulate skeletal and tissue growth, but they also have multiple metabolic effects, like glucose homeostasis by antagonizing insulin and thereby increasing blood glucose, lipolysis by activating lipase or protein anabolism [2,3].

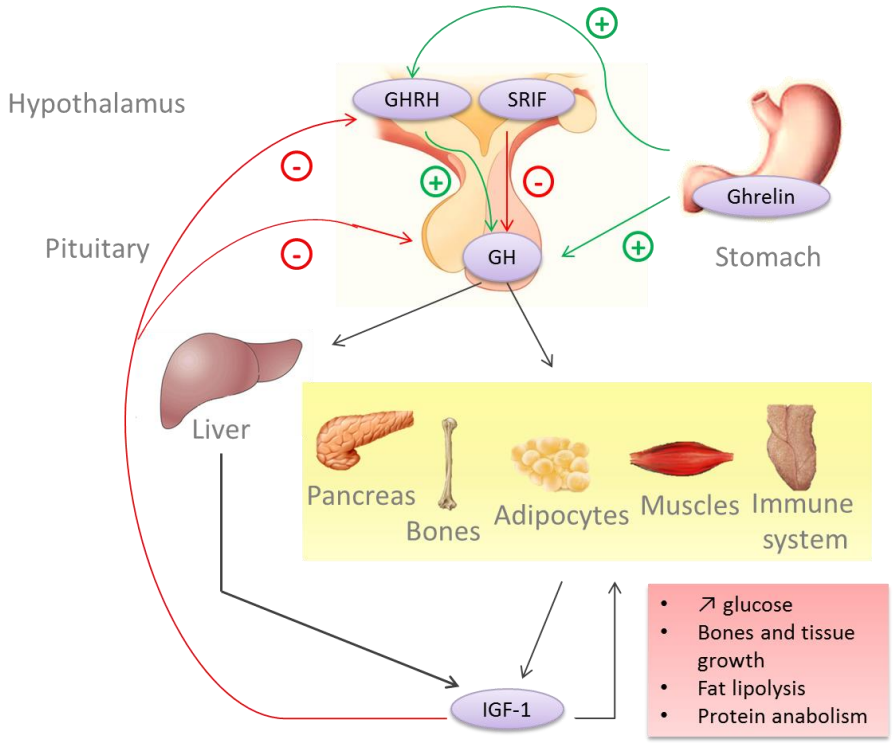

Figure 1.1 – The somatotrope axis. GH production by pituitary somatotroph cells is stimulated by GHRH and ghrelin and inhibited by SRIF and IGF-1. GH acts either directly on target tissues or stimulates IGF-1 production to mediate its growth and metabolic effects.

1.1.1 Growth Hormone releasing hormone (GHRH) and somatotropin release-inhibiting factor (SRIF)

GHRH is a 44-amino acid peptide produced by the arcuate nucleus of the hypothalamus. It was isolated for the first time in 1982 from pancreatic tumors of acromegalic patients [4,5]. GHRH secretion is stimulated by depolarization, α2-adrenargic stimulation, hypoglycemia, hypophysectomy and ghrelin; it is inhibited by SRIF, IGF-1 and GABAergic neurons. Besides its expression in hypothalamus, GHRH mRNA was found in extrahypothalamic neurons, pancreas, epithelial cells of the gastrointestinal tract, placenta, male and female gonads and immune cells [6]. In addition to its role for GH secretion, GHRH is also important for development and proliferation of somatotroph cells.

GHRH binds to a seven transmembrane G protein-coupled receptor, the GHRH-receptor (GHRHR), to increase GH synthesis and release. The binding of GHRH to its receptor activates a stimulatory G-protein which in turn stimulates adenylyl cyclase (AC) to increase intracellular cyclic 3',5'-adenosine monophosphate (cAMP). This increase in

cAMP induces protein kinase A (PKA) which activates the transcription factor cAMP response element binding protein (CREB) by phosphorylation. Activated CREB enhances transcription of Pit-1, the transcription factor specific for pituitary cells, which in turn promotes *GH* and *GHRHR* genes transcription. That leads to increased *de novo* GH production and positive feedback loop increasing GHRHR expression on cell surface. PKA activation also leads to the opening of calcium channels, thus allowing influx of calcium, which directly induces exocytosis of GH stored in secretory granules (**Figure 1.2**) [6,7].

SRIF is a cyclic peptide expressed by neurons of the arcuate nucleus. Its half-life is approximately 2 minutes, thus it is rapidly cleared from the tissue. SRIF secretion is activated by GH and IGF-1, exercise and immobilization and inhibited by hyperglycemia [2,3].

They are five subtypes of receptors for SRIF (SRIFR 1-5) in humans, consisting of seven-transmembrane, G protein-coupled receptors. All five receptors are expressed by human fetal pituitary, but SRIFR4 is no longer present in adult pituitary. Inhibition of GH secretion by somatotroph cells is mostly dependent upon SRIFR2 and SRIFR5 [8]. SRIFR are coupled to an inhibitory G protein, which, upon activation of the receptor, directly inhibits AC and therefore lowers the downstream cascade cAMP – PKA – CREB of the GHRHR signaling [9]. This inhibition of GHRHR signaling decreases GH release and synthesis (**Figure 1.2**).

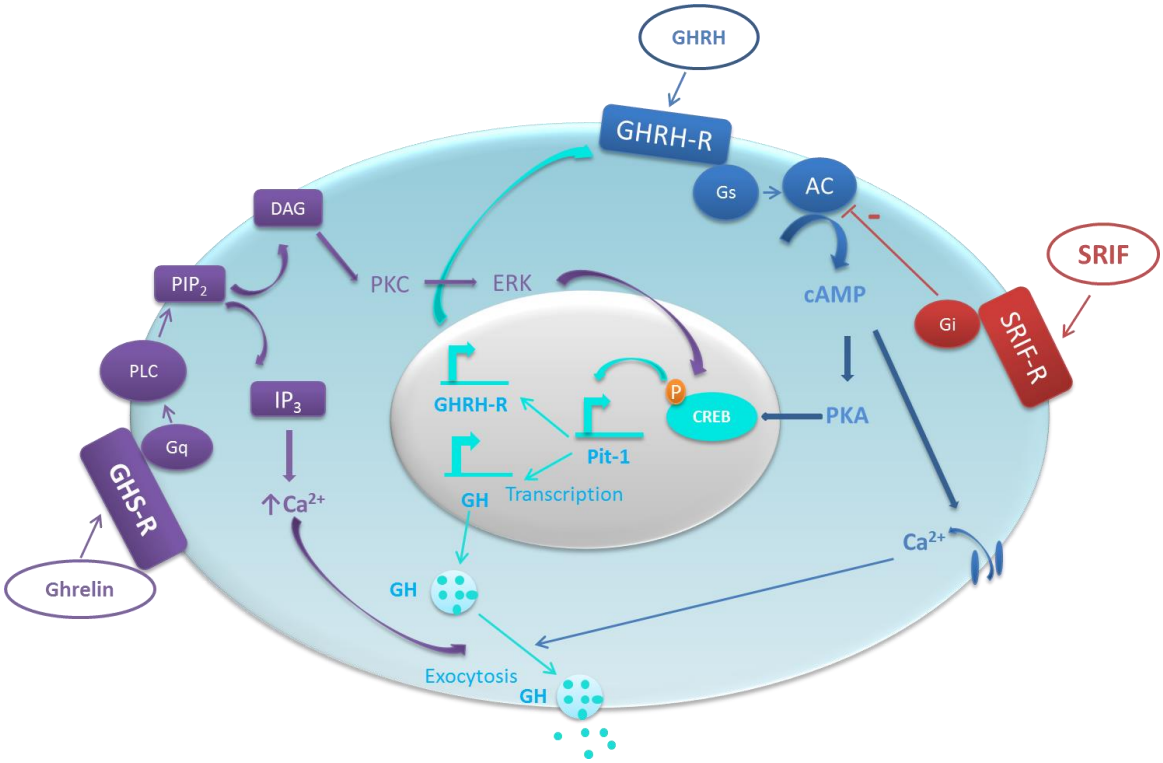

Figure 1.2 – GH regulation in somatotroph cells. GHRH binding to its receptor activates the AC/AMPc/PKA pathway which leads to phosphorylation of CREB. This transcription factor in turn stimulates expression of Pit-1 which activates transcription of *GH* and *GHRHR*. PKA also induces calcium channel opening, leading to calcium influx and triggering exocytosis of GH from secretory granules. SRIFR activation inhibits AC, thus blocking GHRHR signaling. Ghrelin binding to GHSR activates the Gq protein, which stimulates PLC to cleave PIP2 into DAG and IP3. DAG activates PKC/ERK pathway leading to CREB phosphorylation and PIt-1 transcription to increase GH transcription while IP3 increases intracellular calcium triggering GH exocytosis. *Adapted from Hattori N. 2009* [7]

1.1.2 Ghrelin

Ghrelin was discovered in 1999 by M.Kojima as the natural endogenous ligand for growth hormone secretagogue receptor (GHSR) [10]. This 28 amino acid peptide exerts functional activity through GHSR only when acylated on serine 3, a modification mediated by the ghrelin O-acyl transferase which, like ghrelin, is expressed in the stomach [11,12]. Ghrelin has diverse biological actions besides its stimulatory effect on GH release; it is an orexigenic hormone stimulating hunger and food intake, gut motility and gastric acid secretion, but also participates to glucose metabolism, stress, sleep or cardiovascular function [13]. GHSR is a 7 transmembrane domain G protein-coupled receptor found to be expressed mainly in the hypothalamus and pituitary but also in the thyroid, pancreas, spleen, myocardium and adrenal gland [14,15]. Ghrelin-GHSR interaction activates the Gq protein, which in turn stimulates phospholipase C (PLC) to

cleave phosphatidylinositol 4,5-diphosphate (PIP2) into diacylglycerol (DAG) and inositol triphosphate (IP3). On one hand, DAG induces protein kinase C (PKC) to activate extracellular signal regulated kinase (ERK) which finally phosphorylates CREB. Similarly to GHRH signaling, CREB enhances Pit-1 transcription leading to GH transcription. On the other hand, IP3 increases intracellular calcium concentration triggering GH secretory granules exocytosis (**Figure 1.2**) [7,16].

1.1.3 Growth Hormone (GH), GH receptor (GHR) and binding protein (GHBP)

GH, also called somatotropin, is a 191 amino-acid hormone secreted by the somatotroph cells of the anterior pituitary in a pulsatile way, with approximately 8 peaks over 24 hour, mostly during night time. This pulsatile secretion is, at least in part, due to the antagonistic actions of GHRH, ghrelin and SRIF. Nevertheless, patterns for GH secretion are still not fully understood because of their complexity. Indeed, a lot of factors may influence GH secretion such as gender, sexual hormones, fat composition, free fatty acids, body mass index, insulin, leptin or adiponectin. Moreover, GH levels vary during lifetime. Large amounts are needed for growth during childhood, then a rise occurs at puberty and finally in early adulthood, when adult size is reached, GH concentration rapidly declines and continues to slowly decrease throughout adult life [3]. Finally, GHBP also influences GH availability. Discovered in 1986, it consists of the soluble extracellular domain of the GHR[17]. In rodents, it is produced by alternative splicing of the GHR gene [18,19]. In humans and rabbits, GHBP is formed through cleavage of the GHR ectodomain by tumor necrosis factor-α-converting enzyme (also called ADAM17) [20]. Complexation of GH to its BP regulates its bioavailability and bioactivity. Similarly to what is observed for GH, changes of GHBP levels occur during the lifetime, with an increase from childhood to puberty and decrease throughout adult life [21]. Moreover, GHBP concentration is also influenced by body mass index, fat composition or insulin.

GH secretion is regulated by the transcription factor Pit-1, itself controlled by the Prophet of Pit-1 (PROP-1). The two transcription factors are important for pituitary cells development and proliferation [22], and their mutation lead to absence of somatotroph, lactotroph and thyrotroph cells [23,24].

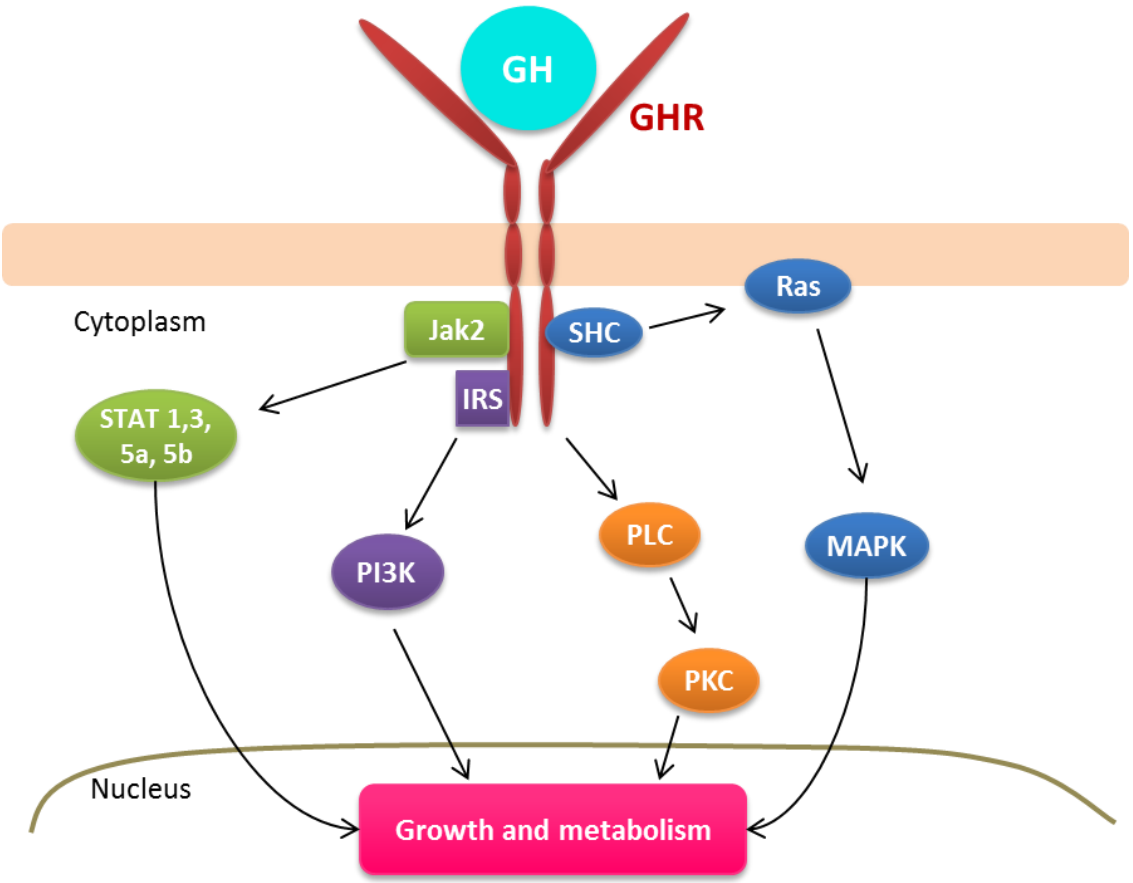

Figure 1.3 – GHR signaling. GH binding to constitutive dimer of GHR induces rotation of subunits leading to activation of several signaling pathways, including Jak2/STAT, IRS/PI3K, PLC/PKC or Ras/MAPK which in turn migrate to the nucleus and activate several gene for growth and metabolism.

GH actions result from the activation of the GHR, a class I cytokine receptor. It consists of a single membrane pass receptor with an extracellular domain containing a cytokine receptor homology domain, and an intracellular domain with a proline-rich Box 1 for binding of tyrosine Janus kinase (JAK) [25]. The general thought is that class I cytokine receptors are activated by ligand-dependent dimerization. Interestingly, it was shown that GHR already exists as a dimer at the cell surface [26], and that GH binding induces rotation of subunits leading to trans-activation of JAK2 [27]. The phosphorylated kinase then recruits and activates the signal transducer and activator of transcription (STAT) proteins to form homo- or heterodimers that migrate to the nucleus and activate transcription of several genes. GH was found to be able to activate 4 members of STAT family: STAT1, 3, 5a and 5b [28,29]. GHR activation also activates others signaling pathways, including Ras/Mitogen Activated Protein Kinase (MAPK), PLC/PKC or insulin receptor substrate (IRS) / phosphatidylinositol 3-kinase (PI3K) [30]. GHR activation signal is summarized in **Figure 1.3**.

1.1.4 Insulin-like growth factor 1 (IGF-1) and receptors

IGF-1 is the main mediator of GH growth actions and this is why it has long been called somatomedin (mediator of somatotropin). It belongs to the large insulin-related system, which includes insulin, IGF-1 and -2, three receptors (insulin receptor, type 1 and type 2 IGF receptor) and six IGF binding proteins (IGFBP 1-6) as well as nine IGFBP related proteins (IGFBP-rP 1-9) [31]. Discovered in 1957 [32], IGF-1 is composed of 70 amino acids and is mainly produced in the liver under the control of GH. However, many peripheral tissues are also able to express IGF-1, suggesting an endocrine, paracrine and autocrine way of actions. IGF-1 release in the circulation induces a negative feedback that inhibits GH production and secretion (**Figure 1.1**). In the periphery, 99% of IGF-1 is complexed to a binding protein and approximately 75% is carried in a ternary structure formed by one IGF-1 molecule, one IGFBP-3 and one acid labile subunit. IGF-1 affinity for these binding proteins is much higher than for its own receptor, and binding of IGF-1 to IGFBP limits its bioavailability and increases its half-life. It also transports IGF-1 to different target tissues [31,33].

Because of the high homology between the members of the insulin-IGF family, IGF-1 is known to bind the three receptors, with the highest affinity for the type 1 IGF receptor (IGF-1R). This receptor is expressed by a wide variety of cells and tissues. IGF-1 binding to the receptor induces activation of IRS-1 that associates with proteins containing src homology 2 (SH2) domains. Amongst those proteins are the PI3K and the growth factor receptor-bound protein 2 (Grb2). The first one leads the formation of PIP3 which is a direct signal for cell growth. The second one activates the Ras/MAPK pathway, which transmits mitogenic and metabolic signals to the nucleus. Grb2 can also be directly activated by SHC and then stimulates Ras, independently of IRS [34] (**Figure 1.4**).

IGF-1 also binds type 2 IGF receptor (IGF-2R), but with a lower affinity than for IGF-1R. IGF-2R is similar to the cation-independent mannose-6-phosphate receptor. The role of this receptor to mediate IGFs signaling is not fully understood, but its effect as a scavenger that regulates uptake and degradation of IGFs is clear [35].

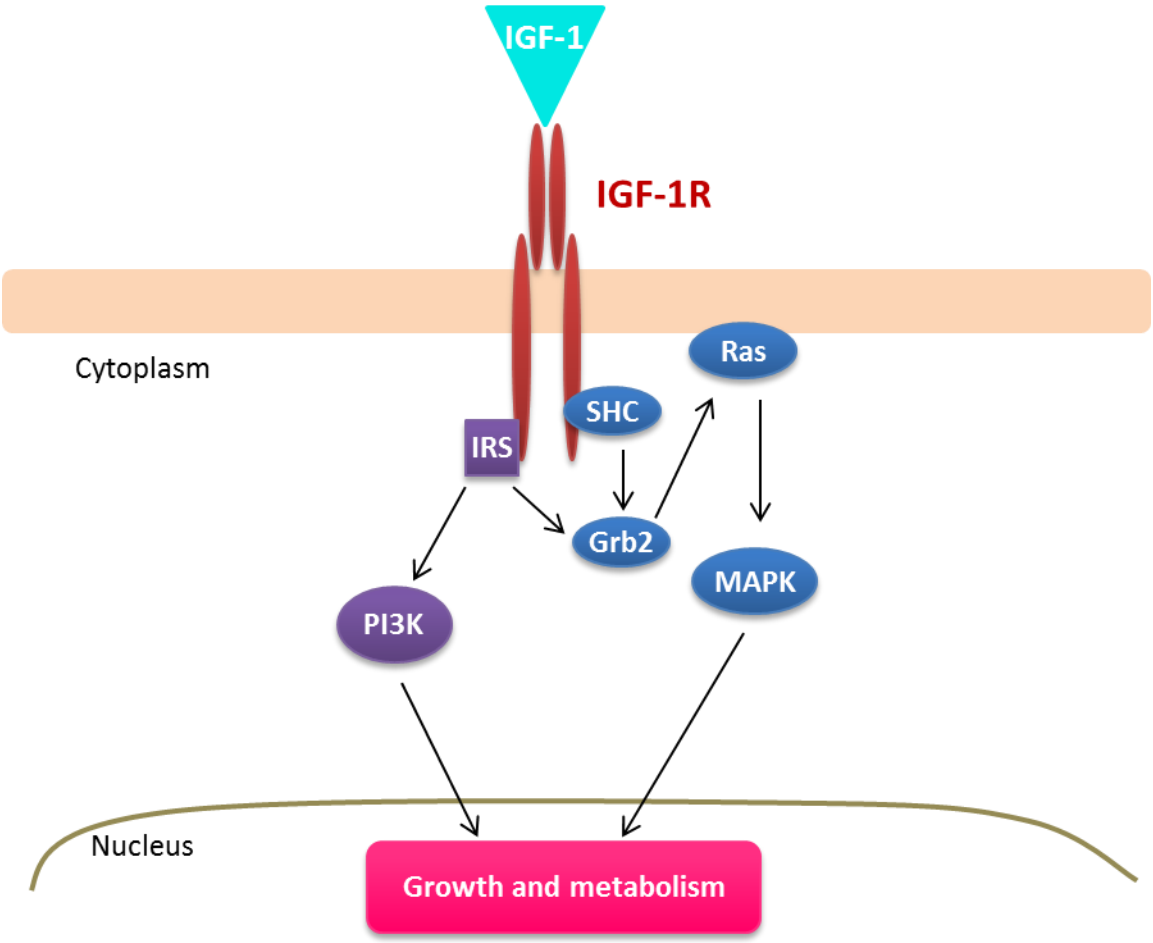

Figure 1.4 – IGF-1R signaling. IGF-1 binding to IGF-1R causes phosphorylation of IRS which activates the Sh2-domains containing proteins PI3K, leading to the formation of PIP3, and Grb2, leading to activation of Ras/MAPK pathway. Grb2 can also be activated by SHC independently of IRS. Downstream signals to the nucleus induce mitogenic and metabolic effects.

Effects of IGF-1, reviewed by Jones and Clemmons [33], include stimulation of cell proliferation, inhibition of cell death, stimulation of cell differentiation and function, promotion of pre- and postnatal bones growth, insulin-like actions or anabolic effects. Most of the growth actions of GH are mediated through IGF-1. This is particularly evidenced in patients with Laron syndrome, a dwarfism characterized by IGF-1 deficiency and high GH concentration caused by a mutation in the GHR gene [36,37]. IGF-1 treatment of children with Laron syndrome increases growth rate and could even restore normal height if treatment is started at an early age [38]. This growth effect is completely independent of GH since GHR function is disrupted in those patients.

1.2 Animal models of somatotrope deficiency

Several mouse models with somatotrope deficiencies exist, deriving from natural mutation or laboratory generated (**Table 1.1**). Mutations occur at different steps of the axis, from defects of hypothalamic GHRH or its receptor to mutation in IGF-1 gene and passing by multiple deficiencies at the pituitary level in Snell-Bagg and Ames dwarf mice or alteration of the GHR gene.

1.2.1 Snell-Bagg and Ames dwarf mice

The first murine models for pituitary deficiency were the Snell-Bagg [39] and Ames dwarf mice [40]. Both strains have spontaneous autosomal recessive mutations that lead to growth failure, absence of GH, thyroid-stimulating hormone (TSH) and prolactin (PRL) and hypopituitarism due to defect in the development of somatotroph, thyreotroph and lactotroph cells. In 1990, Li *et al.* discovered the localization of the mutation affecting the Snell-Bagg mouse, in the Pit-1 gene [23]. The mutation responsible for the Ames Dwarf phenotype was later found localized in the PROP1 gene [24].

1.2.2 Other animal models

Snell-Bagg and Ames dwarf mice have multiple pituitary deficiencies, which make it difficult to identify specific effect of each hormone independently. Fortunately, models of specific somatotrope deficiency also exist. They result from spontaneous or engineered mutations of several members or receptors of the somatotrope axis.

1.2.2.1 Little mouse (lit/lit)

A new dwarf mouse was discovered in 1976, carrying an autosomal recessive mutation on chromosome 6 and called little mice [41]. The mutation was later identified on the GHRHR gene [42]. Little mice (lit/lit) exhibit a dwarf phenotype and reduced GH [42] and IGF-1 production [43]. The amount of IGFBP-3 is also decreased [43].

1.2.2.1 Laron mouse ($GHR^{-/-}$)

In an attempt to obtain a mouse model to study Laron syndrome, Zhou and colleagues generated a mouse with an inactive GHR gene [44]. This mouse, named Laron mouse,

presents growth retardation and dwarfism, absence of GHR and GHBP, decreased serum IGF-1 concentrations and increased GH levels, similarly to what is observed in patients with Laron syndrome. The same group then transferred the mutation into a C57BL/6J background [45].

Table 1.1. Major mouse model of GH deficiencies

Strain	Gene disrupted	Serum concentrations	Reference
Snell-Bagg	Pit-1	↙ GH, PRL, TSH, IGF1	Snell 1929 [39]
Ames dwarf	PROP1	↙ GH, PRL, TSH, IGF1	Schaible and Gowen 1961 [40]
lit/lit	GHRHR	↙ GH, IGF1	Eicher and Beamer 1976 [41]
Laron mouse	GHR	↗ GH ↙ IGF1	Zhou *et al.* 1997 [44]
Igf1$^{-/-}$	IGF-1	↙ IGF1	Powell-Braxton et al. 1993 [46]
Ghrh$^{-/-}$	GHRH	↙ GH, IGF1	Alba and Salvatori 2004 [47]

1.2.2.2 Igf1$^{-/-}$ *mouse*

To investigate the role of IGF-1 in normal development, a research team developed a mouse with targeted disruption of the IGF-1 gene [46]. Unfortunately, 95% of the pups died in perinatal period and those who survived were <60% of body weight of normal pups, showing the importance of IGF-1 for embryonic development.

1.2.2.3 Ghrh$^{-/-}$ *mouse*

The most recently developed mouse model of somatotrope deficiency is the *Ghrh*$^{-/-}$ mouse. Alba and Salvatori generated this new model in order to investigate the functions of GHRH [47]. They disrupted the GHRH gene by replacing part of intron 2 and 3 by a neomycin resistance cassette (Neo^{r}) (**Figure 1.5**). The recombinant GHRH gene was inserted into a plasmid transfected into 129SV embryonic stem cells and then injected into C57BL/6 blastocysts. Resulting chimeric pups were mated with C57BL/6 animals to obtain heterozygous +/- subjects that were mated together afterwards to obtain homozygous -/- mice.

Gnrh$^{-/-}$ mice present a dwarf phenotype with a 55-60% reduction of their weight at 8 weeks of age. As a result of the GHRH disruption, pituitary GH and serum and liver IGF-1 concentrations are decreased compared to normal mice.

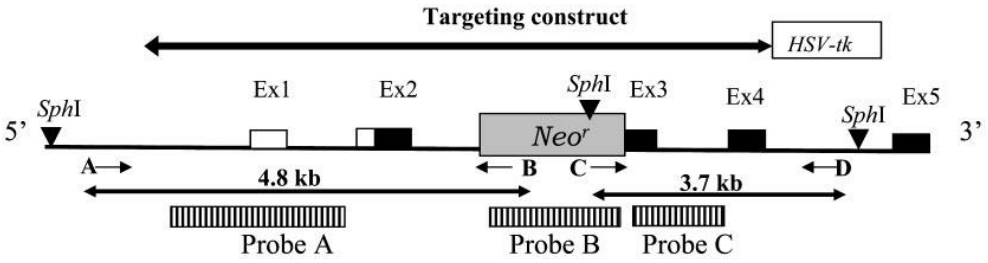

Figure 1.5 — Disruption of GHRH gene. Schematic structure of the targeting construct inserted into the GHRH gene. The boxes represent exons. In *white* are the untranslated exonic sequences. The *Neor* substitutes part of intron 2 and a large part of exon 3. Herpes simplex virus thymidine kinase gene (*HSV-tk*) is attached to the 3' end of the construct. From Alba and Salvatori, 2004 [47].

In this work, we decided to use the *Ghrh*$^{-/-}$mouse model because of the several advantages it presents compared to other models of somatotrope deficiencies:

1) Specific somatotrope deficiency: unlike the Snell-Bagg and Ames dwarf mice, *Ghrh*$^{-/-}$ mice show a specific deficiency of GHRH, GH and IGF-1, with no alterations in the thyreotrope or lactotrope axis. Therefore, this is a very reliable model to identify specific functions and effects of GHRH, GH and IGF-1.
2) Functional pituitary and peripheral sections of the somatotrope axis: by targeting the first member of the axis at the hypothalamic level, this transgenic model allows supplementation at each step of the axis: hypothalamic with GHRH [48], pituitary with GH [49] and peripherally with IGF-1.

1.2.3 GH deficiency and longevity

An extended longevity was reported in each mouse model of GH deficiency (reviewed in [50–52]). Ames Dwarf mice live ~50% longer than normal littermates [53]. Similarly, Snell dwarf mice showed a >40% increased lifespan compared to the long-lived (C3H/HeJ x DW/J)F_1 background [54]. The observed delay in aging seems GH-related since early treatment of Ames Dwarf mice with GH reduces longevity compared to untreated mice [55]. Mice with isolated somatotrope deficiency, such as lit/lit [54], *Ghr*$^{-/-}$ [45] or *Ghrh*$^{-/-}$ [56] mice also present 25 to 50% increased longevity. Similarly, IGF-1

deficiency in *Igf1r*$^{-/-}$ [57] and liver-specific *Igf1*$^{-/-}$ mice leads to enhanced lifespan, but with a more modest effect than GH deficiency [58]. Mechanisms implicated in this improved health span involve increased insulin sensitivity, enhanced cellular stress resistance and decreased inflammation.

1.3 Immune system

The immune system is composed of two interdependent branches: the innate and the adaptive immunity. Innate immunity is the first host response against pathogenic aggressions; it is activated very rapidly but its antigenic repertoire is restraint to a small number of pathogenic common determinants and it lacks memory. On the opposite, the adaptive immunity presents an extreme diversity of the repertoire for antigen receptors (B- and T-cell receptors, BCR and TCR), able to recognize nearly any antigen. Moreover, despite its slow activation, after elimination of the aggression, a memory state is induced and allows a more rapid and efficient response if the same antigen is further encountered. A close relationship exists between the two parts of the immunity: innate cells provide the stimulatory signals required for adaptive cells activation. In turn, adaptive immunity arms innate cells to clear the pathogen. The purpose of this work is of course not to give you an intensive immunity lesson (for a complete but succinct overview, refer to [59]) but to highlight the general principles and notions that will be addressed further.

1.3.1 Innate immunity

The cellular component of the innate immunity is first composed of myeloid cells. They are either resident (macrophages and dendritic cells [DCs]) or circulating (monocytes and granulocytes [neutrophils, basophils and eosinophils]) cells. Circulating cells can be rapidly recruited to the site of infection. The main effector mechanism of myeloid cell is phagocytosis, which leads to pathogen destruction and is also important for activation of adaptive immunity. Indeed, after pathogen uptake, phagocytic cells can process antigens of the pathogen, migrate to lymphoid organs and present antigenic peptides to lymphocytes. They are thus called antigen-presenting cells (APCs). DCs constitute the most effective APC subtype. Besides this phagocytic function, myeloid cells are also able to secrete chemokines (to attract other cells to the site of infection), cytokines (to enhance the functional capacities of immunocompetent cells in an autocrine/paracrine way), as well as soluble effectors (including reactive oxygen species [ROS], histamine or antimicrobial peptides)[60,61].

Recently, a new cellular component of innate immunity has been discovered: the innate lymphoid cells (ILCs) [62]. They derived from lymphoid lineage progenitors and are closely related to T lymphocytes regarding to the transcription factors and cytokines they express, except that they do not express antigen-specific receptors. Natural killer (NK) cells were the first identified ILCs. They possess a cytolytic function, which allows them to directly kill infected cells, and they also produce inflammatory cytokines [63].

1.3.2 Adaptive immunity

The adaptive immune system is subdivided into two arms: B and T lymphocytes. B lymphocytes express BCR, which is an immunoglobulin receptor able to bind soluble antigens, and their effector function is to produce antibodies. T lymphocytes are characterized by the expression of TCR that recognizes antigens presented by other cells through the major histocompatibility complex (MHC). Two effector functions are distinguished amongst T lymphocytes: a cytotoxic function (T cytotoxic, Tc), carried out by CD8-bearing lymphocytes (CD8 T cells), that directly kill infected or abnormal cells; and a helper function (T helper, Th), by CD4 T cells, that activates other cell types through cytokine production or direct cell contacts. Several populations of Th cells are characterized according to their function and cytokine production. For example, Th1 cells secrete interferon γ that activates macrophages and Tc; Th2 produce IL-4, IL-5 or IL-10 and mainly induce eosinophils and B cells; Th17 are IL-17 producing cells with mainly a pro-inflammatory role. Many others subsets have been discovered, and make this field extremely complex [64,65]. Another CD4 T cell subtype has to be mentioned: the regulatory T (Treg) cells. This regulatory subset of T lymphocytes, which expresses the transcription factor Forkhead box protein (FoxP3) and bears a self-specific TCR, plays an important role in peripheral tolerance, by inactivating autoreactive T cells that have escaped intrathymic selection [66,67].

B- and T-cell development presents tightly parallel features, as both pass through several sequential stages of differentiation distinguishable by expression of specific markers. Recombination-activating gene (RAG)-1 and RAG-2 enzymes ensure gene rearrangement of their highly similar receptors; they both depend on receptor checkpoints that block or allow the subsequent cell development, and they share similar

signaling molecules for proliferation and survival, such as IL-7, Flt3 or CXCL12 [68]. The parallel developmental pathways of B and T cells are shown in **Figure 1.6**.

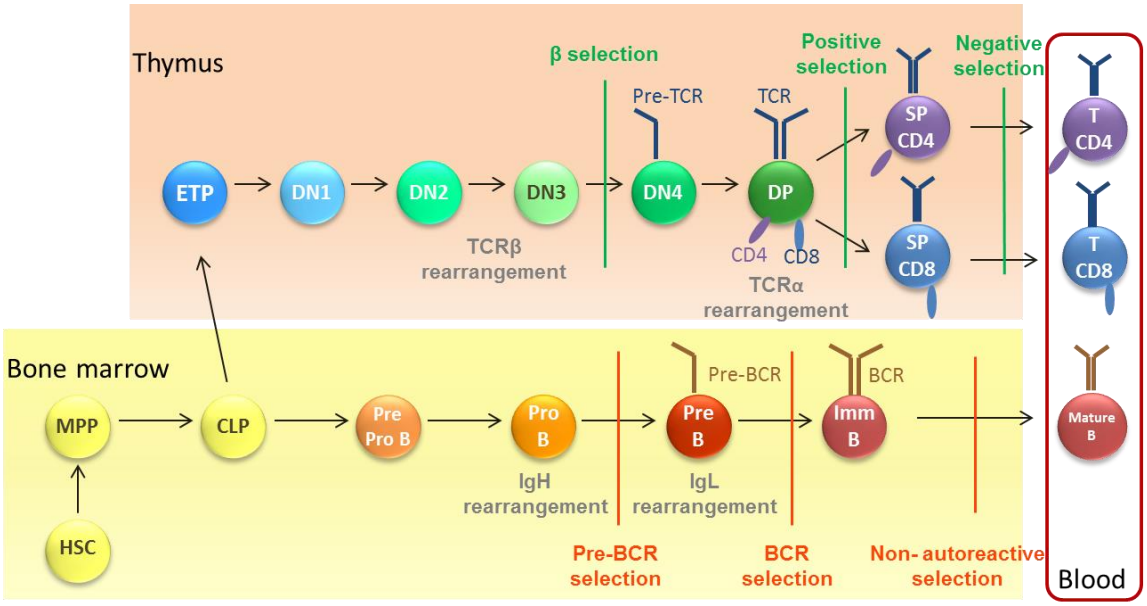

Figure 1.6 — B- and T-cell development in primary lymphoid organs. Lymphocyte lineage cells derive from HSCs in the bone marrow through several steps. After differentiation into MPPs and CLPs, cells committed to B lineage pursue their development in the bone marrow and evolve from pre-pro-B to pro-B, pre-B and finally immature B cells with a functional BCR. Part of CLPs migrate to the thymus, becoming ETPs, and develop into DN cells, which progressively acquire functional TCR during stages 1 to 4 and become DP cells expressing CD4 and CD8, and then commit to CD4 or CD8 lineage in SP cells. Several checkpoints control the quality of gene rearrangements and self-tolerance of the receptors, before exporting to the periphery.

B- and T-cell precursors derive from hematopoietic stem cells (HSCs) in the bone marrow. HSCs are self-renewing cells able to generate all the hematopoietic lineages. To commit into the lymphocytes lineage, HSCs first differentiate into multipotent progenitors (MPPs) with restrained self-renewing capacity. MPPs further develop into common lymphoid progenitors (CLPs), from which originate both B and T cells. B cells pursue their development, named B lymphopoiesis, in the bone marrow while T cells differentiate in a specialized organ, the thymus, in a process called thymopoiesis [68,69]. It should be noted that B- and T-cell development is still under the scope of many studies, and our knowledge in the field is rapidly growing. The reality is much more complex than described here, as new intermediate developmental stages are more and more characterized. Moreover, the classical view of multipotent progenitors evolving toward more specialized cells in dedicated organs needs to be reviewed since cells committed to a specific lineage seem still able to give rise to other lineages [69] and a

population of B cells was found to develop within the thymus [70]. We will propose here a synthetic overview of B lymphopoiesis and thymopoiesis.

1.3.2.1 B lymphopoiesis

B-cell development takes place in the bone marrow and gives rise to immature B cells, which migrate to secondary lymphoid organs such as spleen and lymph nodes (**Figure 1.6**). Differential stages of maturation can be distinguished, according to expression of cell surface markers, immunoglobulins and transcription factors. Unfortunately, human and mouse cells express different markers [71], so we will try here to synthetically describe the common features between both species. First CLPs differentiate into pre-pro-B cells, the first B-cell lineage committed progenitor, which further develop into CD19-expressing pro-B cells. Activation of RAG-1 and RAG-2 enzymes at this pro-B stage activates the immunoglobulin (Ig) genes rearrangement, which is required to generate the BCR. First, D-to-J and V-to-DJ rearrangement of the heavy chain locus leads to the expression of a pre-BCR composed of Igα and Igβ associated with an Ig heavy (H) and a surrogate light (L) chain characterizing the pre-B cell stage. Finally, V-to-J rearrangement of the IgL chain induces the expression of a functional IgM-BCR on immature B cells [71,72]. This highly regulated process allows the export of B cells bearing a functional non-autoreactive BCR via several checkpoints [73,74]. A first control takes place after IgH rearrangement, to ensure that a complete pre-BCR composed of Igμ, Igα, Igβ and surrogate light chains is expressed. After IgL rearrangement, another checkpoint ensures that immature B cells possess a complete BCR with replacement of surrogate light chains by Igκ or Igλ. Finally, after interaction with stromal cells presenting autoantigens, B cells with an autoreactive BCR undergo receptor editing to replace their receptor by rearrangement of other heavy and light chains. If receptor editing fails to produce a new non-autoreactive BCR, cells are eliminated by deletion or anergy. Those who successfully pass through the successive controls are exported to the periphery. An adequate microenvironment is crucial for B lymphopoiesis to take place. It provides necessary chemokines, cytokines, signaling molecules and cell contacts to support and trigger B cell development [75–78]. Notably, IL-7R signaling is required for B-cell progenitor proliferation and survival in mice [79] but

not in humans [80], where the key factor implicated in B-cell development is still to be identified.

1.3.2.2 Thymopoiesis

The generation of the large repertoire of functional self-tolerant T lymphocytes occurs in the thymus, the unique organ with the capacity to support T-cell differentiation program and to induce central tolerance [81,82]. Two types of T lymphocytes are generated in the thymus: αβ and λδ TCR-bearing cells. λδ cells represent only a small proportion of the cells generated by the thymus, and will not be discussed here (for reviews about λδ cells development, please refer to [83,84]). As for B lymphopoiesis, thymopoiesis is a multi-step process highly regulated, avoiding the production of nonfunctional or autoreactive cells (**Figure 1.6**). Progenitors coming from the bone marrow enter the thymus where they are called early T-cell progenitors (ETPs). The exact nature of these incoming progenitors is not fully elucidated, but it is generally acknowledged that they are closely related to marrow CLPs [69,85].

Inside the thymus, the successive differentiation stages encountered by the thymocytes (*i.e.* intrathymically developing T lymphocytes) can be distinguished according to the expression of two surface markers: CD4 and CD8 [86,87]. The most immature subset, counting for 5% of total thymocytes, is called double negative (DN) cells, because they express neither CD4 nor CD8 markers. Four sub-populations can be distinguished in this DN stage, according to the expression of CD44 and CD25 [88]. Indeed, DN1 cells (or thymic lymphoid progenitors) are $CD44^+$ and $CD25^-$. This population of precursor is not completely committed to the T lineage, since transfection experiments showed that they can generate DCs, NK or B cells in addition to their T-cell potential [85]. DN1 thymocytes evolve to DN2 (also called Pro-T cell) after acquisition of CD25 expression. A massive proliferation step is characteristic of this stage. Evidence demonstrated that DN2 precursors still retain NK and DC potential [85]. Thus, the first strictly T-lineage committed stage is achieved at DN3 (or early pre-T cells) stage, after loss of CD44 expression. Finally, down-regulation of CD25 characterizes the DN4 cells (also termed late pre-T cells). TCR gene rearrangement is induced at the DN2 and DN3 stages and leads to the expression of a pre-TCR composed of a CD3 complex associated with a

rearranged β chain and a pre-α chain. The expression of a pre-TCR is a required signal to induce survival and progression to the next step of differentiation, the double positive (DP) stage. DP cells express both CD4 and CD8 molecules at their surface. They represent the majority of thymic T cells (around 80%). Successful β-rearrangement allows rearrangement of the α-chain and expression of a complete TCR at the surface of DP cells. Signaling of this mature TCR after interaction with the MHC class II or class I expressed by stromal cells induces a lineage restriction which generate respectively $CD4^+$ or $CD8^+$ single positive (SP) cells, the most mature subset of thymocytes ready to be export to peripheral lymphoid organs. The exact mechanism underlying CD4/CD8 lineage choice is still under the scope of many investigations, but two main hypotheses are debated: the stochastic (random) and the instructive (determined) model [89,90]. Amongst this SP population, counting for 15% of total thymocytes, are found $CD8^+$ cytotoxic, $CD4^+$ helper and also $CD4^+$ Treg cells.

The thymus is also the organ for central tolerance: by maintaining several control steps, it ensures that only functional and self-tolerant T cells are exported in periphery [91]. A first checkpoint takes place at the DN3 stage, the β-selection, which rescues from apoptosis cells with a functional β-chain rearrangement. The second control, the positive selection, ensures that DP cells express a functional TCR, able to link with a certain affinity to the MHC-peptide complex presented by cortical thymic epithelial cells (cTEC). Cells that do not receive survival signal through their TCR (around 90% of DP thymocytes) die by 'neglect'. Finally, at the SP stage, autoreactive TCR-bearing cells are eliminated after interaction with MHC-self peptides carried by medullar TEC (mTEC) and DCs, a phenomenon called negative selection, since only non-self-signaling TCR survived. The same association with MHC-self peptide complex also gives rise to Treg cells. How the same mechanism leads in some case to deletion of autoreactive clones or in other case to the stimulation of regulatory function in $CD4^+$ SP cells is still unknown, even though two major hypotheses are suggested: the instructive model suggests that medium avidity of TCR for self-antigen leads to Treg generation while strong avidity induces apoptosis; the selective model proposes that regulatory fate is determined prior to TCR signaling and allows to rescue self-specific cells from negative selection [92,93].

As in the bone marrow for B-cell development, thymic microenvironment is crucial for thymopoiesis. Thymocytes follow a highly regulated migration throughout thymic compartments in order to reach the appropriate niches providing the correct cell interactions, ligands, chemokines or cytokines required by each developmental step (**Figure 1.7**)[87]: precursors enter the thymus at the cortico-medullary junction (CMJ) and then migrate to the sub-capsular zone (SCZ) of the cortex during DN stages and finally return back to lower cortex and then medulla while evolving to DP and SP stages respectively. Notch signal has been shown to be essential for early T-cell development: it stimulates survival and proliferation and is implicated in T-lineage commitment [87,94]. Stem cell factor (SCF) [95], the ligand of c-Kit, and IL-7 [76,79] are important cytokines for survival and proliferation during early thymopoiesis. IL-7 is also implicated in TCR rearrangement [96]. Chemokines including CXCL12, CCL19, CCL21 and CCL25 play a role in thymocyte trafficking, by favoring homing of precursors into the thymus, regulating CMJ-to-cortex and cortex-to-medulla migrations and inducing export of mature thymocytes to the periphery [97,98]. TEC constitute the major component of thymic stroma. Besides their role in MHC-peptide presentation for positive and negative selection, they provide the principal source of cytokines, chemokines and cell contacts needed for T-cell development. The transcription factor Foxn1 regulates several functions in TECs, including antigen processing and presentation, attraction of T-cell precursors or positive and negative selection [99]. Disturbance of Foxn1 gene leads to the 'nude' (hairless) phenotype in mouse model, characterized by lack of thymus and immunodeficiency due to the inability to produce T cells.

The thymus is known to encounter drastic histological and functional changes with aging: this process named thymic involution is characterized by thymus size decrease together with replacement of epithelial space by adipose tissue and decline in thymopoiesis [100–102]. The diminution in thymus function starts after puberty in humans and slowly progresses with time, inducing steady decrease in the export of naïve T cells. However, the repertoire diversity of naïve T cells is ensured at least until the age of 70 years and drops afterward [103].

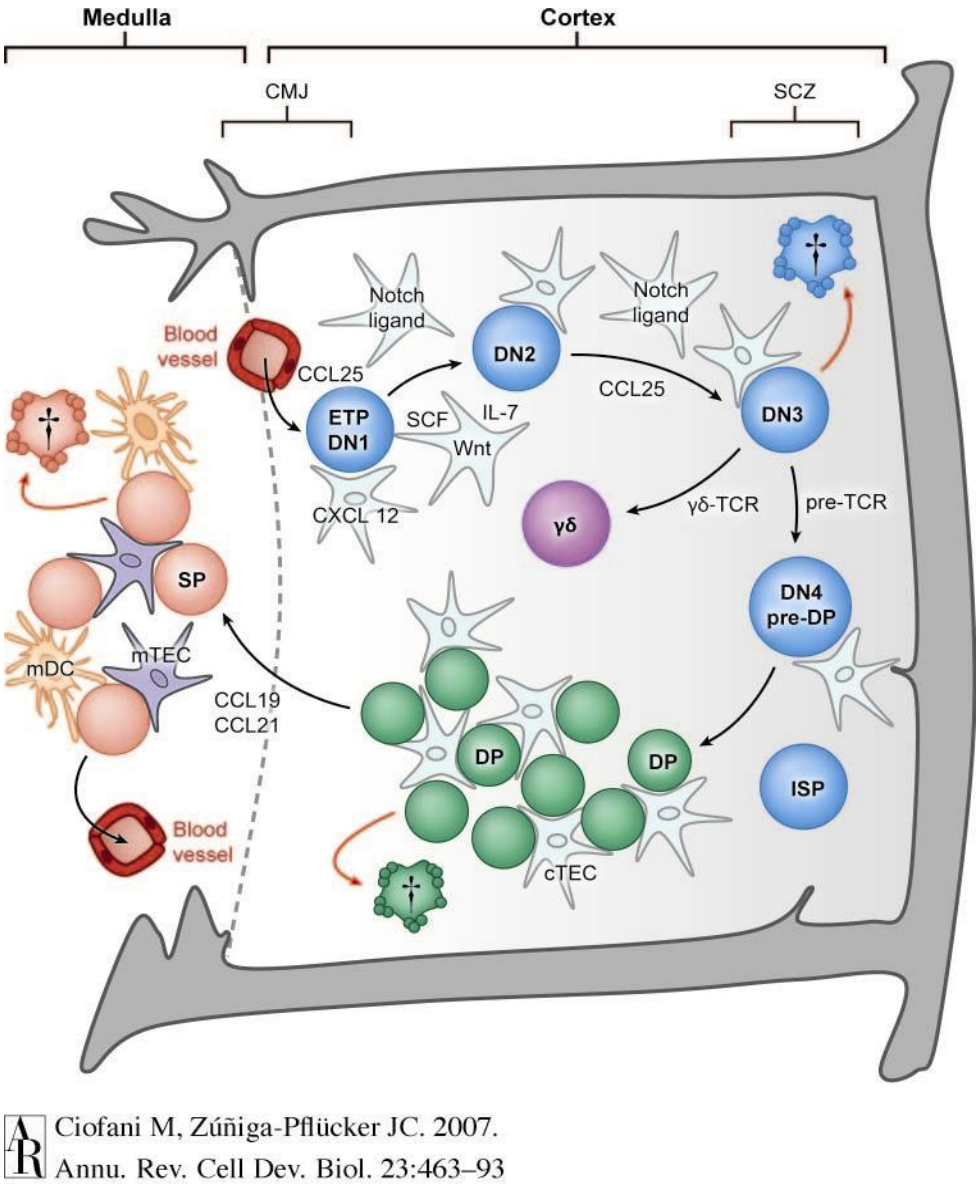

Ciofani M, Zúñiga-Pflücker JC. 2007.
Annu. Rev. Cell Dev. Biol. 23:463–93

Figure 1.7 — Thymocyte migration, microenvironmental signals and checkpoints during thymopoiesis. ETPs enter the thymus at the CMJ and migrate to the SCZ of the cortex while evolving from DN1 to DN4 stages. DN3 cells undergo TCR β-chain rearrangement and β-selection, which rescues cells with functional β-rearrangement from death (†). Selected DP cells migrate back through the cortex and endure positive selection to pursue with SP-cells bearing a functional αβ TCR, which is tested for auto-reactivity during negative selection in the medulla. Several signals from the thymic microenvironment control survival, proliferation, migration and differentiation of the developing thymocytes, including ligands (Notch, Wnt), cytokines (SCF and IL-7), chemokines (CXCL12, CCL19, 21 and 25) or cell interactions with TECs or DCs. From Ciofani and Zuniga-Pflucker, 2007 [87].

1.3.2.3 B- and T-cell receptor gene rearrangement

The adaptive immune system is unique in regard to the wide diversity of the repertoire of BCR (or Ig) and TCR, which allows lymphocytes to recognize virtually any antigen. This repertoire diversity is achieved as a result of a unique process that occurs in developing lymphocytes: the rearrangement of the genes that encode for antigen receptors. Non-

functional in germ-line, the rearrangement of the variable (V), diversity (D; not present in all loci) and joining (J) gene segments (*i.e.* the V(D)J recombination) activated during early lymphocyte development leads, in case of successful recombination, to the expression of a functional BCR or TCR at the cell surface (for a complete overview of V(D)J recombination process and regulation, please refer to Schatz and Ji, 2001 [104] and chapters 5 and 9 of Kuby Immunology [105]). As shown in **Figure 1.8**, the genes coding for each chain of B (IgH and IgL) and T receptors (TCRβ and TCRα-TCRδ) are composed of several V, D (not for IgL and TCRα) and J segments in germ-line configuration, followed by constant regions. For example, the TCRβ gene possess 30 V segments and two D segments, each one being associated with 6 J segments. To be expressed, genes need to rearrange in order to ensure the fusion of one V with one D (if required) and one J segments. This random association offers a multitude of possibilities, assuring a part of the repertoire diversity estimated in the mouse to 2.41 $x10^6$ combinations for immunoglobulin and $3x10^6$ for TCR.

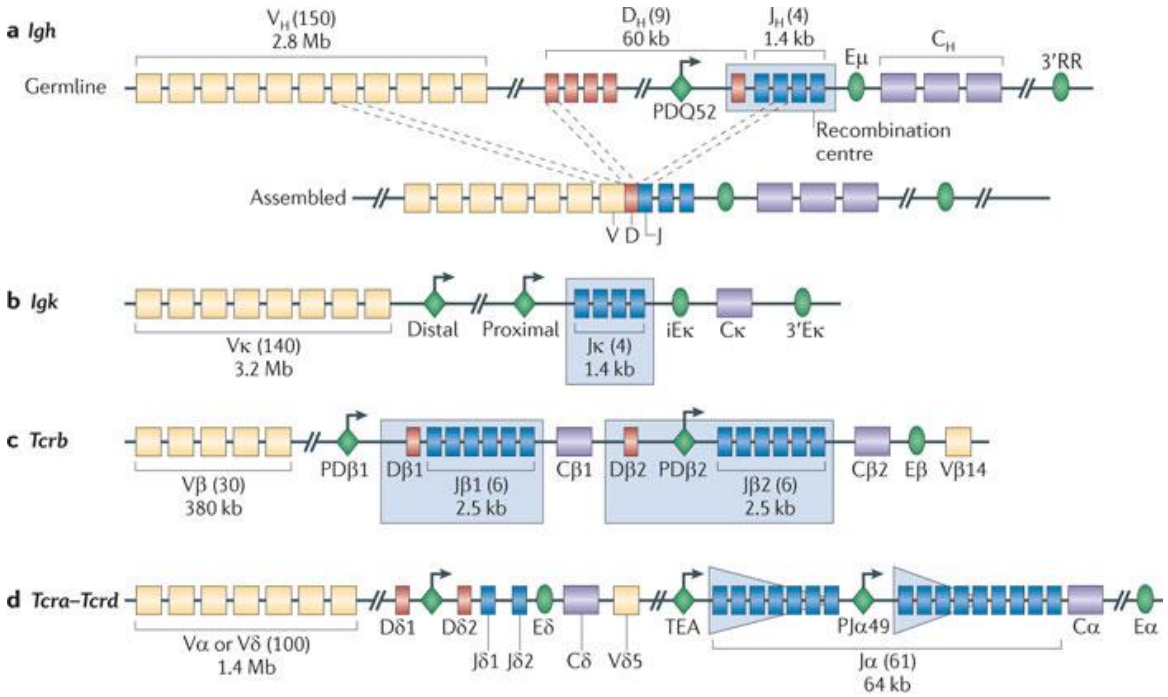

Figure 1.8 — Structure of the mouse antigen receptor genes. Schematic representation of the germ-line configuration of the BCR and TCR chains loci. V (yellow), D (red) and J (blue) segments are shown with their approximate number and the approximate size of the region. The constant regions are in grey, the green ovals represent enhancer elements and green diamonds with arrows are promoters. The blue squared areas are the regions where RAG complex bind to initiate the recombination. One example of assembly is shown for IgH locus. From Schatz and Ji, 2011 [104].

The order of gene recombination is highly regulated: first the IgH and TCRβ chain rearrange in B and T cells, respectively, with D-to-J recombination followed by V-to-DJ assembly. If this first rearrangement passes the control step, IgL and TCRα loci recombination are initiated, with only V-to-J assembly.

V(D)J recombination requires: 1) the cleavage of DNA by RAG complex (RAG1 and RAG2) at specific coding regions (recombination signal sequences RSS) that flank each V, D and J gene segment and 2) the reparation of the DNA double strand break by DNA repair enzymes. This result in the deletion of the portions of gene that are between the RSS sequences of the selected V(D)J segments. During this process, the joining of the two gene segments after RAG cleavage is imprecise and this junctional flexibility can lead either to nonfunctional rearrangement or to productive fusion with diversity in the sequence of amino acids at the joining sites. Moreover, increased diversity also comes from P- and N-nucleotides addition. P-nucleotides are added to complete the single strand that results from cleavage of the hairpin structure that appears at the end of the sequence after RAG-induced cleavage. N-nucleotides are added by terminal deoxynucleotidyl transferase during the joining of D-J or V-DJ segments. Up to 15 N-nucleotides can be randomly added, largely increasing the receptor diversity.

The particular phenomenon of excision of the by-products generated during TCR gene rearrangement is a very interesting tool to experimentally evaluate thymic function [106]. Indeed, the DNA excised during D-to-J and V-to-DJ recombination circularizes and forms what is called TCR rearrangement excision circles (TRECs). They are stable in the cells and non-duplicated during mitosis, therefore progressively diluted by cell divisions. TRECs are formed during any TCR gene rearrangements, but classically only two types are quantified to assess thymic function [107]: the DJβTREC formed during β chain rearrangement and the sjTREC created by the excision of δ locus located inside α locus (**Figure 1.9**). As sjTRECs are produced at a late stage of thymopoiesis, when cells do not proliferate anymore, they are found in almost each cell that leaves the thymus (called recent thymic emigrant [RTE]) and are thus a good marker of the quantity of cells exported by the thymus. DJβTRECs are then created during D-to-J rearrangement of TCRβ chain at the DN2 stages, just before the intensive proliferation phase. By calculating the ratio of sj/DJβTREC, the extent of this intrathymic proliferation can thus

be assessed. TRECs are currently the best tool to investigate thymic function. The experimental method for TREC quantification is detailed in the "Material and Methods" part of this work.

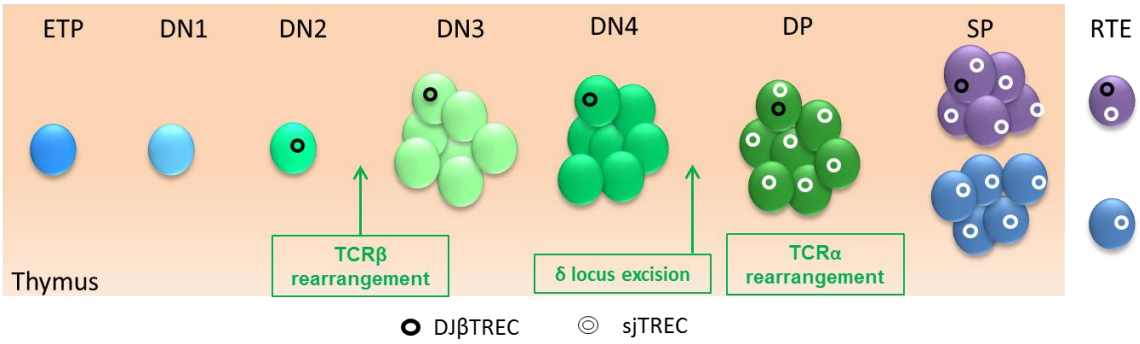

Figure 1.9 —TREC formation during thymopoiesis. DJβTREC (black ring) is formed by bypass product of TCRβ chain rearrangement at DN2 stage. A proliferation burst occurs thereafter, that dilutes DJβTREC. Before TCRα chain rearrangement, the δ locus located inside the α locus need to be excised, leading to the production of an sjTREC (white ring) in each DP cell. Proliferation is almost undetectable thereafter, thus sjTREC exists in virtually each cell that leaves the thymus (RTE) and is a good marker of thymic export. The ratio sj/DJβTREC is a good surrogate of intrathymic proliferation between DN and DP stages.

1.4 Somatotrope axis and immune system

The link existing between the endocrine and immune systems has been known for a long time and the field was the focus of numerous researches in the past century. Philip E. Smith was the first to establish the direct relationship between endocrine gland and lymphoid organ when he observed that hypophysectomy in rats induced thymus involution [108]. It was only forty years later that the somatotrope axis was clearly evidenced as one of the actors of this relationship. Researchers showed that GH treatment could reverse or prevent the thymo-dependent immunodeficiency observed in Snell-Bagg mice [109–111]. Moreover, old rats treated with GH3 cells (pituitary adenoma cells secreting GH and PRL) exhibited regeneration of their aged-atrophic thymus [112]. Finally, expression of GHRH, GH, IGF-1 and their receptors by immune cells is a further evidence of the close relationship between the somatotrope axis and the immune system. Studies to investigate the effects and mechanisms of somatotrope hormones upon immune cells reveal their pleiotropic actions and multiple targets. Indeed, the somatotrope axis is able to influence development and function of innate lymphoid cells, as well as T and B lymphocytes. A large part of research in this field has particularly focused on the T-cell compartment, although it appears now that main targets for GH effects in immune system are B cells, neutrophils and monocytes/macrophages.

1.4.1 Expression for GHRH, GH and IGF-1 receptors by immune cells

Receptors for GHRH, GH, IGF-1 and ghrelin have been described on the cell surface of various immune cells, in rodents and humans (**Table 1.2**). The first observation of GHR expression by a human lymphoid cell line was made on IM-9 cells, a B lymphoblast cell line. They showed that GH could actively regulate the concentration of GHR [113]. Using flow cytometry with biotinylated bovine GH, Gagnerault found GHR expression in several murine lymphoid organs [114]. In the bone marrow, 25-30% of lymphoid cells were positive, including B cells, T cells, macrophages and granulocyte progenitors. In the thymus, 25-30% of thymocytes were stained, with the lowest expression on SP CD4 thymocytes. GHR expression was also found in 50% of blood and spleen cells and 20% of lymph nodes cells, with a higher proportion of positive cells in the B-cell and

macrophage subsets (50% of stained cells compared to 20% for T cells). Moreover, they showed that T-cell activation with concanavalin A or anti-CD3 antibodies increases GHR expression [114]. In human also, thymocytes and TECs express GHR mRNA [115]. They confirmed the presence of GHR protein in human TEC by immunohistochemistry. Flow cytometry analysis of thymocyte subpopulations showed that GHR was predominantly expressed by the immature DN subset [115]. Another team analyzed leucocytes from healthy subjects and found GHR mRNA in blood B cells, T cells and neutrophils, with the highest proportion in B cells [116]. Both studies also searched for GH mRNA, and they found expression of GH in the same cell populations than for GHR [115,116]. GH expression has also been described in human TECs [117] and thymocytes [118], as well as in rat leukocytes isolated from blood, spleen, thymus and bone marrow [119].

As for GH and GHR, IGF-1 and its receptor are present in immune cells. By immunohistochemistry, Hansson detected intracytoplasmic IGF-1 in stromal and lymphoid cells of lymph nodes, thymus, spleen and bone marrow of adult rats [120]. Expression of functional type 1 and type 2 IGFR was described by Verland and Gammeloft on rat thymocytes and murine thymoma cell lines [121]. In humans, presence of IGF-1R was detected in peripheral blood mononuclear cells (PBMCs), with high expression on monocytes, NK cells and CD4 T cells, intermediate in CD8 T cells and low in B cells [122]. Functional IGF-1R was also found on human thymocytes [123], especially in the DN subset which present 3 to 4 time more receptors per cells than DP or SP cells [124]. Another group confirmed the presence of IGF1 and IGF-1R in the thymus by measuring mRNA expression in human and murine thymocytes and TECs [125]. Our laboratory has also shown the importance of the intrathymic IGF system in T-cell development [126,127].

The ability of immune cells to express GH, IGF-1 and their receptors strongly suggests an autocrine-paracrine way of action, besides the classical endocrine way. Indeed, it has been shown that GH treatment increases IGF-1 production by TECs and thymocytes [118,128]. Moreover, IGF-1 antisera or antibodies against IGF-1 and IGF-1R are able to inhibit the GH-stimulatory effect on TECs and thymocytes [118,129]. Collectively, this data demonstrates that at least a part of GH actions in the thymus are mediated through

IGF-1. However, the physiological role, if any, of GH expression in lymphoid cells is still unknown.

Table 1.2. Somatotrope axis members and receptors expression by immune cells

Molecule / receptor	Cell	Reference
GH	Leukocyte from blood, bone marrow, thymus and spleen B-cell T-cell Neutrophil Thymocyte TEC	De Mello-Coelho *et al.* 1998 Hattori *et al.* 2001 Maggiano *et al.* 1994 Sabharwal and Verma 1996 [115–118]
GHR	IM-9 (human B-lymphoma) Bone marrow progenitors (B-T-granulocytes-monocytes) B-cell T-cell Macrophage Neutrophil Thymocyte TEC	Lesniak *et al*. 1976 Gagnerault *et al.* 1996 De Mello-Coelho *et al.* 1998 Hattori *et al*. 2001 [113–116]
IGF-1	Stromal and lymphoid cells of LN, thymus, spleen and bone marrow Thymocyte TEC	Hansson *et al.* 1988 De Mello-Coelho *et al.* 2002 Kecha *et al*. 1999 – 2000 [120,125–127]
IGF-1R	Monocyte NK cell T-cell B-cell Thymocyte TEC	Verland and Gammeloft 1989 Kooijman *et al.* 1992-1995 De Mello-Coelho *et al.* 2002 Kecha *et al.* 1999 – 2000 [121,122,124–127]

Another question is still to be elucidated: are GH and IGF-1 acting directly on immune cells or do they induce intermediate mechanisms to mediate their effects? We had focused on that question in previous research. One possible intermediary is IL-7, an important cytokine for B- and T-cell survival and proliferation during lymphopoiesis [76](and for VD(J) rearrangement of T cell receptor [96]. IGF-1 treatment of human TEC primary cultures increases IL-7 expression and production, suggesting a role for IL-7 as a downstream effector of IGF-1 effects [130].

1.4.2 Somatotrope axis and innate immunity

Innate immunity is the first host defense against pathogens and is also crucial for activation of adaptive immunity, via antigen presentation to lymphocytes by APCs. Numerous studies describe effects of somatotrope axis members upon innate cells (**Table 1.3**). First, they have been shown to prime and increase the phagocytic function of myeloid cells, and therefore enhancing their ability to eliminate pathogen and to present antigenic peptides to activate lymphocytes. Indeed, Keith Kelley's group was the first to show, both *in vitro* and *in vivo*, that GH could prime macrophages to increase their production of superoxide anion, an important ROS needed to kill ingested pathogen [131]. They later demonstrated a similar effect on polymorphonuclear cells (PMNs, also called neutrophils), another type of phagocytic myeloid cells. Moreover, IGF-1 was similarly able to induce this enhanced ROS production by PMNs, even though it did not mediate GH effects, as anti-IGF1 antibody abrogated increased superoxide anion production caused by IGF-1 but not GH [132]. Nevertheless, it seems that in humans, unlike in porcine or bovine species, the GH-mediated increase in superoxide anion production by neutrophils is dependent upon the PRL receptor (PRLR) instead of GHR [133]. It is well known that human GH interacts with both human GHR and PRLR. Other groups confirmed the priming effect of GH and IGF-1 on macrophages and neutrophils, even if some contradictory results appeared. Warwick-Davies demonstrated *in vitro* that GH, but not IGF-1, primes human monocytes for increased production of hydrogen-peroxide (H_2O_2) [134]. GH also enhanced superoxide anion production by human monocytes, but failed to induce tumor necrosis factor (TNFα) production or killing activity against *Mycobacterium tuberculosis* [135]. In peripartum cows, GH treatment increased the intensity of phagocytosis and ROS release, probably through the stimulation of IGF-1 production, while numbers of granulocytes and lymphocytes remained unchanged [136]. IGF-1 was shown to directly prime PMNs for increased H_2O_2 production, enhanced phagocytosis *of Staphylococcus aureus* and *Candida albicans*, stronger degranulation and higher expression of complement receptors [137]. Furthermore, a synthetic GHS (compound A233) was found to increase superoxide anion production by fish leukocyte cultures [138]. These experimental data were confirmed by human studies: in GH-deficient children, analyses showed an impaired phagocytic

function compared to normal controls in neutrophils and monocytes for one study and only neutrophils in the other; long-term GH treatment restored normal phagocytosis in those cells [139,140]. Similarly, a 12-months GH treatment in malnourished hemodialysis patients stimulated phagocytic function of PMNs [141].

Another aspect of innate cells influenced by the somatotrope axis is their migratory and motility abilities. *In vitro* chemotaxis experiments on PMN isolated from acromegalic patients (*i.e.* excessive GH production) revealed a decreased formylpeptide-stimulated migration compared to patients with normal GH levels [142]. Similar results were obtained when normal PMNs were treated with GH in a modified Boyden chamber chemotaxis assay: chemotaxis toward formylpeptide was decreased, probably through stimulation of PMN adhesiveness [143]. Same group showed that GH, when tested alone in Boyden chamber assay, was chemoattractant for blood-derived human monocytes, but when used in combination with other chemoattractant peptides (including formylpeptide), GH deactivated the migratory response [144]. Same observations were obtained *in vivo* after a single GH injection in healthy patients [145]. Study with canine PMNs showed that canine GH potentiated shape change, adhesion and integrins expression, resulting in increased transendothelial migration [146]. Similarly, GH treatment of human neutrophils resulted in increased adhesion to plastic substratum and shape changes. These effects were mediated through the activation of the Jak2/STAT3 pathway and subsequent phosphorylation and focal localization of focal adhesion kinases $p125^{FAK}$ and paxillin, two important molecules in neutrophil adhesion [147]. Altogether, this data suggests that GH is a potent chemoattractant for lymphoid cells, but in combination with other chemoattractants it reduces chemotactic response and induces cell adhesion, which is required for cell recruitment from bloodstream toward infected sites.

NK cell activity is also influenced by GH. Indeed, impaired NK cell cytotoxicity was observed in case of GH-deficiency (GHD) [148,149], while NK cell proportion was found either normal [149,150] or decreased [148]. Long-term GH or GHRH treatments were unable to restore normal NK parameters. On the opposite, *in vitro* pre-treatment with GH increased killing activity of NK cells against a NK-sensitive cell line and against glioma

cells [151]. Furthermore other i*n vitro* studies demonstrated that IGF-1 was able to stimulate NK cell cytotoxicity of both GH-deficient and normal patients [122,150].

In addition, somatotrope axis members are also implicated in proliferation, survival and cytokine production of innate cells. GH treatment of cultured human PMNs, besides the enhancement of ROS production, decreased PMN apoptosis [152]. Similarly, IGF-1 was shown to inhibit apoptosis in progenitor myeloid cells and in granulocytes [153,154]. Moreover, IGF-1 [155] but not GH [135,155] stimulates TNFα production by monocytes/macrophages. Nevertheless, it seems that IGF-1 does not stimulate cytokine production (IL-6, IL-8 or TNFα) of granulocytes *in vitro* [154]. In another study, GH was shown to stimulate DC functions. Indeed, they observed an increased expression of MHC and co-stimulatory molecules and higher production of IL-12, resulting in a better activation of lymphocytes [156]. In patients with adult GH deficiency (AGHD), GH treatment resulted in increasing the number of neutrophils and the granulocyte colony-stimulating factor (G-CSF) plasmatic concentration [157]. G-CSF is a cytokine that induces neutrophil production and activation. This study however could not differentiate if the effect of GH was direct or IGF-1-mediated. Similar neutrophil accumulation and activation was observed in septic rats treated with GH [158]. However, this resulted in aggravation of the lung microvascular injury. This last study raises the important question of the fragile equilibrium between beneficial and deleterious effects of GH treatment. Of course, in light of the various promoting effects of GH and IGF-1 described here upon innate cells, it is tempting to use them in therapy to ameliorate innate immune response. However, inducing a too strong response could be harmful. Further studies are needed to better understand the safety and benefits of GH administration in various conditions (infections, cancer, sepsis, etc).

In conclusion, both *in vitro* experiments and studies in human patients with GHD suggest that the somatotrope axis influences innate immunity by promoting activation, survival and function of innate cells. More specifically, GH and IGF-1 are able to increase phagocytic and cytotoxic activity of myeloid and lymphoid innate cells, respectively, as well as their cytokine production, all crucial functions of the innate immune response.

Table 1.3. Effects of somatotrope axis upon innate immunity

Effects on innate cells	Hormones	Reference
↗ Phagocytic function of monocytes, macrophages and PMN	GH IGF-1 GHS	Edwards *et al.* 1988 Fu *et al.*1991 - 1992 Warwick-Davies *et al.* 1995a+b Manfredi *et al.* 1994 Kotzmann *et al.* 2003 Bjerkness and Aarskog 1995 Martinez *et al.* 2012 [131–135,137–139,141]
↗ Migration, ↗ adherence, ↘ chemoattractants-induced migration of PMNs and monocytes	GH	Fornari *et al.* 1994 Wiedermann *et al.* 1991-1992-1993 Petersen *et al.* 2000 Ryu *et al.* 2000 [142–147]
↘ Apoptosis of myeloid cells and progenitors	GH IGF-1	Matsuda *et al.* 1998 Burgess *et al.* 2003 Kooijman *et al.* 2002 [152–154]
↗ Cytokine production by innate cells	GH IGF-1	Sohmiya *et al.* 2005 Liu *et al.* 2010 Renier *et al.* 1996 [155–157]
↗ Neutrophil accumulation	GH	Sohmiya *et al.* 2005 Liu *et al.* 2002 [157,158]
↗ NK cell activity	GH IGF-1	Sneppen *et al.* 2002 Kiess *et al.* 1988 Shimizu *et al.* 2005 Kooijman *et al.* 1992 Auernhammer *et al.* 1996 [122,148–151]
↗ DC functions	GH	Liu *et al.*2010 [156]

1.4.3 Cellular immunity: thymus and T responses

The somatotrope axis has been shown to affect both development and function of T lymphocytes (**Table 1.4**). Indeed, studies in dwarf mouse models revealed early thymic atrophy and T lymphopenia, partially reversible with GH treatment [109,110,159,160]. Other *in vivo* studies have shown that GH or IGF-1 treatment enhanced thymic output of naïve T cells (or RTE) [161,162]. The same observations were obtained in some human conditions. For example, our laboratory has evaluated thymic function in AGHD with or without GH treatment. Results demonstrated that TREC numbers, markers of thymopoiesis (see section 1.2.3.3), were decreased after GH withdrawal, but returned to starting values after GH resumption (**Figure 1.10**), revealing the important role of GH for

maintenance of a normal thymic function in human adults. Moreover, TREC numbers were correlated to IGF-1 plasmatic concentrations, suggesting a role of IGF-1 in mediating GH actions [163].

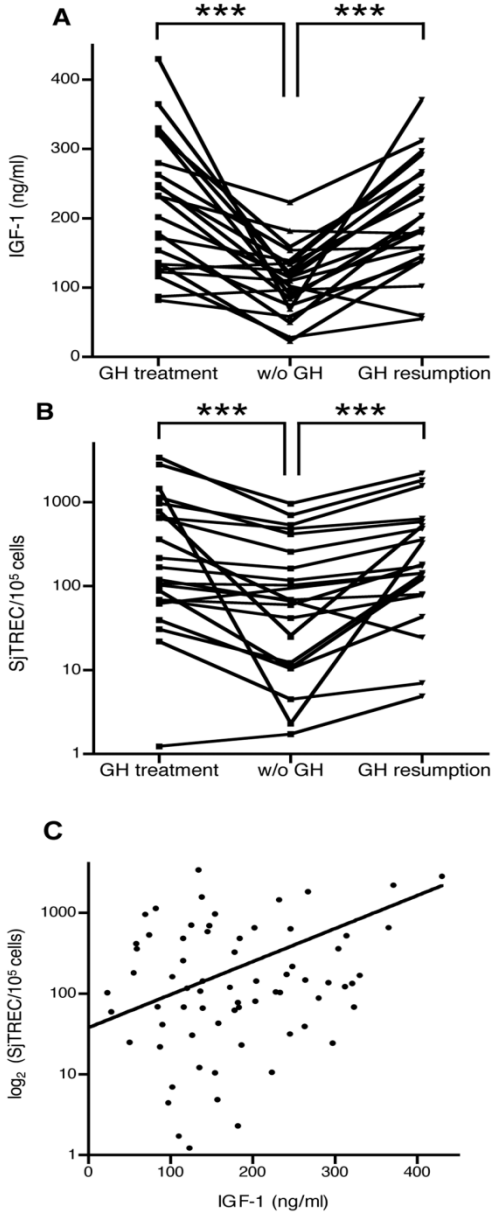

Figure 1.10 — Plasma IGF-1 concentrations and sjTREC frequency in PBMCs from patients with GH deficiency and on GH treatment. The interruption of GH-treatment for 1 month induced a very significant decrease in blood IGF-1 (A) and sjTREC levels (B). Both parameters were restored at initial levels one month after GH resumption. ***P<0.001 (by Wilcoxon's signed rank test, $n = 22$). As shown in C, there was a significant positive correlation between blood IGF-1 levels and sjTREC frequencies ($R = 0.61$, $P<0.01$ by Spearman's analysis). From Morrhaye *et al*. 2009 [163].

Evidence of the thymopoietic effects of GH also come from HIV^+ patients. In infected patients under antiretroviral therapy, GH administration reduced thymic atrophy, enhanced thymic output, as assessed by TREC quantification, and allowed $CD4^+$ T cells recovery, since frequency and numbers of $CD4^+$ T cells were higher in GH-treated patients [164,165]. However, GH treatment has no additional effect on viral load, compared to antiretroviral therapy alone [165].

Altogether this data reveals a role for the somatotrope axis in stimulating thymopoiesis. This potentiating effect results from both direct action on thymocyte proliferation and trafficking, and stimulation of the thymic microenvironment. In Dwarf mice treated with GH, analysis showed a bigger thymus compared to control mice, with increased number of thymocytes, especially the DP subset [160]. Same enhanced cellularity of the thymus was observed in normal mice intrathymically injected with GH or in transgenic mice overexpressing GH [161]. Similarly, IGF-1 treatment induced an increase in the number of thymocytes, in the thymic mass and in the number of peripheral T precursors [162,166]. This higher number of thymocytes results from a direct stimulation of cell proliferation by GH [118,167] and IGF-1 [118,124,128,162,166], as assessed by DNA synthesis, tritiated thymidine incorporation or BrdU measurements. GH action could be mediated by IGF-1, since IGF-1 antisera inhibited GH-stimulated thymocyte proliferation [118].

In addition, GH has an impact on thymocyte trafficking inside the thymus. GH treatment increased human T-cell engraftment in the thymus of severe combine immmunodeficient mice (SCID) [168,169], suggesting that the hormone could favor homing to the thymus through a direct effect on T cells, since ovine GH, which could interact with murine but not human GHR, was unable to promote thymus engraftment [169]. GH further enhances thymocyte adhesion and migration to and through laminin, as demonstrated by cell adhesion and Transwell assays with thymocytes isolated from GH overexpressing mice or mice intrathymically injected with GH [161].

Finally, thymic microenvironment, which actively takes part in the thymopoiesis process (see section 1.3.2.2.), is also affected by GH and IGF-1. Both hormones were shown to stimulate TEC proliferation *in vitro* [118,129] and *in vivo* [162]. They further stimulate TEC production of chemokines CXCL12 and CCL25 [161,162] as well as of ligands and receptors of extracellular matrix (type IV collagen, laminin, fibronectin, VLA-5 and VLA-6) [161,170]. Moreover, GH enhanced production of cytokines IL-1α, IL-1β and IL-6 by bovine fetal thymic stromal cells in culture [171]. Interestingly, it appears that actions of IGF-1 on TECs are sufficient to promote thymopoiesis, despite the stimulating effects on thymocytes. It was demonstrated, in an elegant experiment using a mouse model of

specific IGF-1R deletion on thymocytes, that IGF-1 treatment had the same effect on thymic function than in normal mice [162].

Table 1.4. Effects of somatotrope axis upon cellular immunity

Effects on cell	Hormones	Reference
↗ Thymopoiesis and export of naïve T-cell	GH IGF-1 Ghrelin, GHS	Morrhaye *et al.* 2009 Napolitano *et al.* 2002-2008 Dixit *et al.* 2007 Koo *et al.* 2001 [163–165,172,173]
↗ Thymic mass and thymocyte proliferation	GH IGF-1 Ghrelin, GHS	Murphy *et al.* 1992 Smaniotto *et al.* 2005 Clark *et al.* 1993 Chu *et al.* 2008 Yamada *et al.* 1993 Kooijman *et al.* 1995 Sabharwal and Varma 1996 Postel-Vinay *et al.* 1997 Dixit *et al.* 2007 Koo *et al.* 2001 [118,124,128,160–162,166,167,172,173]
↗ Migration and adherence of thymocytes	GH	Taub *et al.* 1994 Murphy *et al.* 1992 Smaniotto *et al.* 2005 [161,168,169]
↗ Proliferation and function of TECs	GH IGF-1 Ghrelin	Sabharwa and Varma 1996 Timsit *et al.* 1992 Chu *et al.* 2008 Smaniotto *et al.* 2005 Mello-Coelho *et al.* 1997 Dixit *et al.* 2007 [118,129,161,162,170,172]
↗ Mature T-cell proliferation	GH IGF-1? GHS	Clark *et al.* 1993 Postel-Vinay *et al.* 1997 Koo *et al.* 2001 [166,167,173]
↗ Migration and adherence of mature T-cell	GH	Taub *et al.* 1994 Smantiotto *et al.* 2010 [169,174]

Thus, an abundant literature describes the role of the somatotrope axis upon T-cell development. Additionally, mature lymphocytes are also influenced by GH and IGF-1, although this is far less documented. Similarly to what was observed in the thymus, *in vivo* IGF-1 treatment leads to increased number of splenocytes, including T cells [166]. Nevertheless, one *in vitro* study failed to show any proliferating effect of IGF-1, while GH significantly potentiated the proliferation of activated T lymphocytes [167]. Similarly,

peripheral T-cell survival and proliferation were unaffected by IGF-1 treatment as assessed by Ki67 staining or in thymectomized mice, despite a marked effect on thymopoiesis [162]. A stimulation of the mitogenic response of concanavalin A-activated T cells was observed after 14 days of IGF-1 treatment, while antigen-specific response was unaffected [166]. In addition, stimulation of migration and adhesion of mature T cells by GH have been described [169,174].

Finally, few studies investigated the effect of ghrelin and GHS (both bind to GHSR) on thymopoiesis and T cells. Ghrelin increased thymopoiesis and TCR diversity in aged rats, through enhancement of thymocytes, ETP and TEC numbers [172]. GHS similarly enhanced thymocyte number in aged mice and increased T-cell engraftment in thymus of SCID mice. In addition, GHS was shown to stimulate B- and T-cell proliferation [173].

In conclusion, *in vitro* and *in vivo* experiments with GH, IGF-1, ghrelin or GHS treatments highlighted the capacity of the somatotrope axis to promote thymopoiesis and T-cell function, by direct effect on proliferation and trafficking of developing and mature T-cell or indirectly via stimulation of the microenvironment.

1.4.4 Humoral immunity

It is well acknowledged that B cells show the strongest expression for GH and its receptor [114,116]. Hence, it is quite surprising that little interest has been shown to investigate GH or IGF-1 effects upon those cells. Studies in dwarf mice revealed a defect in B lymphopoiesis due to markedly decreased number of B progenitors, as well as B lymphopenia in the spleen. Both parameters were partially restored by GH or IGF-1 treatment [175,176]. Further investigations in lit/lit and *Igf1*$^{-/-}$ mouse models pointed out that GH and IGF-1 were rather implicated in maintenance of peripheral B cells than in their development in the bone marrow, since both mice present normal level of bone marrow B progenitors but decreased splenic B cells [177]. This is in contradiction with the observation that IGF-1 treatment in normal mice increases the number of bone marrow B-lineage cells and faster B-lineage reconstitution after irradiation and bone marrow cell transplantation [178]. The promoting effect on B lymphopoiesis was confirmed by *in vitro* experiments showing that addition of IGF-1 or IGF-1-producing stromal cells to pro-B cell cultures stimulated the expression of μ-heavy chain specific of

the pre-B stage [179]. Moreover, IGF-1 was shown to potentiate the proliferative signal provided by IL-7, although it was ineffective to stimulate pro-B cell proliferation by itself [179,180]. GH similarly promotes B-lineage differentiation from bone marrow stem cells, possibly through autocrine stimulation of IGF-1 expression [181].

In addition, stimulation of peripheral B-cell proliferation and function by GH or IGF-1 has been described. IGF-1 treatment in mice increased the number of splenic B cells, at least partially by directly promoting their proliferation [166,178]. It also improves B-cell response, as demonstrated by the improved IgG synthesis after *in vivo* and *in vitro* antigenic stimulation [166,182]. Likewise, GH showed stimulatory effect on B-cell proliferation and Ig synthesis *in vitro* [183]. A higher IgG response was also observed in peripartum cows challenged with ovalbumin and injected with GH [136]. However, researchers failed to observe any proliferative effect of GH in LPS-activated B cells [167]. Finally, as was observed for peripheral T cells, GH could enhance migratory capacity of B cells in secondary lymphoid organs [174].

Table 1.5. Effects of the somatotrope axis on humoral immunity

Effects on cell	Hormones	Reference
↗ B-lymphopoiesis	GH IGF-1	Jardieu *et al.* 1994 Landreth *et al.* 1992 Gibson *et al.* 1993 Sumita *et al.* 2005 [178–181]
↗ Proliferation of peripheral B cells	GH IGF-1	Clark *et al.* 1993 Jardieu *et al.* 1994 Yoshida *et al.* 1992 [166,178,183]
↗ Antigen-specific Ig synthesis	GH IGF-1	Clark *et al.* 1993 Robbins *et al.* 1994 Yoshida *et al.* 1992 Silva *et al.* 2005 [136,166,182,183]
↗ Migration of peripheral B cells in secondary lymphoid organs	GH	Smaniotto *et al.* 2010 [174]

Therefore, even if few studies focused on the role of the somatotrope axis upon humoral immunity, some evidence exists for the positive actions of GH and IGF-1 in promoting B-cell development in the bone marrow and in stimulating proliferation, Ig synthesis and migration of peripheral B cells (**Table 1.5**).

1.4.5 Immune system in animal models of somatotrope deficiency

As described below, numerous studies evidence the immunostimulatory capacity of the somatotrope axis on both innate and adaptive immunity. However, the physiological reality of those effects is not yet understood. If the somatotrope axis is required for immune system development or function, we could speculate that somatotrope deficiency would induce immunodeficiency. It was indeed the case in several studies performed with dwarf mice. Histological and autoradiographic analyses showed decreased absolute and relative weight of the thymus and spleen, in parallel with disturbed architecture and lymphopenia in primary and secondary lymphoid organs. Moreover, their immunological capacity was also reduced, as assessed by the defect in production of plaque-forming units in response to sheep erythrocytes, which requires the cooperation of both B and T cells [109]. All parameters were restored by GH treatment [110,111]. Further investigations in Snell-Bagg mice showed that thymic hypoplasia was mainly due to the disappearance of DP thymocytes, which instead were found in lymph nodes. Again, DP count returns to normal in the thymus and lymph nodes after GH treatment [160]. Antigen-specific T-cell response was found normal in this study. Regarding B-cell compartment, normal distribution for B and T lymphocytes were observed in the spleen, despite the reduced size of the organ. However, B-cell progenitors were almost absent in bone marrow, and GH treatment was unable to restore this population [175]. Similar observations were made in the Ames-Dwarf model [159]. They present a smaller relative weight of spleen and thymus, peripheral lymphopenia and faster thymic involution. Immune response to sheep erythrocytes and graft-*vs*-host activity were deteriorated, but counts and function of bone marrow cells and peripheral Ig levels were found normal, thus leading to the conclusion that only the thymo-dependent system was defective.

Conversely, several studies failed to observe any immunodeficiency in dwarf mice. Thymic cellularity and mitogenic responsiveness of thymocytes to phytohaemagglutinin and concanavalin A were comparable between Snell-Bagg and normal mice [184]. The unique difference detected was a reduced number of splenic B and T cells, together with higher frequency of T cells and lower frequency of B cells in this organ, but mitogenic activities of both lymphocytes were normal. Splenic abnormalities were partially

restored by GH treatment. Collectively, this data suggests that thymus physiology is unaffected by somatotrope deficiency, while peripheral lymphocyte populations were disturbed, more profoundly for B cells. Similar conclusions were obtained in a study comparing Snell-Bagg mice with specific models of hormones deficiency including hypothyroid, lit/lit and *Igf1*$^{-/-}$ mice, deficient for thyroid hormones, GH and IGF-1 or IGF-1 alone respectively [177]. All the analyzed models present normal thymic cellularity when normalized to the smaller size of the animal, as well as a normal distribution of the four thymocyte subpopulations (DN, DP and SP CD4 or CD8), thus suggesting no impact of the somatotrope axis on thymus function. The total number of cells in spleen and bone marrow were also identical between normal and deficient mice. Nevertheless, Snell-Bagg and hypothyroid mice showed a defect in the number of progenitors and mature B cells in the bone marrow, while Snell-Bagg and lit/lit mice shared a decreased B cellularity in their spleen. This last result supports the conclusion that thyroid hormones are important for B-cell development in the bone marrow, while somatotrope hormones are implicated in maintenance of the peripheral pool of B cells. Further analysis to evaluate the humoral, cellular and innate immune response in those mouse models showed no differences in the B- and T-cell immune capacities, independently of the type of the hormonal defect [185]. Innate response was slightly defective in Snell-Bagg and hypothyroid mice, but normal in lit/lit mouse model, suggesting a role for thyroid but not somatotrope hormones in innate cell function.

There is a confounding discrepancy in the results obtained from mouse models of somatotrope deficiency, between those showing a major impact on thymus and T-cell compartment and those finding only slow differences, mainly in the peripheral B-cell subset. Dorskhind and Horseman came with a theory that could reunify those contradictory data: the stress hypothesis [186]. According to this hypothesis, the main immune role of hormones, such as GH or IGF-1, is to counteract negative effects of immunoregulators, like glucocorticoids (GCs), produced during stressful situations. When a stress is applied to an organism, a ‘general adaptation syndrome’ occurs, including production of steroids and subsequent immunodeficiency [187]. Somatotrope hormones may be produced in response to ensure homeostasis, not only of the immune system but of the complete organism. By carefully reviewing literature about immune

system in dwarf mice, Dorshkind and Horseman realized that studies where immune system was deficient were performed with mice housed in stressful conditions, either because of an unsanitary environment or because of psychological stress when dwarf mice and normal littermates were housed in the same cage [188]. An evidence of this is that, in those studies, dwarf mice lifespan was about 45-60 days [109,111,159] while normally GH deficient mice exhibit extended lifespan (see section 1.2.3). On the opposite, studies that found no striking immune defects were held in more stringent housing conditions. They further reinforced their hypothesis by performing experiments where Snell-Bagg mice were housed either separately or together with their normal-sized littermates [189]. Mice kept in the same cage as larger littermates had striking reduced thymic cellularity compared to dwarf mice housed alone. GH treatment restored comparable number of cells. This data clearly revealed that housing stress is an important factor that leads to thymus deficiency in dwarf mice and bring a plausible explanation to the contradictory results previously obtained in those mice.

1.4.6 Immune system in GH deficient patients

Various GH deficiencies exist in human, from genetic defect leading to growth failure in children to acquired deficiency due to pituitary tumors and irradiation. Very few studies have been conducted to investigate the immune system of those patients, despite the interrogation about GH requirement for immune system development and function. Most of the work performed in children or AGHD found normal distribution of circulating leukocyte populations, including B cells, CD4 and CD8 T cells, NK cells, granulocytes and monocytes [139,140,149,190]. Leukocyte frequencies were not modified after GH treatment. Only innate immune function seems altered in GHD patients, since decreased phagocytic function of granulocytes [139,140] and lower NK activity [148–150] compared to normal controls were observed. Despite the apparent involvement of GH in thymopoiesis of AGHD patients [163], the immune response of T and B cells were not different in GHD children compared to age-matched controls, and clinical history revealed no increased susceptibility to infections in those deficient children [191]. A recent study aimed to evaluate infectious disease and immune response in a cohort of 35 patients with untreated GHD resulting from GHRHR gene mutation [192]. According to their clinical questionnaire and serological tests, those

patients do not exhibit higher frequency of infections. Their total IgG levels were lower than controls, albeit within normal range, but it did not affect their vaccination response against hepatitis B, tetanus or BCG. A positive response to tests of delayed hypersensitivity was also comparable to normal adults, suggesting normal cellular response, although papule diameter was smaller. Altogether, this data showed that GHD did not alter immune response in adulthood, but the authors do not exclude that some unfavorable effects could be seen in severe and acute infections, especially when GHD children seem more vulnerable to childhood infections [192]. Unfortunately, to our knowledge, there is no study investigating the gravity of infections in GHD children, and such a study would be difficult to perform since most GHD children are under GH therapy.

2 Objectives

They are numerous reports arguing for pleiotropic effects of the somatotrope axis upon immune cells and organs. However, the physiological reality of those effects is still obscure. Contradictory findings were obtained regarding the necessity of somatotrope hormones for immune system development. Some groups claimed they are crucial for thymus function, based on the thymo-dependent immunodeficiency observed in dwarf mice that could be corrected by GH injection. Others found no or little effects of somatotrope deficiency in mouse models or humans. Therefore, further investigations are needed to solve this issue and to better understand the physiological role of GH during development, function and homeostasis of the immune system.

To this purpose, we decided to investigate the developmental and functional immunology of the *Ghrh*$^{-/-}$ mouse model (described in section 1.2.2.4). A previous study revealed that *Ghrh*$^{-/-}$ mice are less prone to the induction of experimental autoimmune encephalomyelitis (EAE), showing that the somatotrope axis is involved in the immune response to the myelin oligodendrocyte glycoprotein (MOG) used to induce EAE. Moreover, GH but not GHRH treatment restored normal susceptibility to EAE in *Ghrh*$^{-/-}$ mice, without normalizing serum IGF-1 concentrations [193]. Thus, it seems that GH (but not GHRH or IGF-1) protects mice against EAE. This data points out the impact of somatotrope deficiency upon immune response in *Ghrh*$^{-/-}$ model, here in the case of autoimmunity.

In my thesis, I have first characterized adaptive immune system of *Ghrh*$^{-/-}$ mice in basal conditions, so to see if there is any immunodeficiency or immune alterations resulting from the somatotrope defect. Then, I evaluated the impact of somatotrope deficiency upon immune aging, by analyzing immunological parameters in aged mutant and control mice. Then, *Ghrh*$^{-/-}$ mice were supplemented with GH to investigate the restoration of some immune parameters. Finally, in an attempt to test the stress hypothesis, I submitted mice to a metabolic stress by injecting DXM, a synthetic GC that induces a severe but reversible thymic atrophy.

3 Material and methods

3.1 Mice

A *Ghrh*$^{-/-}$ colony (also referred to as knock-out – KO mice) was established at the animal facility of the University of Liège from 2 males and 4 females sent by Pr Roberto Salvatori. Control C57Bl/6J (or wild-type – WT) mice were obtained from the colony maintained at the animal facility of the University of Liège. We performed a backcross between those two strains, in order to obtain animals with completely identical genetic background. Briefly, *Ghrh*$^{-/-}$ and C57Bl/6J mice were bred together to obtain a F1 generation of heterozygous (HZ) animals. F1 animals were mated together and gave rise to F2 mice with *Ghrh*$^{+/+}$ (WTb for backcrossed), *Ghrh*$^{+/-}$ (HZb) and *Ghrh*$^{-/-}$ (KOb) animals (respectively 25% - 50% - 25% proportion expected). Mouse genotype was identified phenotypically: original *Ghrh*$^{-/-}$ mice have agouti color, a dominant trait, where agouti gene is located near the *Ghrh* mutated gene, so they are transmitted together. Therefore, WTb F2 mice are black and normal-sized; HZb animals are agouti and normal-sized and KOb mice are agouti and dwarf. Normal-sized and dwarf mice were separated at least 4 weeks before any experiment. Male and female mice of 3 months (mo; 9-12 weeks) were used for the basal characterization and DXM experiment; 3, 6 and 18mo for the aging investigation and 3 and 18mo for the GH supplementation. All the experiments were conducted with approval of the Institutional Animal Care and Use Committee of the University of Liège (permit n°1305) in strict accordance with the guidelines for the care and use animals set out by the European Union.

3.2 Tissue and cell preparation

Mice were weighed and euthanized by i.p. injection of Ketamine (100mg/kg) – Xylazine (10mg/kg) followed either by puncture of cardiac blood in K2-EDTA microtainer tubes (BD biosciences) or by removal of the heart to ensure death. Thymus, spleen and inguinal lymph nodes (LN) were removed and weighed. For *Igf1* quantification in GH supplementation experiments, a piece of liver (approximately 30mg) was also removed and placed at 4°C in RNA later (Qiagen) until extraction. For analysis of B lymphopoiesis, bone marrow cells were isolated from one femur in WT and two in KO mice, then passed

through a MACS SmartStrainer 70µm (Miltenyi Biotec) and washed in Dubelcco's PBS (DPBS, Gibco, Life Technologies; 500g for 5min, RT). PBMCs were isolated from whole blood by centrifugation in Lympholyte®-Mammal density separation medium (Cedarlane) or by lysis of red blood cell with RBC lysis buffer (eBioscience), according to the manufacturer's instructions. Thymus, spleen and LN were disrupted mechanically and resulting cell suspensions were washed twice (5min, 500g, RT) in DPBS. To ensure elimination of red blood cells from splenic cell suspensions, a lysing step was performed by 5min incubation in 1ml RBC Lysis Buffer Hybri-Max (Sigma-Aldrich) followed by a washing step in DPBS. Cell suspensions were then filtered through a MACS SmartStrainer 70µm to avoid debris and aggregates. Cells were counted in Neubauer Chamber with trypan blue exclusion of dead cells, diluted in DPBS and distributed for later experiments.

3.3 Flow cytometry analyses of lymphocyte populations

Approximately 500,000 cells were stained for detection of specific lymphocyte populations in the different organs analyzed. The following mAbs were used: anti-mouse CD45.2 FITC (clone 104), CD19 Brilliant Violet (BV) 510 (1D3), CD3 APC-Cy7 (145-2C11), CD44 APC (IM7), CD62L PE (MEL-14), IgM PE (R6-60.2), B220 – CD45R PE-Cy7 (RA3-6B2), CD43 APC (S7) and Ki67 (B56) were purchased from BD Biosciences. Anti-mouse CD4 eFluor®450 (RM4-5), CD8a Pe-Cy7 (53-6.7), CD90.2 – Thy-1.2 APC (53-2.1), CD69 APC (H1.2F3) and Foxp3 PE (FJK-16s) were purchased from eBioscience. Anti-mouse CD28 PE (clone 37.51) was purchased from Miltenyi Biotec. The viability dye 7-AAD (BD Biosciences) was used to exclude dead cells from some analysis.

Briefly, cells were centrifuged and the pullet was resuspended in 100µl of surface mAbs cocktail diluted in DPBS + 2% fetal bovine serum (FBS, Life Technologies), before 20min of incubation at 4°C protected from the light. The several cocktails used for staining of thymus, spleen, lymph nodes, PBMC and bone marrow are described in **Table 3.1**. Cells were next washed in DPBS + 2% FBS and resuspended in 150µl of DPBS medium alone. For intracellular staining of FoxP3 and Ki67, after a first step of staining of surface antigens, cells were fixed and permeabilized with Fixation/Permeabilization solution (Anti-Mouse/Rat Foxp3 Staining Set, eBioscience) according to the manufacturer's

instructions, prior to 30min incubation with FoxP3 or Ki67 antibody diluted in Perm Buffer (Anti-Mouse/Rat Foxp3 Staining Set). After two washing steps in Perm Buffer, cells were diluted in 150µl of DPBS and analyzed on a BD FACS Verse (BD Biosciences) using BD FACS Suite Software and FlowJo Software.

Table 3.1. Surface antibodies cocktails for staining of lymphoid organs

Organ – staining	Surface antibody	Volume per sample (µl)
Thymus[a]	Thy1.2 APC diluted 1/20	3
	CD8 PE Cy7	1
	CD4 e450	1.25
Spleen, LN, PBMC (B – T staining)	CD45.2 FITC	1
	CD62L PE	1
	CD8 PE Cy7	1
	CD44 APC	1
	CD4 e450	1.25
	CD3 APC-Cy7	1
	CD19 BV510	1
Spleen, LN, PBMC (Treg staining[a])	CD45.2 FITC	1
	CD8 PE Cy7	1
	CD4 e450	1.25
	CD3 APC-Cy7	1
Bone marrow	IgM PE	1
	B220 PE Cy7	0.5
	CD43 APC	1
	CD19 BV510	1

[a] for Treg staining, 1µl of FoxP3 PE antibody was added separately after fixation/permeabilization step.

3.4 TREC quantification

Thymus function was evaluated by quantification of sj and DβTREC, by adapting a protocol previously described by Dulude *et al.* [194]. Total sjTREC number was estimated by quantification of δREC1 rearrangement with jα61 and jα58 segments, since they represent almost 100% of sjTREC frequency in mice [194]. DJβ2TREC production was found to be unproductive [194]; therefore DβTREC content was measured by quantifying Dβ1 rearrangements with Jβ1.1 to 1.6. The CD4 gene was used as a single copy gene, allowing estimation of the number of cells (each cells possess two alleles of the CD4

gene, so the number of cells = number of CD4 copies/2). The relative numbers of copies of CD4 gene and TREC were obtained by multiplex nested real-time PCR quantification (RT-qPCR), by comparison with plasmids containing both CD4 and sj61 or DJβ4 sequences respectively for sj- or dβTREC quantification. First, to release DNA content, cells were lysed 30min at 56°C in lysing buffer constituted with Tris-HCl (10mM; pH 8.3), Tween 20 (0.05%), Igepal (0.05%) and proteinase K (100µg/ml) followed by 10min at 95°C to inactivate proteinase K. Cell lysates and plasmids were then pre-amplified for CD4 gene and sj- or DβTREC in a step called "pre-PCR", using outer primers (**Table 3.2**). Briefly, 10µl of samples were added to 90µl of a mix composed of 1µl of each primer at 100mM (CD4 1 and 2, REC1 and Jα58 and 61 for sjTREC; CD4 1 and 2, Dβ1 and Jβ1.1-1.6 for DβTREC), 20µl of 5X colorless GoTaq® Flexi buffer (Promega), 14µl of MgCl2 25mM (Promega), 4µl of dNTP 10mM (Promega), 0.8µl of GoTaq® Flexi DNA Polymerase (Promega) completed with nuclease-free water (Ambion). Amplification was performed in an iCycler thermocycler (Bio-Rad) with the following program: initial denaturation at 95°C for 10min; 22 cycles (for spleen and PBMC) or 19 cycles (for thymus) of amplification at 95°C for 30s; 60° for 30s; 72°C for 2min; final elongation 72°C for 10min and cooling at 15°C. PCR products were diluted 400x for spleen and PBMC and 500x for thymus samples and then relative CD4 and TREC number of copies were determined by RT-qPCR in a LightCycler480 thermocycler (Roche Diagnostics) by adding 4µl of diluted PCR products to 7µl of Takyon™ No Rox SYBR MasterMix Blue dTTP (Eurogentec), 0.2µl of CD4 or TREC inner primers (**Table 3.2**) and completed with nuclease-free water to reach a total volume of 14µl. The amplification program was 5min of initial denaturation at 95°C; 40 cycles of amplification at 95°C for 10s; 60°C for 15s; 72°C for 10s and cooling at 40°C. Results were analyzed on the LightCycler480 Software by the second derivative max method. Standard curves with arbitrary determined numbers of copies were obtained by performing a 10-fold serial dilution of each plasmid. Number of TREC and CD4 were calculated by reporting Ct of each sample to the standard curve. Finally, TREC were expressed in number per 10^6 cells. To evaluate run-to-run variation, an internal control was added to each run of RT-qPCR. When the standard deviation of the control was above 10% compared to the mean for all runs, a correction factor (control's TREC number in this run / mean control's TREC number in all runs) was applied to each sample of the run.

Table 3.2. Outer and inner primers for sj and DβTREC quantification

Name	Sequences Out	Sequences In
CD4 1	CCAACCAACAAGAGCTCAAGGA	AGCTCAAGGAGACCACCATGT
CD4 2	CCCAGAATCTTCCTCTGGT	TGGTCAGAGAACTTCCAGGT
Jα61	AACTGCCTGGTGTGATAAGAT	GGAGTATCTCTTTGGAGTGA
Jα58	CCCAGGACACCTAAAAGGAT	AACTCGCACAGTGGAGGAAA
REC1	AGTGTGTCCTCAGCCTTGAT	GAAAACCTCCCCTAGGAAGA
Dβ1	TATCCACTGATGGTGGTCTGTT	GACGTTGGCAGAAGAGGATT
Jβ1.1	CATGTTTGACATTGCCACAAGT	AGCGATTACTCCTCCTATGGT
Jβ1.2	CTCTCTTCACCCCTTAAGATT	GTAAAGGAACCAGACTCACAGTT
Jβ1.3	TGAGGCTGGATCCACAAAGGT	TCAAGATGAACCTCGGGTGGA
Jβ1.4	GGGCCATTAGGAAACGTGAT	GCAGGAAGCATGAGGAAGTT
Jβ1.5	GGAGGAAGGAAGGATGGTGA	CAGAGTCCTGCCTCAAAGAA
Jβ1.6	CCTGTGACATGCCTCATGGTA	TCAGGTCTCAGGGATCTAAGA

3.5 *In vitro* stimulation of B- and T-cell function

B or T cells were isolated from splenic cell suspensions by MACS separation in LS column (Miltenyi) with Pan Bcell Isolation Kit II or Pan Tcell Isolation Kit II (Miltenyi) respectively, according to the manufacturer's instructions. Cell purification assessed by flow cytometry was above 90%. Isolated cells were next labeled with 1µl CFSE (CellTrace CFSE, Life Technologies) under agitation and incubated 6min at 37°C with vortexing each 2min. Labeling was stopped by addition of 3ml of cold FBS and incubation 5min in ice. Then cells were washed 3 times (500g for 5min RT) in RPMI (Gibco, Life Technologies) + 10% FBS. CFSE-labeled cells were counted and 100,000 cells were added in 200µl of RPMI + 10% FBS + 1% Penicilin/streptamycin (Lonza) + 1% L-glutamine (Gibco, Life Technologies) + 5µM 2-mercaptoethanol (Gibco, Life Technologies) in each well of a 96 wells U-plate (VWR). For B-cell activation, 2µg/ml of LPS (Sigma) was added to the cells. For T-cell, plates were pre-coated with 50µl of purified anti-CD3 antibody 5µg/ml (eBioscience) and 2µg/ml of purified CD28 antibody (eBioscience) were then added to the cells in the well. Each sample had its own control non-stimulated, to obtain basal values. Stimulated cells were finally incubated for 24h, 48h or 72h. At each time, cells were harvested and prepared for flow cytometry to measurement of cell proliferation

with CFSE dilution and activation with CD69 expression (antibodies cocktails are shown in **Table 3.3**). For experiments with B cells, 50µl of supernatant were sampled for IgM measurement by ELISA using the Mouse IgM ELISA Ready-set-go kit according to the manufacturer's instructions (Affymetrix, eBioscience). In some experiments, CD8 naïve T cells ($CD3^+$ $CD8^+$ $CD44^{low}$) were sorted by FACS from MACS-separated T cells and further labeled with CFSE and stimulated with CD3-CD28 antibodies in 96 wells U-plate. In another experiment, purified T-cells were treated with GH (Genotonorm, Pfizer) or IGF-1 (Increlex, Ipsen) 10 and 100nM at the same moment than CD28 addition.

Table 3.3. Antibodies cocktails for analysis B- and T-cell function

Organ – staining	Surface antibody	Volume per sample (µl)
B-cell	CD19 BV510	1
	CD69 APC	1
T-cell	CD3 APC-Cy7	1
	CD4 V450	1.25
	CD8 PE-Cy7	1
	CD69 APC	1

3.6 GH supplementation

Ghrh$^{-/-}$ and C57Bl/6J young and aged mice were injected daily with human recombinant GH (100µl i.p. at 1mg/kg) for 6 weeks. Control mice were injected with DPBS. Before the first injection (referred to as d0) and once per week after the beginning of the treatment, glycaemia and weight were monitored in order to assess metabolic effects of the treatment. In addition, a blood sample (130µl in WT and 65µl in KO mice) was taken from the tail weekly for flow cytometry analysis or TREC quantification (each analysis was alternatively performed every second week). Basal level of blood TREC was determined two weeks before d0. After 6 weeks, mice were killed by i.p. injection of Ketamine/Xylazine and cardiac blood puncture. Thymus, spleen and LN were removed for immunological analysis and a piece of liver was taken for quantification of *Igf1* expression.

3.7 *Igf1* quantification by RT-qPCR

Liver and thymic *Igf1* expression was analyzed by RT-qPCR as previously described [195]. Briefly, RNA was extracted with the NucleoSpin® RNA kit (Macherey-Nagel) according to the manufacturer's instructions. RNA concentration was measured by NanoDrop ND-1000 (Thermo Scientific) and 500ng were used for reverse-transcription with oligo-dT using Transcriptor first strand cDNA synthesis Kit (Roche) following manufacturer's instructions. Transcript quantification was performed using Taqman probes technology and iQ Supermix (Bio-Rad) with the following primers: *Igf1* forward CAGGCTATGGCTCCAGCATT; *Igf1* reverse ATAGAGCGGGCTGCTTTTG; probe 6-FAM-AGGGCACCTCAGACAGGCATTGTGG-BHQ-1. Mouse hypoxanthine-guanine phosphoribosyltransferase (HPRT, Mm01324427_m1 TaqMan Gene Expression Assays, Applied Biosystems) was used as a housekeeping gene. Amplification was performed in an iCycler thermocycler (Bio-Rad) with the following conditions: polymerase activation at 50°C for 2min; denaturation at 95°C for 10min; amplification for 50 cycles at 95°C for 15s and 60°C for 1min. A calibration curve was generated from serial dilutions of plasmids containing either IGF-1 or HPRT sequence and number of copies of each transcript was calculated by linear regression.

3.8 DXM administration

Mice were injected i.p. with 100µl of Dexamethasone dihydrogenophosphat-dinatrium 20mg/kg (Aacidexam 5mg/ml, Aspen) or DPBS as control. The day of injection was referred to as d0. MRI sessions were performed at day 0, 2, 5, 10 and 14 in order to follow thymic involution and recovery. At each time point, individual groups of mice were euthanized and thymus, blood, spleen and LN were removed for further analysis. The d0 group was analyzed before DXM injection to obtain basal values. Results for other time points were expressed in percent of this basal value.

3.9 Thymic volume follow-up by MRI

Anaesthesia was induced with isoflurane 4 % in air, and then maintained by reducing the ratio to 1.5 % for the duration of the acquisition (flow rate: 0.8 L/min). The mice were placed prone in a stereotaxic holder (Minerve, France). The breathing rate was

monitored during the entire scan and the body temperature maintained at 37 ± 0.5 °C with an air warming system (Minerve, France). MRI anatomical images were acquired on a 9.4 Tesla MRI DirectDrive VNMRS horizontal bore system with a shielded gradient system (Agilent Technologies, Palo Alto, CA) and a 40 mm inner diameter volumetric coil (Agilent Technologies, Palo Alto, CA). Fast spin echo multislices sequence were acquired using the following parameters adapted from Brooks *et al*. and Beckmann *et al*. [196,197]: TR/TE_{eff} = 2000/40 ms, matrix = 192 x 192, FOV = 20 x 25 mm, 10 contiguous slices focused on the region of interest (thickness = 1.0 mm, in-plane voxel size: 0.104 x 0.130 mm). Anatomical images were analyzed using PMOD software version 3.6 (PMOD Technologies Ltd., Zurich, Switzerland). The thymus was manually segmented, because of its difference in signal intensity from the surrounding tissues, on each contiguous slice (thereafter referred as region-of-interest, ROI). The PMOD tools allow direct computing of the organ volume, by multiplying the effective slice thickness with the surface areas of each ROI.

3.10 Statistical analyses

Statistical analyses were performed on the Prism 4.0 software (GraphPad). Kolmogorov-Smirnov and Shapiro-Wilk normality tests were performed to evaluate the Gaussian distribution of data. When Gaussian distribution was verified unpaired t-test was applied, while Mann-Whitney test was used for non-Gaussian distributions. For multi-parametric analysis of GH supplementation and DXM administration, two-way ANOVA with Bonferroni post-test was used.

4 Results

To investigate the impact of somatotrope deficiency upon immune system development and function of the *Ghrh*$^{-/-}$ mice, I first characterized their immune system in basal conditions. Then I studied the effect on aging and immunosenescence. In a third step, mice were supplemented with GH to observe if it corrected immunological parameters. Finally, I tested the stress hypothesis by following DXM-induced thymic atrophy and recovery.

4.1 Immune system of the *Ghrh*$^{-/-}$ mouse in basal conditions

The first objective of this thesis is to reassess to necessity of the somatotrope axis for immune system development. To that purpose, I analyzed several immunological parameters in 3mo-old mice, comparing weight and cell content of lymphoid organs, thymus phenotype and function, peripheral lymphocyte distribution and function and B-lymphopoiesis between mutant and normal animals. Here, I analyzed backcrossed mice, and compared results with original strains[i] to verify if mice from WT and KO colonies are identical to backcrossed mice or if they present further differences caused by a non-similar genetic background.

4.1.1 Weight and cellularity of lymphoid organs

As shown in **Figure 4.1**, mutant mice were half the size of normal or heterozygous animals. WTb and HZb females were smaller than male counterparts, while no statistical differences were found between male and female homozygous mutant mice. The body weight of original mice was similar to backcrossed animals. Because of this smaller size, weight and cellularity results were normalized in function of total body weight or organ weight respectively.

[i] C57Bl/6J and *Ghrh*$^{-/-}$ homozygous colonies were handled by the animal facility of the University of Liège. Data for WT and KO mice here are the same as d0 groups in DXM experiment, except for TREC quantification where backcrossed groups were compared to 3mo WT and KO groups of aging experiment. Therefore, original and backcrossed groups were not analyzed in the same experiment.

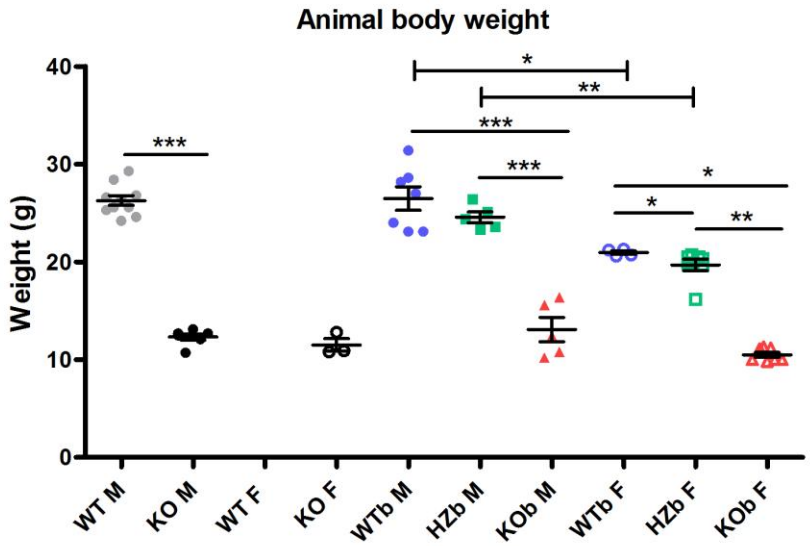

Figure 4.1 – Animal body weight. Original (WT, *n*=10M; KO *n*=7M-3F) and backcrossed (WTb, *n*=7M-4F; HZb, *n*=5M-7F; KOb, *n*=5M-7F) male (M, full symbol) and female (F, open symbol) mice were weighed after euthanasia. Data (mean ± SEM) are representative of 3 or 4 independent experiments. Unpaired t-test was used for statistical analysis of male and Mann Whitney test for female mice. *** $p < 0.001$, ** $p < 0.01$, * $p < 0.05$.

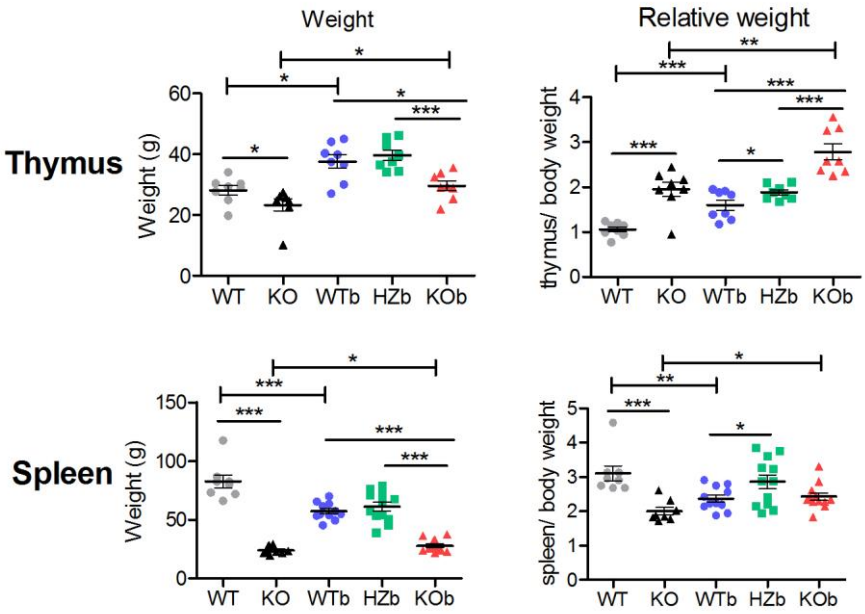

Figure 4.2 –Thymus and spleen weight. Absolute and relative (organ weight/body weight) weight of original (WT, KO) and backcrossed (WTb, HZb, KOb) thymus and spleen. Data (mean ± SEM) are representative of 3 or 4 independent experiments. Unpaired t-test or Mann Whitney test were used for statistical analysis, according to the Gaussian distribution of each group. *n*=8-12 per group *** $p < 0.001$, ** $p < 0.01$, * $p < 0.05$.

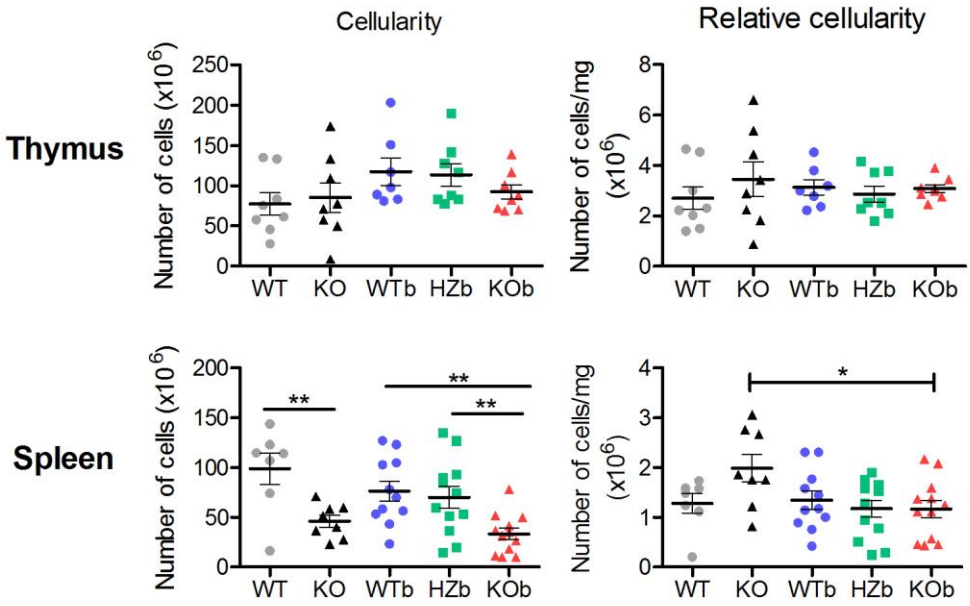

Figure 4.3 –Thymus and spleen cellularity. Absolute and relative (number of cells/mg of tissue) number of cells in original (WT, KO) and backcrossed (WTb, HZb, KOb) thymus and spleen. Data (mean ± SEM) are representative of 3 or 4 independent experiments. Unpaired t-test was used for statistical analysis. *n*=8-12 per group. *** $p < 0.001$, ** $p < 0.01$, * $p < 0.05$.

Thymus absolute weight was smaller in KO mice compared to WT, but when corrected to their smaller size they showed proportionally 2-fold bigger thymus (**Figure 4.2**). Similar results were obtained in backcrossed animals. Mutant mice showed markedly reduced absolute weight of their spleen, but relative weight is lower only for original but not backcrossed KO mice (**Figure 4.2**; 3.1 ± 0.22 for WT *vs* 2.0 ± 0.11 for KO and 2.4 ± 0.10 for WTb *vs* 2.4 ± 0.11 for KOb). Results obtained in original mice were different from that of the corresponding backcrossed group. For the thymus, this could be explained by the difference in the ratio male/female in each group. Indeed, female mice exhibited bigger thymus than male mice (data not shown). As original strain groups contained almost only male mice while a higher proportion of female were analyzed in backcrossed groups, mean thymus weights in the latter groups are bigger than in the firsts. However, spleen weights were similar whatever the gender. Thus sex ratio did not explain the difference of spleen weight between original and backcrossed animals.

Numbers of cells in cell suspensions obtained from each organ were counted in a Neubauer Chamber and divided by the organ's weight to calculate relative cellularity. No differences of absolute or relative cellularity were found in the thymus of original or backcrossed mice (**Figure 4.3**). The total number of splenic cells was lower in KO and

KOb mice compared to WT and WTb or HZb groups respectively. When normalized to the weight, the number of cells per gram of tissue was similar between normal and mutant mice. However, relative cellularity in KOb mice was smaller than in original KO mice (**Figure 4.3**).

In conclusion, thymus in *Ghrh*$^{-/-}$ mice was not reduced in parallel to the total body weight and was therefore proportionally bigger than in normal-sized animals, with no differences in the number of cells. On the opposite, the spleen in dwarf animals was either smaller (in original groups) or equal (in backcrossed groups) to that in normal mice, but with comparable relative cellularity.

4.1.2 Thymus phenotype

Characterization of the thymus was first assessed by controlling thymocyte distribution by flow cytometry. Gating strategy is shown in **Figure 4.4** and results in **Figure 4.5**. No statistical difference was obtained between original WT and KO mice, although DN subset tended to be lower in KO mice (p=0.0725). KOb mice had a higher proportion of DP cells (89.0% ± 0.43 *vs* 87.5% ± 0.46 and 87.3% ± 0.27) and reduced proportion of SP CD4 (6.7% ± 0.25 *vs* 7.5% ± 0.17 and 7.7% ± 0.17) compared to WTb and HZb. They also showed a tendency to DN diminution (p=0.0515). They were no difference in the percentage of intrathymic Treg cells (around 4% in all groups). Comparison between original and backcrossed groups showed that the percentage of DN was higher in WT than in WTb, while other parameters were similar. Original KO mice had a decreased percentage of DP and an increased percentage of SP CD4 compared to KOb mice. The number of cells was calculated for each sample by multiplying the number of cells/µl recorded by the FACS by the dilution factor applied to the analyzed cell suspension. Unfortunately, results were hardly interpretable because of a huge distribution of results (standard deviation above $2x10^7$ cells for total thymocyte number, data not shown)[ii].

[ii] In addition, an important lack of data occurs, due to an unknown error of the FACS device that was unable to record the volume of cells analyzed for some sample (almost one out of two data are missing).

Altogether, this data demonstrated that distribution of the four developmental stages of thymocytes is almost unaffected in *Ghrh*$^{-/-}$ mice, despite a trend toward a slight DN diminution and a significant 2% increase and 1% decrease of DP and SP CD4 subpopulations, respectively.

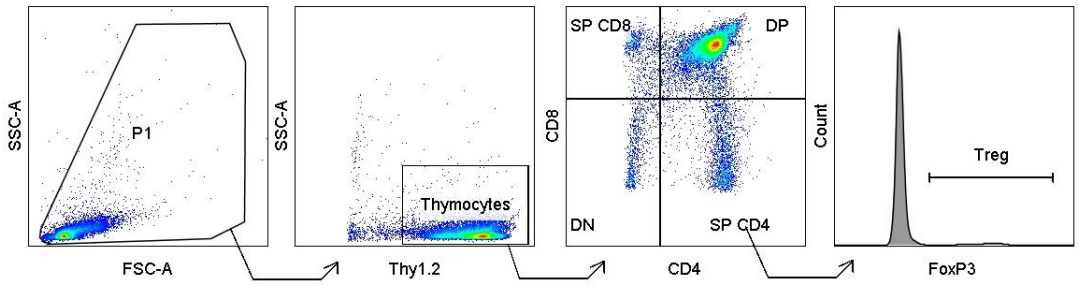

Figure 4.4 – Gating strategy for thymus flow cytometry. 500,000 cells were labeled and analyzed on FACS Verse. Debris and dead cells were excluded in function of their SSC-A/FSC-A profile (P1) and Thy1.2^{+} thymocytes were selected. Four thymocyte sub-populations were distinguished according to their expression of CD4 and CD8: DN CD4^{-}CD8^{-}; DP CD4^{+}CD8^{+}; SP CD4 CD4^{+}CD8^{-} and SP CD8 CD4^{-}CD8^{+}. Treg FoxP3^{+} cells were found amongst the SP CD4 population. 30,000 events were recorded.

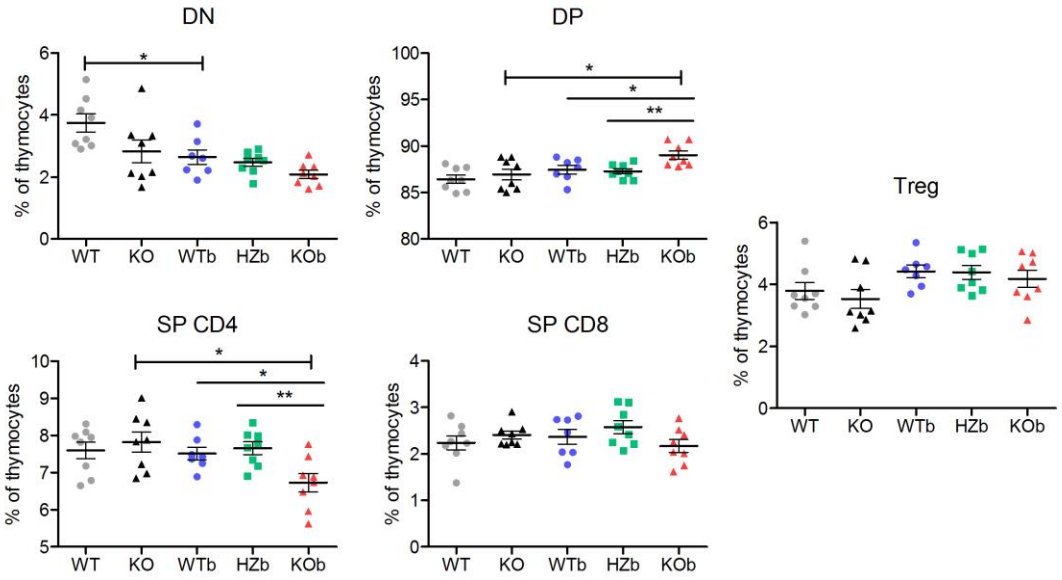

Figure 4.5 – Thymocyte distribution. Percentage of DN, DP, SP CD4, SP CD8 and Treg thymocytes analyzed in the thymus of original (WT, KO) and backcrossed (WTb, HZb, KOb) mice. Data (mean ± SEM) are representative of 3 independent experiments. Unpaired t-test was used for statistical analysis. *n*=8 per group. ** $p < 0.01$, * $p < 0.05$.

4.1.3 Thymus function

Thymus characterization was further assessed by the quantification of TRECs, markers of thymopoiesis. TRECs were measured peripherally in the splenocytes. Number of sjTRECs/10^6 cells was higher in mutant mice compared to normal-sized mice, both in original and backcrossed groups. KO mice also had a higher number of dβTRECs, but in backcrossed mice the increase was significant only compared to HZb and not WTb mice. The sj/Dβ ratio was reduced in WT mice compared to KO (127.7 ± 13.92 in WT *vs* 62.3 ± 6.83 in KO), while backcrossed groups showed similar ratios (**Figure 4.6**). The discrepancy of results between original and backcrossed groups was explained by the high difference obtained between WT and WTb groups for sjTRECs (18960 ± 1026 for WT *vs* 34106 ± 2966 for WTb), dβTRECs (166.1 ± 20.94 for WT *vs* 767.5 ± 34.85 for WTb) and the ratio (127.7 ± 13.92 for WT *vs* 44.8 ± 4.06 for WTb).

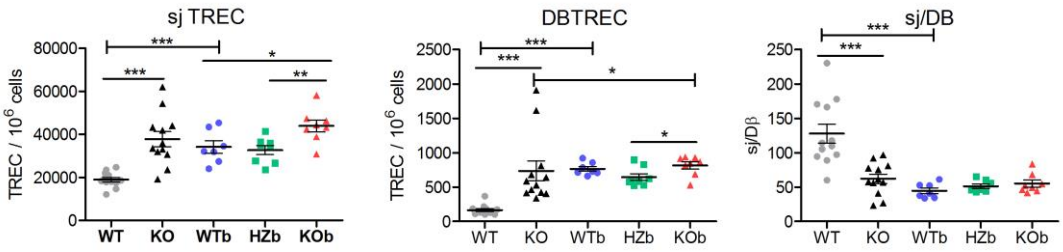

Figure 4.6 – Quantification of TRECs as markers of thymopoiesis. The number/10^6 cells of sjTRECs, DβTRECs and sj/Dβ ratio were quantified in splenocytes of original (WT, KO) and backcrossed (WTb, HZb, KOb) mice. Data (mean ± SEM) are representative of 3 independent experiments. Unpaired t-test was used for statistical analysis. *n*=8-12 per group. *** $p < 0.001$, ** $p < 0.01$, * $p < 0.05$.

Those results indicated that *Ghrh*$^{-/-}$ mice have a higher thymic export, since sjTREC are markers of naïve T cells leaving the thymus; and possibly have a reduced intrathymic proliferation, as assessed by the sj/Dβ ratio. Two hypotheses could explain those apparently contradictory results. First, a higher export of naïve cells with decreased or equal intrathymic proliferation could happen if more progenitors infiltrated the thymus. Keeping in mind that TREC numbers are influenced by cell proliferation, a second and non-exclusive explanation is that *Ghrh*$^{-/-}$ T cells proliferate less in periphery than WT cells, therefore diluting TREC to a lesser extent. This latter hypothesis was tested by measuring T-cell proliferation in the spleen of WT and KO mice with anti-Ki67 labeling. As shown in **Figure 4.7**, no difference in the proportion of proliferative cells was observed between WT and KO mice for T-cell population. Inside this population, CD4 T-

cell proliferation was also similar but CD8 T cells proliferated less in KO mice (10.9 ± 0.65% for KO *vs* 13.5 ± 0.62% for WT). On the opposite, B cells proliferated more in KO mice compared to WT mice. Comparable results were obtained in PBMCs (data not shown). The overall global mean of lymphocytes proliferation showed a higher percentage of Ki67^{+} cells in KO compared to WT mice (data not shown). Therefore, those results invalidated the hypothesis of a reduced cell proliferation to explain the increase in TREC numbers of *Ghrh*$^{-/-}$ mice.

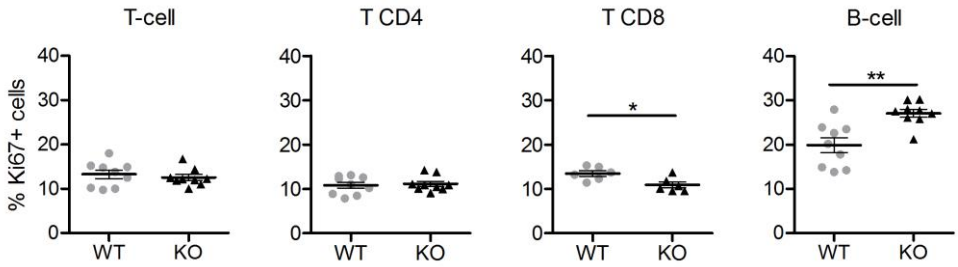

Figure 4.7 – *In-vivo* T-cell proliferation. Proportion of Ki67^{+} proliferative cells were analyzed by flow cytometry amongst T-cell (CD3^{+}), T CD4 (CD3^{+}CD4^{+}), T CD8 (CD3^{+}CD8^{+}) and B-cell (CD19^{+}) populations from spleen cell suspensions of original (WT, KO) mice. Data (mean ± SEM) are representative of 3 independent experiments. Unpaired t-test was used for statistical analysis. *n*=6 per group. * $p < 0.05$.

4.1.4 Spleen phenotype

The immune system was next investigated by analyzing peripheral distribution of mature lymphocytes. The spleen was chosen as a representative peripheral lymphoid organ. Gating strategies for flow cytometry analyses of B and T lymphocytes and of Treg cells are shown in **Figure 4.8 A and B** respectively. Results showed that KO mice exhibited a decreased proportion of B cells and an increased proportion of T cells (around 5% for both differences), while percentages of CD4, CD8 and Treg cells were comparable to WT mice (**Figure 4.9**). The same conclusions were obtained in backcrossed animals, with an even higher difference (around 8%) of B and T cells proportions between HZb and WTb mice. In order to verify if this difference in proportion was due to a change in the number of B cells, T cells or both, total numbers of B and T lymphocytes were calculated, using two different methods. First method was based on the number of cells/µl recorded with the FACS Verse, which is multiplied by the total volume of labeled cells and by the dilution factor applied to the cell suspension before antibodies labeling. The second method consisted of reporting the percentage of total events for B and T cells to

the total number of splenic cells counted with Neubauer chambers. Numbers of cells were then normalized per mg of tissue to take into account the smaller size of spleen in dwarf mice. Both methods had some disadvantages: with the first method, some data were lost because of the inability of the FACS device to record volume of the cell suspension analyzed. The second method was influenced by the proportion of debris and dead cells in the cell suspension analyzed by flow cytometry, which could strongly vary from one sample to another. As cell number was calculated from the percentage of B and T cell amongst total events analyzed, they were reduced if the number of debris and dead cells was higher. Results shown in **Figure 4.10** reveal that in original groups, B and T cells numbers per mg of spleen were reduced in KO compared to WT mice. In backcrossed groups, the dispersion of results was too important to distinguish any differences in the number of cells. The two methods of calculation seemed comparable, since they gave similar results. Unfortunately, this investigation did not allow understanding of how the number of B and T cells varied to give rise the observed differences in their proportions.

To investigate the naïve and memory profile of T lymphocytes, cells were labeled with anti-CD44 and anti-CD69 antibodies. CD44 is a marker of activation, while CD62L is an adhesion molecule expressed on naïve cells. Therefore, naïve T cells express high level of CD62L and low level of CD44 while T effector memory cells (TEM) have the opposite profile ($CD44^{hi}$ $CD62^{low}$). An intermediate population expressing both CD44 and CD62L represents T central memory cells (TCM), a memory cell population found in peripheral lymphoid organs. As shown in **Figure 4.9**, KO mice had a higher proportion of naïve T-cells and decreased proportion of TCM for both CD4 and CD8 populations (the difference reached 20% in CD4 and 15% in CD8 T cells) compared to WT controls. A similar increase of naïve cells proportion was observed in KOb mice, but the memory pool diminution was distributed between both memory subsets in CD8 T-cells and only in TEM in CD4 population. Nonetheless, both original and backcrossed groups revealed that *Ghrh*$^{-/-}$ mice exhibit a higher proportion of naïve T cells at the cost of memory T cells, which was consistent with the higher number of TRECs observed in those mice.

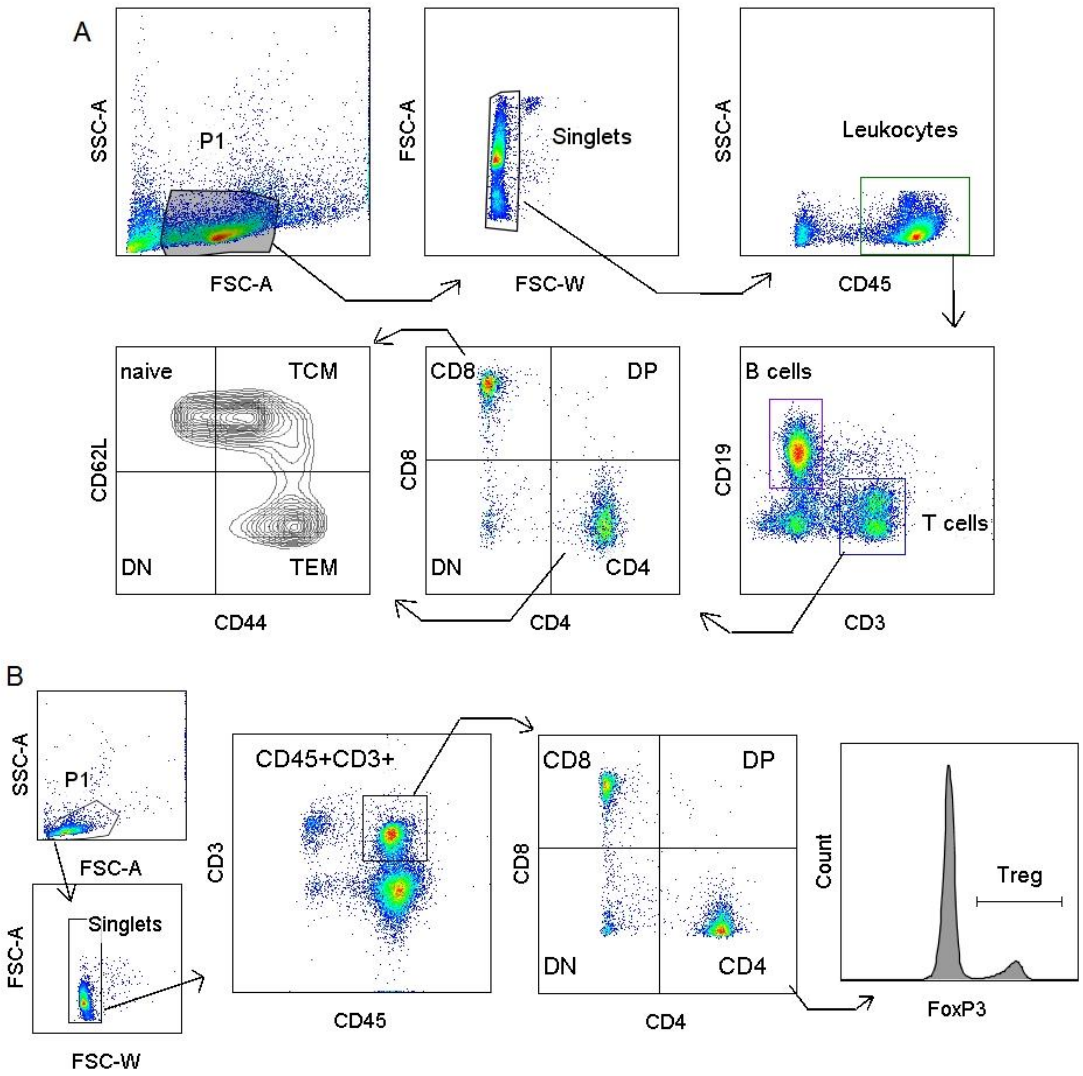

Figure 4.8 – Gating strategy for flow cytometry of peripheral lymphocytes. 500,000 cells were labeled and analyzed on FACS Verse. Debris and dead cells were excluded in function of their SSC-A/FSC-A profile (P1) and single cells were selected by FSC-A/FSC-W gating. (**A**) B-T analysis in periphery. 20,000 $CD45^+$ events were recorded. $CD3^+$ T cells and $CD19^+$ B cells were distinguished amongst the $CD45^+$ leukocytes population. T cells were next divided into $CD4^+$ and $CD8^+$ subsets. Finally, naïve ($CD44^{low}CD62L^{hi}$), central memory (TCM; $CD44^{hi}CD62L^{hi}$) and effector memory (TEM; $CD44^{hi}$ $CD62^{low}$) T cells were analyzed within de $CD3^+CD4^+$ or $CD3^+CD8^+$ populations. (**B**) Treg analysis in periphery. 20,000 $CD45^+$ events were recorded. T cells were gated as $CD45^+CD3^+$ cells and then divided into $CD4^+$ and $CD8^+$ cells. $FoxP3^+$ Treg cells were analyzed within the $CD4^+$ subset.

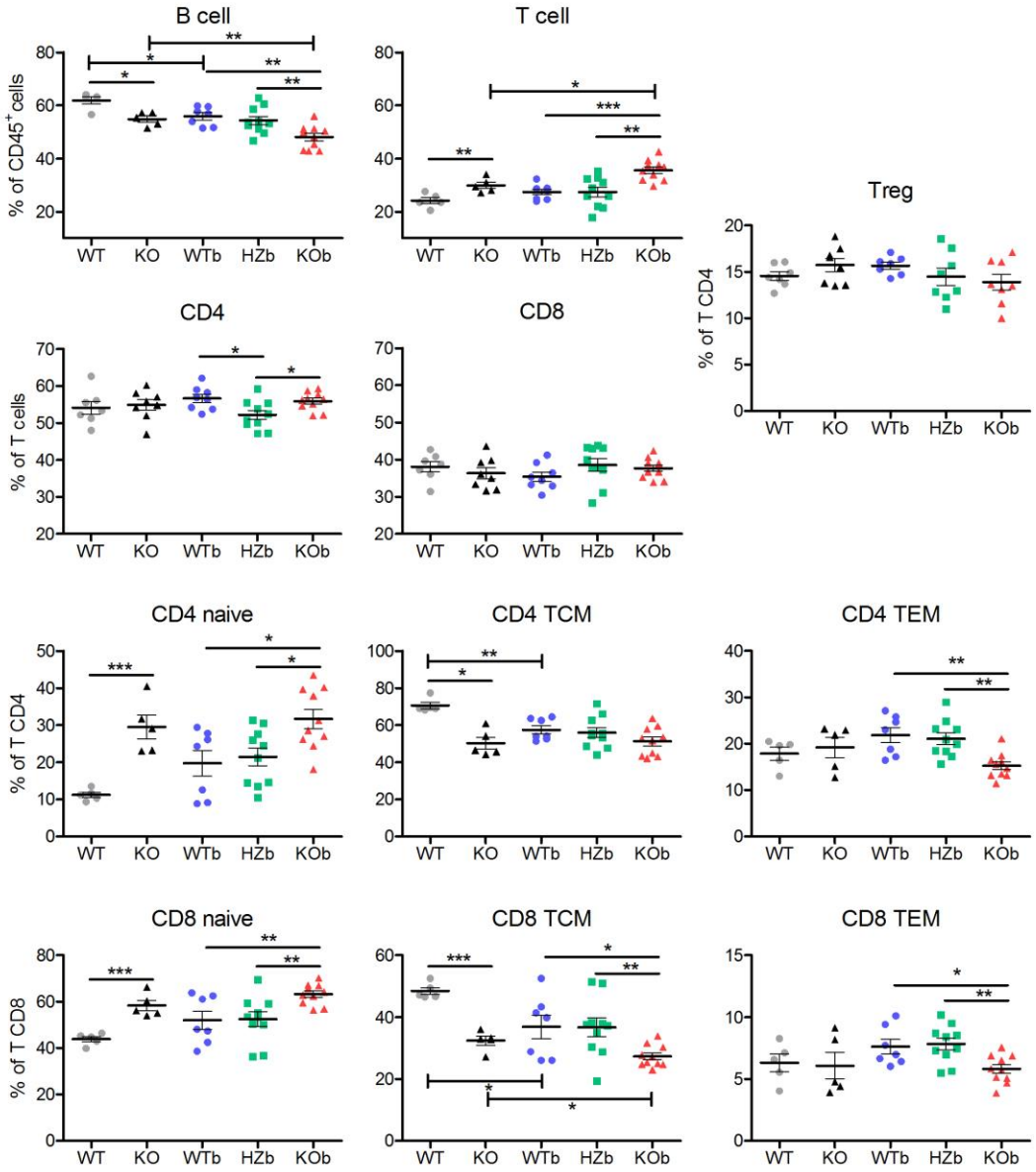

Figure 4.9 – Lymphocyte distribution in the spleen. Percentage of B and T cells amongst leukocytes; CD4 T and CD8 T amongst T cells; Treg cells amongst CD4 T cells. The naïve-memory profile of CD4 or CD8 T-cell populations were analyzed in the spleen of original (WT, KO) and backcrossed (WTb, HZb, KOb) mice. Data (mean ± SEM) are representative of 3 independent experiments. Unpaired t-test or Mann Whitney test were used for statistical analysis, according to the Gaussian distribution of each group. *n*=5-8 in original and 7-10 per group in backcrossed groups. *** $p < 0.001$, ** $p < 0.01$, * $p < 0.05$.

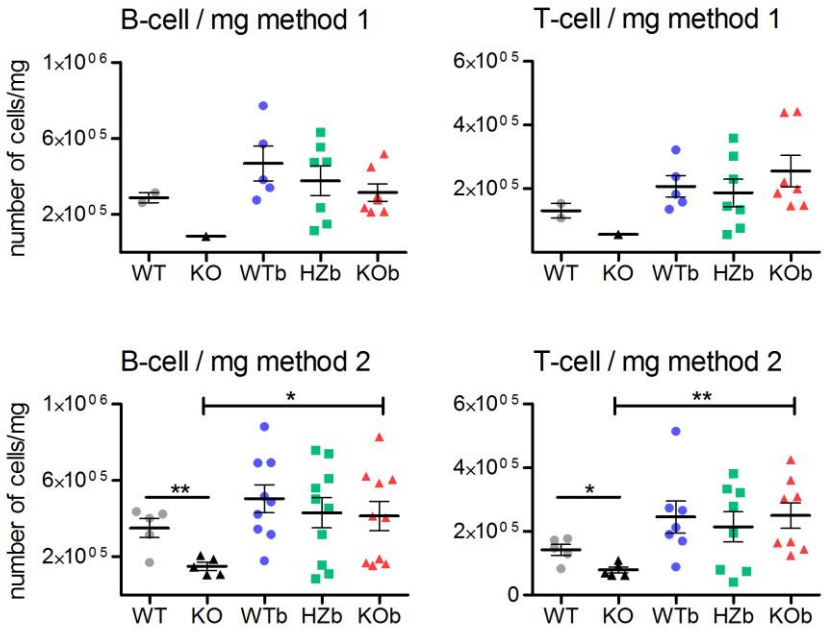

Figure 4.10 – Relative numbers of B and T splenocytes calculated by two methods. Number of B and T lymphocytes per mg of spleen in original (WT, KO) and backcrossed (WTb, HZb, KOb) mice were calculated from FACS Verse counts multiplied by the total volume of labeled cells and the dilution factor (Method 1) or from Neubauer counts of total cellularity divided by the percentage of B and T cells from total events (Method 2). Data (mean ± SEM) are representative of 2 or 3 independent experiments. Unpaired t-test or Mann Whitney test were used for statistical analysis, according to the Gaussian distribution of each group. *n*=4-5 in original and 5-10 per group in backcrossed groups. ** $p < 0.01$, * $p < 0.05$.

4.1.5 B lymphopoiesis

In order to analyze if the peripheral B-cell defect observed in *Ghrh*$^{-/-}$ mice resulted from a problem in B-cell development in the bone marrow, B lymphopoiesis was investigated by flow cytometry. B-lineage committed cells expressed B220. Four developmental stages were distinguishable (**Figure 4.11**): PreProB (CD43^{+} CD19^{-} IgM^{-}), ProB (CD43^{+} CD19^{+} IgM^{-}), PreB (CD43^{-} CD19^{+} IgM^{-}) and immature B cells (CD19^{+}IgM^{+}). As shown in **Figure 4.12**, KOb mice had an almost two-fold higher proportion of B-committed B220^{+} cells compared to WTb or HZb animals. In addition, the percentage of PreProB and ProB was significantly reduced in KOb compared to WTb while the percentage of PreB tended to increase (p=0.0611). However, immature B proportion was similar between the three groups. Therefore, B lymphopoiesis seemed to be not deficient and those results could not explain the decreased proportion observed in peripheral B cells.

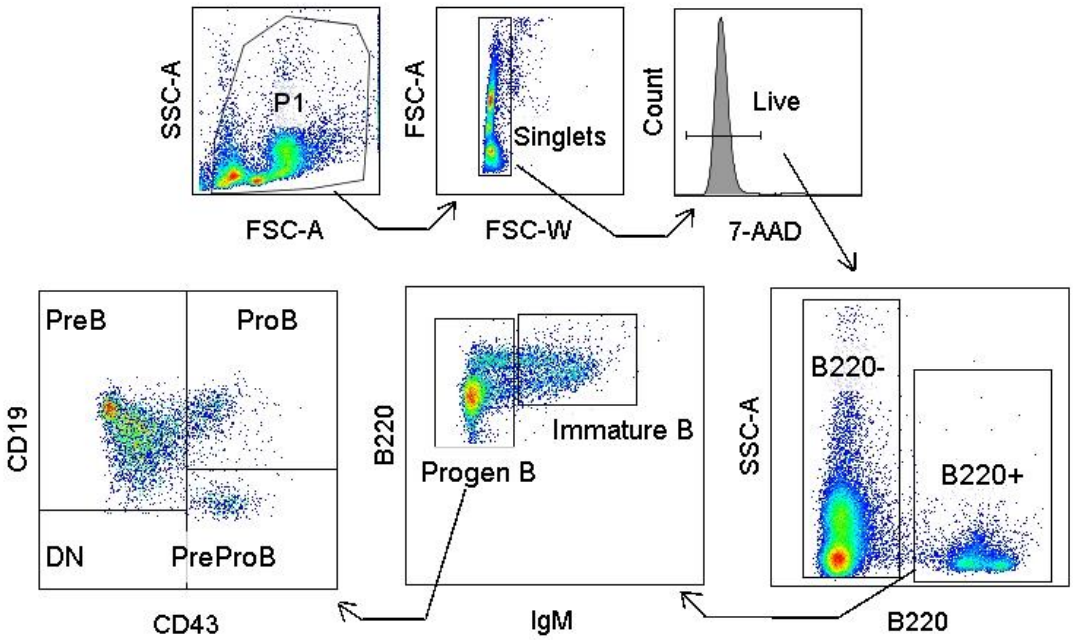

Figure 4.11 – Gating strategy for flow cytometry of B lymphopoiesis in bone marrow. 500,000 cells were labeled and analyzed on FACS Verse. Debris and dead cells were excluded in function of their SSC-A/FSC-A profile (P1) and single cells were selected by FSC-A/FSC-W gating. 20,000 living cells (7-AAD negative) were recorded. B-lineage committed cells were gated as $B220^+$ cells. IgM expression distinguished immature B cells from earlier progenitors. Amongst IgM^- progenitors, PreProB cells ($CD43^+CD19^-$) evolved into ProB cells ($CD43^+CD19^+$) that further differentiate into PreB cells ($CD43^-CD19^+$).

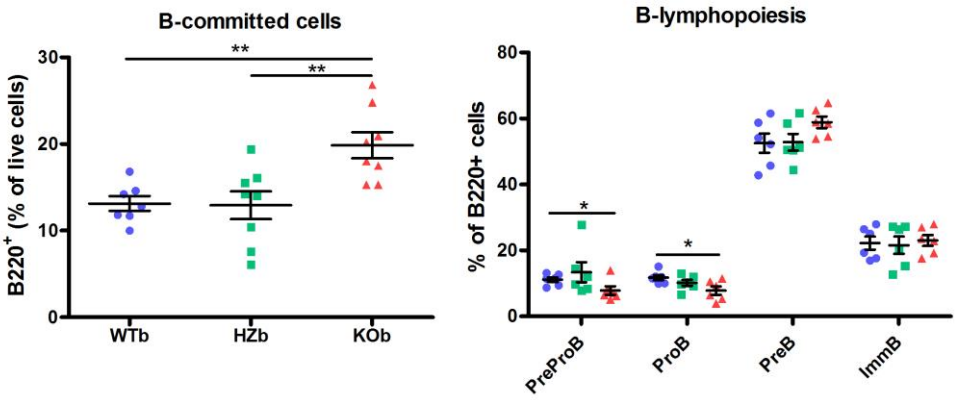

Figure 4.12 – B lymphopoiesis in bone marrow. The percentage of B-committed cells amongst living cells (left panel) and the proportion amongst $B220^+$ population of the four developmental stages of B-cell development (right panel) were analyzed by flow cytometry in the bone marrow of backcrossed (WTb blue circle, HZb green square, KOb red triangle) mice. Data (mean ± SEM) are representative of 3 independent experiments. Unpaired t-test was used for statistical analysis. *n*=7-8 per group. ** $p < 0.01$, * $p < 0.05$.

4.1.6 *In vitro* T- and B-cell function

Following adequate stimulation, activated lymphocytes starts to clonally proliferate. Ability of T and B cells to respond to non-antigen-specific stimulation was tested *in vitro*. After MACS separation, isolated T and B cells were stimulated with anti-CD3/anti-CD28

antibodies or LPS respectively. After 24, 48 and 72h the activation status of cells was controlled by their expression of CD69, an early activation marker, and proliferation was followed by CFSE dilution method. Non-stimulated control cells did not proliferate nor expressed CD69 (data not shown). As illustrated in **Figure 4.13 A**, the proportion of activated $CD69^+$ cells was higher in CD3/CD28 stimulated T cells from KO mice compared to WT. Similarly, proliferation was more important in KO cells, as assessed by the smaller D0 peak (non-divided cells). The difference was significant only for T-cell proliferation after 72h (**Figure 4.13 B**). T-cell activation was higher in KO cells after 24h and then reached a plateau at 48h, where no difference with WT cells was found. After 72h, CD69 expression decreased since it is an early activation marker. The higher the activation was, the higher CD69 diminution was. In backcrossed animals, similar tendency for higher activation and proliferation of KOb T cells was observed, although without reaching statistical significance, probably because of the small number of samples analyzed (*n*=4). Comparable results were obtained regarding B-cell response after LPS-stimulation. KOb mice showed a higher proportion of $CD69^+$ cells at 24 and 48h post-stimulation and more cells had proliferated after 48h (**Figure 4.14**). IgM release in the supernatant followed the same tendency, however without reaching statistical significance. Surprisingly, the situation in HZb mice seemed intermediate between that in WTb and KOb, for both B- and T-cell responses. This suggested that carrying one mutated *Ghrh* gene is sufficient to induce enhanced *in vitro* response to stimulation. One possible explanation for this enhanced response of T lymphocytes after CD3/CD28 stimulation could be the higher proportion of naïve cells, which could be more prompted for activation than memory cells. However, $CD8^+CD44^-$ naïve cells isolated by FACS and stimulated in the same way with CD3/CD28 showed similar results to unsorted T cells, *i.e.* higher activation and proliferation of KO cells (data not shown). Finally, GH or IGF-1 treatment (10 and 100nM) was unable to reduce response of KO T cells to a level comparable to that in WT cells (data not shown). Therefore, the mechanism responsible for the difference in response was independent of the GH/IGF-1 local environment.

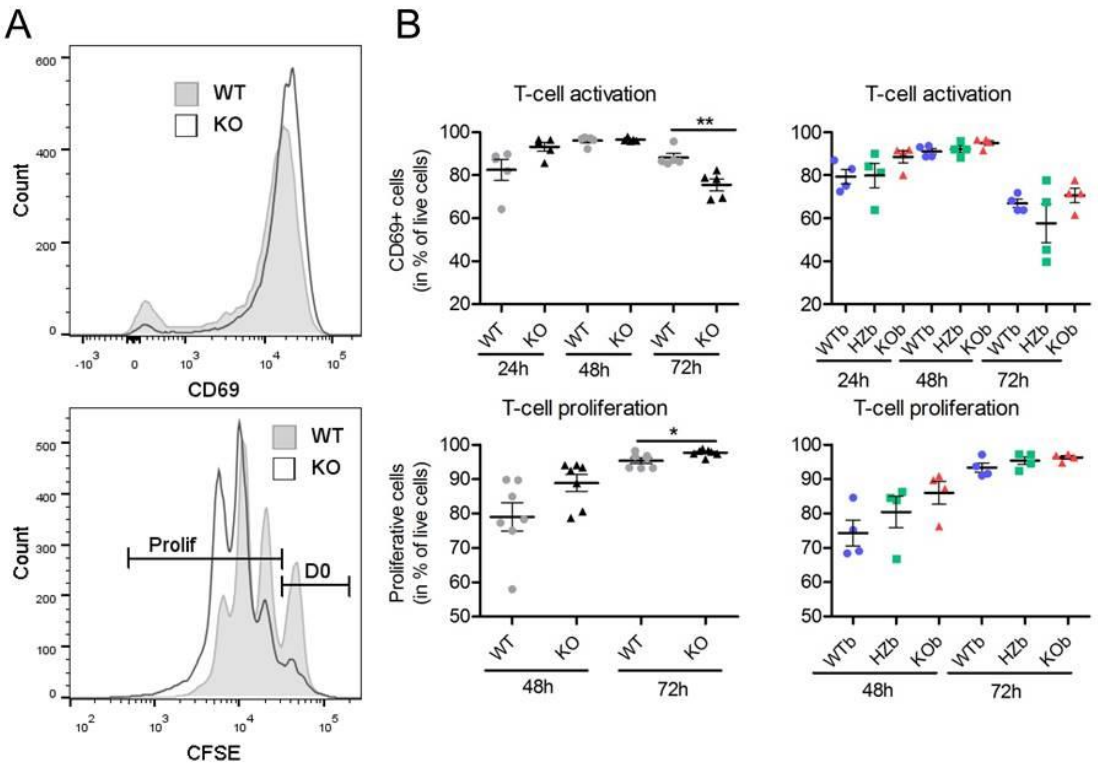

Figure 4.13 – T-cell activation and proliferation after *in vitro* stimulation. T cells from original (WT, KO) and backcrossed (WTb, HZb, KOb) spleen cell suspensions were isolated by MACS separation and 100,000 cells were stimulated *in vitro* with anti-CD3/anti-CD28. (**A**) Representative graphs of CD69 expression by T-cells after 24h of culture and CFSE dilution after 48h of stimulation. The D0 peak represents cells that have not proliferated and the rest are proliferative cells where each peak counts for one division cycle. (**B**) Activation (%CD69$^+$ cells) and proliferation (% of non-D0 cells) of T cells after 24, 48 or 72h of stimulation. Data (mean ± SEM) are representative of 2 or 3 independent experiments. Unpaired t-test was used for statistical analysis. *n*=7 per group for original and 4 per group for backcrossed. ** $p < 0.01$, * $p < 0.05$.

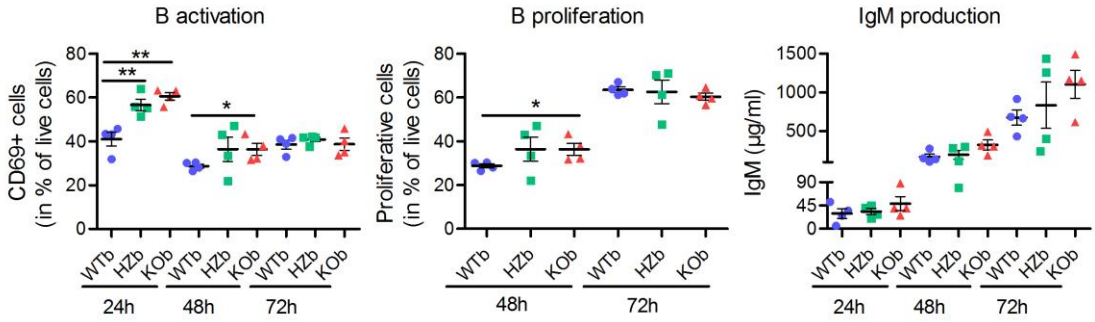

Figure 4.14 – B-cell activation and proliferation after *in vitro* stimulation. B cells from backcrossed (WTb, HZb, KOb) spleen cell suspensions were isolated by MACS separation and 100,000 cells were stimulated *in vitro* with LPS. Activation (%CD69$^+$ cells), proliferation (% of non-D0 cells) and IgM production in the supernatant of B cells were analyzed after 24, 48 or 72h of stimulation. Data (mean ± SEM) are representative of 2 independent experiments. Unpaired t-test was used for statistical analysis. *n*=4 per group ** $p < 0.01$, * $p < 0.05$.

4.1.7 Conclusions

The first objective of this part was to characterize immune system of *Ghrh*$^{-/-}$ mice to evaluate if they present any immunodeficiency or immune defect due to a severe deficiency of the somatotrope GHRH/GH/IGF-1 axis. Mutant mice did not exhibit thymic atrophy but possibly some slight splenic atrophy compared to non-GH deficient animals. Their thymus presented only modest alterations of thymopoiesis, with a 2% increase of DP cells, a parallel decrease of SP CD4 cells and a trend for DN diminution. In addition, markers of thymic export (sjTREC) were more abundant in peripheral lymphocytes, while intrathymic proliferation (assessed by the sj/DβTREC ratio) was equal or decreased. Since the hypothesis of reduced peripheral proliferation to explain the higher TREC number was excluded by Ki67 proliferation analysis, those results suggest that thymopoiesis in *Ghrh*$^{-/-}$ mice is enhanced, either by increased influx of progenitors into the thymus, faster commitment of DN to DP stages (as suggested by the decrease in DN and increase in DP percentages) and/or decreased apoptosis of thymocytes. Enhancement of thymopoiesis in *Ghrh*$^{-/-}$ mice is consistent with the higher proportion of naïve T cells observed in their spleen. In addition, lymphocyte distribution in the spleen was also disturbed in *Ghrh*$^{-/-}$ mice, with an approximately 5-8% decrease in B cells and inversely an increase in T-cell proportion, leading to a lower B/T ratio. It is still unclear if this alteration resulted from a defect in B-cell number, increase in T-cell count or both. Indeed, the two counting methods used to calculate B- and T-cell cellularity were not reliable enough to obtain solid results. Nevertheless, it appeared that B-cell diminution did not find its origin in B-cell development in the bone marrow, since the proportion of immature B-cells ready to be exported to the periphery was not different between normal and deficient mice. Furthermore, B-committed lineage cells were even more abundant in *Ghrh*$^{-/-}$ bone marrow than in WT mice. Surprisingly, peripheral mature B cells proliferated more in mutant mice, which might be a compensatory mechanism to restore B-cell population to a normal level. Altogether, those results did not allow understanding of the exact mechanism underlying the diminution of B/T ratio in *Ghrh*$^{-/-}$ mice. We postulate that improved thymopoiesis in *Ghrh*$^{-/-}$ mice resulted in the release of more T-cells in periphery, therefore shrinking B-cell proportion. However, a diminution

in B-cell number cannot be excluded based on available data, even though the origin of this diminution remains unknown.

Finally, B- and T-cell response to *in vitro* non-specific stimulation was functional in *Ghrh*$^{-/-}$ mice. Maximal levels of activation and proliferation were similar in normal and mutant mice (more than 90% of T-cells were activated and proliferated), but it seems that they occurred more rapidly in the latter. Acceleration of the time-response curve should be confirmed by analyzing CD69 expression and CFSE dilution each 12 hours after stimulation.

In conclusion, characterization of the immune system of *Ghrh*$^{-/-}$ mice at 3mo reveals that mutant mice do not exhibit any immunodeficiency and rather present an improved thymopoiesis, as well as cellular and humoral *in vitro* responses. **Therefore, it seems that a functional somatotrope axis is not required for the normal development of the immune system, at least regarding the adaptive arm.**

A second objective of this part of the work was to validate the use of *Ghrh*$^{-/-}$ and C57Bl/6J colonies from the University of Liège to perform my work. *Ghrh*$^{-/-}$ mice are on a C57Bl/6J genetic background, with a small participation of 129SV genome coming from embryonic stem cells, notably responsible of the agouti color [47]. Moreover, *Ghrh*$^{-/-}$ mice originated from the United States, while our C57Bl/6J mice have been bred in the animal facility of the University of Liège for many years. Therefore, some genetic drift could have occurred in one or the other colony. To evaluate this possibility and the impact of 129SV genome in *Ghrh*$^{-/-}$ background, the immune system of the two original colonies were analyzed in parallel to backcrossed WT, HZ and KO mice carrying identical genetic background. The mean of certain parameters was different between original and corresponding backcrossed group. This could be attributed to experimental bias since experiments were not conducted in the same period. All backcrossed experiments were conducted within one month while original groups were analyzed over 4 months almost one-year away from backcrossed groups. Despite all our efforts to minimize experimental variations, we could not exclude uncontrolled changes in housing conditions, lot products, devices calibration or manipulator skills over this long time-period. However, globally the same differences were found in WT *vs* KO and in WTb *vs*

KOb mice — *i.e.* increased relative thymic weight, higher TREC number and proportion of naïve T cells, lower B/T ratio and improved *in vitro* T-cell response — therefore validating the WT-KO model in original colonies. In the next part of this work, only original WT and KO mice will be used, for time, costs and breeding contingencies. Indeed it is easier and faster to obtain a sufficient number of WT and KO mice from two distinct homozygous colonies than in backcrossed breeding, where theoretically only 25% of the pups inherit of +/+ or -/- genotypes. It thus requires more couples in backcross colony to obtain comparable numbers of WT and KO mice compared to homozygous breeding. In addition, this avoids the social stress of being held with normal-sized littermates for dwarf KO mice, which could induce immunological alterations [189].

4.2 Aging in *Ghrh*$^{-/-}$ mice

With aging, the immune system becomes deficient, especially in mammals, with reduced resistance to infections, decreased efficiency of vaccines, and a higher risk of cancers. This immunosenescence is characterized by a pro-inflammatory state (TNFα, IL-6), a reduced diversity of TCR repertoire, an increase in memory lymphocytes, and reduced B as well as T lymphopoiesis [198,199]. One hallmark event of immunosenescence is thymic involution: epithelial areas slowly disappear and are replaced by perivascular adipose tissues, leading to decreased thymopoiesis [101]. In addition, hormonal fluctuations also occur during aging, notably somatopause — the age-related reduction in GH and IGF-1 concentrations [200]. Some argue that somatopause is one of the events that trigger thymic involution, even though the causal link is not firmly established. Several studies in rodents showed partial rejuvenation of aged-atrophic thymus and restoration of thymopoiesis after treatment of aged animals with GH, IGF-1 or ghrelin and GHS [112,172,201–204]. Nevertheless, the role of reduced somatotrope hormones in inducing aged-related immune defects is less clear. An early thymic atrophy was observed in Snell-Bagg and Ames-Dwarf mice, partially reversible with GH treatment [109,110,159] but lit/lit mice exhibit thymus involution similar to control aged-animals [205].

Therefore, after investigating the role of the somatotrope axis upon immune system development, the second part of this work aims to evaluate the role of somatotrope hormones during immune aging. To this purpose, thymus and peripheral lymphoid organs were analyzed in young (3mo), middle-aged (6mo) and aged (18mo) WT and KO mice.

4.2.1 Evolution of weight and cellularity of lymphoid organs with aging

Thymus and spleen of mutant and control mice were weighed and the total number of cells was calculated by the FACS Verse method (see section 4.1.4) after flow cytometry analyses of cell suspensions. As shown in **Figures 4.15** and **4.16**, thymus in mutant mice were almost half the size at 3 and 6mo but, in aged mice, thymus weight was similar between WT and KO mice, because of the shrink in WT thymus weight between 6 and 18mo (almost 2.5-fold decrease), while thymus weight in KO mice was stable across

time. Similarly, the total number of cells in thymus of KO mice was lower than in WT thymus, but both mice exhibited a diminution (2.9 for WT and 3.5 times for KO) in total cellularity with age. When normalized to total body weight, thymus weight was similar between WT and KO mice at 3mo, but was significantly reduced at 6mo and inversely higher at 18mo. Both WT and KO relative thymus weight did not change between 3 and 6mo, and thymic atrophy occurred between 6 and 18mo. No difference in the number of cells per mg of thymus was observed between WT and KO mice. Diminution of relative cellularity with age happened in both WT and KO mice, but it seemed to appear as soon as 6mo in KO mice while it occurred later in WT animals. Altogether, this data suggests that thymic involution occurred a little bit earlier in mutant mice (between 3 and 6mo of age while it seemed to start after 6mo in WT animals), but with a less severe impact on the relative weight at advanced age.

Absolute and relative spleen weights were diminished in KO compared to WT mice, regardless of the age. However, only WT spleen weight increased between 3 and 18mo. Similarly, absolute number of cells in the spleen of KO mice was reduced at 3 and 6mo, while relative cellularity was not different. On the opposite, at 18mo, both absolute and relative spleen cellularity decreased in WT mice but increased in KO mice, leading to a surprising 4-fold higher number of cells/mg of spleen in aged KO compared to WT mice (**Figures 4.15** and **4.16**).

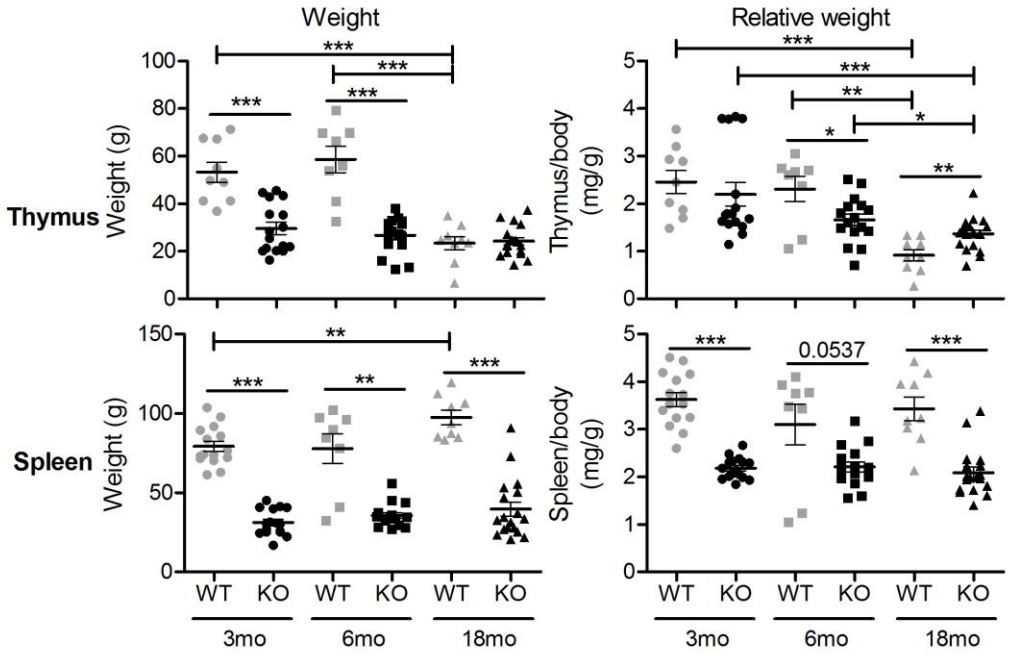

Figure 4.15 –Thymus and spleen weight. Absolute and relative (organ weight/body weight) weight of thymus and spleen of 3mo-, 6mo- and 18mo-old WT and KO mice. Data (mean ± SEM) are representative of 2 or 3 independent experiments. Unpaired t-test or Mann Whitney test were used for statistical analysis, according to the Gaussian distribution of each group. *n*=8-18 per group *** $p < 0.001$, ** $p < 0.01$, * $p < 0.05$.

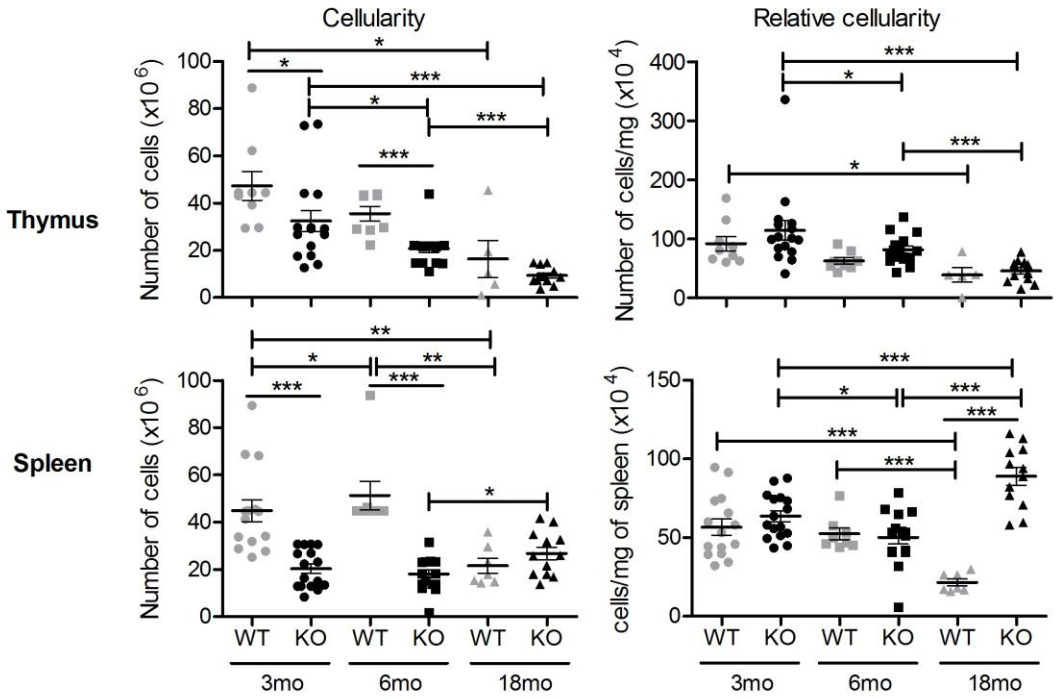

Figure 4.16 –Thymus and spleen cellularity. Absolute and relative (number of cells/mg of tissue) number of cells in the thymus and spleen of 3mo-, 6mo- and 18mo-old WT and KO mice, assessed by the FACS Verse method. Data (mean ± SEM) are representative of 2 or 3 independent experiments. Unpaired t-test or Mann Whitney test were used for statistical analysis, according to the Gaussian distribution of each group. *n*=5-16 per group *** $p < 0.001$, ** $p < 0.01$, * $p < 0.05$.

4.2.2 Thymus phenotype and function during aging

Flow cytometry analysis of thymic cell suspensions was performed to evaluate the distribution of the four thymic subpopulations, as well as intrathymic Treg cells. Gating strategy is shown in **Figure 4.5** and results in **Figure 4.17**. Proportion of immature DN cells was slightly decreased in 3mo- and 6mo-old KO mice compared to WT. This 1% diminution was compensated by increase of DP subset at 3mo and $CD8^+$SP population at 6mo. Furthermore DN proportion constantly increased with age in KO but not in WT mice. Percentage of $CD8^+$SP cells was reduced of around 1% in aged mice, but the diminution occurred earlier in WT than in KO mice. On the opposite, $CD4^+$SP T cells did not vary with age, except the slight decrease observed between 3 and 6mo in WT mice only. Finally, intrathymic Treg population in KO animals was slightly higher in young and aged, but not middle-aged mice compared to WT. Proportion of Treg cells increased in 18mo-old KO mice compared to younger mice.

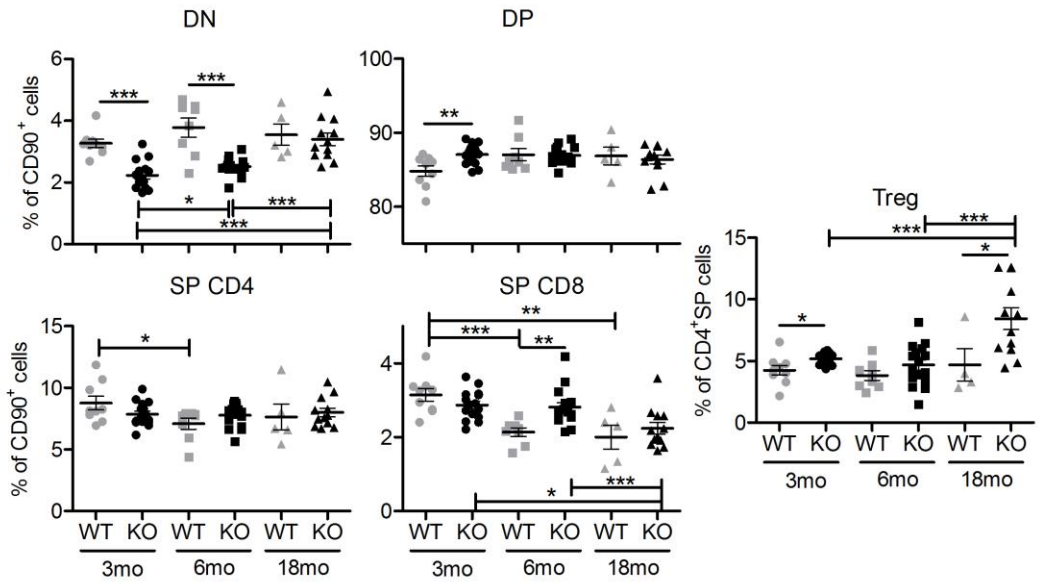

Figure 4.17 – Thymocyte distribution. Frequencies of DN, DP, SP CD4, SP CD8 and Treg thymocytes in the thymus of 3mo-, 6mo- and 18mo-old WT (*n*=5-9) and KO (*n*=12-16) mice. Data (mean ± SEM) are representative of 2 or 3 independent experiments. Unpaired t-test or Mann Whitney test were used for statistical analysis, according to the Gaussian distribution of each group. *** $p < 0.001$, ** $p < 0.01$, * $p < 0.05$.

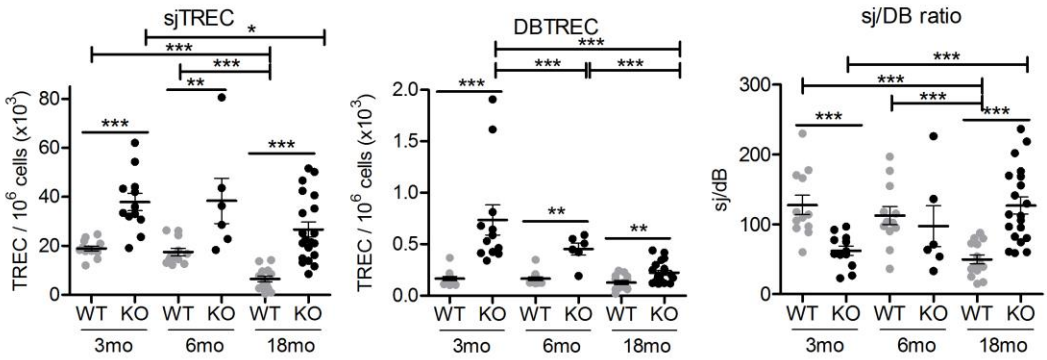

Figure 4.18 – Quantification of TREC as markers of thymopoiesis. The number/10^6 cells of sjTRECs, DβTRECs and sj/Dβ ratio were quantified in splenocytes of 3mo-, 6mo- and 18mo-old WT (*n*=12-14) and KO (*n*=6-20) mice. Data (mean ± SEM) are representative of 3 independent experiments, except for KO 6mo where only one experiment was performed. Unpaired t-test or Mann Whitney test were used for statistical analysis, according to the Gaussian distribution of each group. *** $p < 0.001$, ** $p < 0.01$, * $p < 0.05$.

Thymopoiesis was then assessed by quantification of TRECs in splenocytes[iii]. Results presented on **Figure 4.18** confirmed the increase of sj and DβTRECs in KO mice compared to WT animals throughout life. The sj/Dβ ratio was lower in 3mo-old KO mice than in age-matched WT, but it was equal at 6mo and higher at 18mo. Aging induced a decrease in the number of sjTRECs in both WT and KO mice after 6mo. DβTREC number was also lower at each time in KO mice, while it was stable in WT animals. Therefore, in WT mice where sj but not DβTRECs were reduced with time, the sj/Dβ ratio was lower in aged mice compared to young or middle-aged WT animals. On the opposite, KO mice presented an increase in sj/Dβ ratio between 3 and 18mo because the diminution of DβTRECs was more pronounced than for sjTREC (4-fold decrease *vs* one third respectively). Taken together, those results indicate that in WT normal mice, aging induced a decrease in intrathymic proliferation and in thymic export, revealing a reduced efficiency of thymopoiesis after the DN stage (since DβTRECs are created in DN2 cells). The situation in mutant mice seemed different. The number of early DβTRECs diminished with age and this was probably compensated by an increased intrathymic proliferation between DN and DP stages, that could explain the slight increase in DN

[iii] It should be noticed that the 18mo-old WT and KO groups presented here corresponded to the basal data of the groups of the GH supplementation experiment analyzed two weeks before starting GH treatment (see chapter 4.3). Unfortunatley, we were unable to quantifiy TRECs of the aged groups normally used in this part because of the lack of available biological material.

proportion seen with time. The compensation was not sufficient since thymic export was still reduced in aged mice.

4.2.3 Peripheral lymphocyte variation with age

Next, the peripheral distribution of lymphocytes was studied across time in spleen, lymph nodes and blood of WT and KO mice (see gating strategy **Figure 4.8**). Mutant mice showed a higher T-cell frequency and lower B-cell frequency compared to WT mice in the three organs at the three ages analyzed, even though statistical significance was not reached in the blood of 3mo- and 6mo-old mice (**Table 4.1**). Aging had almost no impact upon B- and T-cell distribution in mutant mice, except an increase in blood B-cell frequency and a decrease in splenic T-cell frequency in 18mo-old KO mice. Similar increased B-cell and decreased T-cell frequency was found in LN and blood but not in the spleen of 18mo-old WT mice. Comparison of CD4 and CD8 T-cell distribution between WT and KO mice revealed more disparate results: there was either no difference or higher CD4 (LN at all ages, blood 18mo) and lower CD8 (LN at all ages, blood 3mo and 18mo, spleen 18mo) proportion in function of age and organ studied (**Table 4.1**). Unexpectedly, the inverse result (lower CD4 and higher CD8 frequencies) occurred in the spleen of 6mo-old KO mice, but the difference was slight (around 3%), therefore suggesting rather a stochastic result. Effect of aging upon CD4-CD8 distribution was also heterogeneous: percentage of CD4 decreased in LN and blood of aged WT and KO mice while CD8 proportion increased in LN and blood of WT mice only, and decreased in spleen of aged KO mice. Consequently, the CD4/CD8 ratio decreased in LN and blood of both mice (for example in LN: 1.2 ± 0.04 at 3mo *vs* 0.9 ± 0.04 at 18mo in WT and 1.5 ± 0.08 at 3mo *vs* 1.2 ± 0.08 at 18mo in KO mice, data not shown). Finally, Treg cells frequency was not different between WT and KO mice, besides the slight increase in spleen of 3mo-old KO mice. In both mice, Treg frequency increased with aging in the three lymphoid organs.

Study of the evolution of naive and memory of T-cells across time in peripheral organ of WT and KO mice is described in **Table 4.2**. Despite some exceptions, KO mice exhibited a bigger pool of naïve cells than WT, lower proportion of TCM and normal TEM, for both CD4 and CD8 T cells, whatever the organ or age. As expected, aging was accompanied by

a decrease in the pool of naïve cells and an increase in memory cells in the spleen and LN of WT and KO mice. Results were more heterogeneous in the blood (see **Table 4.2**). Within the memory pool, CD4 and CD8 TEM were markedly increased at 18 months. CD8 TCM also increased while CD4 TCM were reduced, already at 6 months of age.

Table 4.1. Lymphocyte subpopulations in peripheral lymphoid organs of 3mo-, 6mo- and 18mo-old WT and KO mice.

Frequency (% of parent population)	3mo		6mo		18mo	
	C57BL/6J WT (n = 15)[3]	*Ghrh*$^{-/-}$ KO (n = 16)[3]	C57BL/6J WT (n = 8)[2]	*Ghrh*$^{-/-}$ KO (n = 16)[3]	C57BL/6J WT (n = 9)[3]	*Ghrh*$^{-/-}$ KO (n = 12)[2]
Spleen						
B-cell	60.0 ± 1.36	52.5 ± 1.18 ***	61.4 ± 0.85	51.7 ± 1.06 ***	61.9 ± 1.67	54.1 ± 1.46 **
T-cell	30.6 ± 1.23	35.5 ± 1.17 **	28.9 ± 1.25	33.9 ± 1.41 *	28.3 ± 1.84	30.2 ± 1.29 aaa
T CD8	36.7 ± 0.61	36.9 ± 1.08	36.0 ± 0.67	38.8 ± 0.81 *	37.1 ± 0.93	30.5 ± 1.76 ** aa, bbb
T CD4	57.4 ± 0.66	56.2 ± 1.04	57.0 ± 0.40	54.3 ± 0.86 *	55.7 ± 1.08	58.5 ± 1.93 b
Treg	14.0 ± 0.38	17.3 ± 0.60 ***	17.9 ± 0.69 aaa	18.0 ± 0.61	29.3 ± 1.98 aaa, bbb	29.2 ± 2.43 aaa, bbb
Lymph node						
B-cell	33.8 ± 1.85	26.5 ± 1.56 **	39.8 ± 3.42	27.6 ± 1.94 **	53.6 ± 2.50 aaa, bb	22.9 ± 2.02***
T-cell	63.2 ± 1.82	70.1 ± 1.60 **	56.5 ± 3.43	68.2 ± 2.27 *	43.3 ± 2.66 aaa, b	67.7 ± 2.23***
T CD8	43.5 ± 0.74	39.0 ± 1.15 **	44.5 ± 0.38	40.8 ± 1.00 *	49.8 ± 1.07 aaa, bbb	41.8 ± 1.49 **
T CD4	53.1 ± 0.71	57.8 ± 1.13 **	50.4 ± 0.48 a	55.5 ± 1.05 **	42.0 ± 0.95 aaa, bbb	50.4 ± 1.48 ** aaa, bb
Treg	12.5 ± 0.53	12.5 ± 0.22	16.1 ± 0.51 aaa	16.3 ± 0.70 aaa	30.3 ± 2.13 aaa, bbb	30.7 ± 2.12 aaa, bbb
Blood						
B-cell	46.1 ± 2.65	43.3 ± 2.55	54.2 ± 3.10	43.1 ± 5.39	75.7 ± 3.58 aaa, bb	54.2 ± 2.63 *** aa
T-cell	38.7 ± 1.64	30.4 ± 3.62 *	29.8 ± 3.83 a	33.3 ± 6.31	17.2 ± 2.00 aaa, b	26.9 ± 2.19 *
T CD8	42.5 ± 1.58	37.3 ± 1.43 *	44.9 ± 2.09	46.1 ± 2.95 a	58.2 ± 2.53 aaa, bb	37.5 ± 2.71 *** b
T CD4	54.9 ± 1.55	55.3 ± 0.96	52.2 ± 1.94	49.6 ± 3.53	35.5 ± 2.03 aaa, bbb	47.5 ± 2.24 ** aa
Treg	9.2 ± 0.98	8.0 ± 0.63	7.5 ± 0.90	7.8 ± 0.44	13.0 ± 0.92 a, bb	11.2 ± 1.99 b

Data (mean ± SEM) are representative of two[2] or three[3] independent experiments.
Unpaired t-test or Mann-Whitney test was used according to the Gaussian distribution of each set of data.
KO mice compared to age-matched WT: *** $p < 0.001$, ** $p < 0.01$, * $p < 0.05$.
Comparison of 6mo or 18mo vs 3mo (a) and 18mo vs 6mo (b) within the same strain: aaa, bbb: $p < 0.001$; aa, bb: $p < 0.01$; a, b: $p < 0.05$

Table 4.2. Naïve and memory T-cell distribution in peripheral lymphoid organs of 3mo-, 6mo- and 18mo-old WT and KO mice.

Frequency (% of parent population)	3mo		6mo		18mo	
	C57BL/6J WT (n = 15)[3]	*Ghrh*$^{-/-}$ KO (n = 16)[3]	C57BL/6J WT (n = 8)[2]	*Ghrh*$^{-/-}$ KO (n = 16)[3]	C57BL/6J WT (n = 7)[3]	*Ghrh*$^{-/-}$ KO (n = 6)[1]
Spleen						
CD4 naive	12.0 ± 0.62	29.7 ± 1.30 ***	12.1 ± 0.75	21.0 ± 1.36 *** aaa	3.4 ± 0.36 aaa, bb	9.6 ± 2.67 aaa, bbb
CD4 TCM	61.7 ± 2.20	45.6 ± 1.42 ***	52.1 ± 2.03 aa	50.7 ± 1.39 a	21.2 ± 2.57 aaa, bbb	21.5 ± 4.04 aaa, bbb
CD4 TEM	24.6 ± 1.62	23.7 ± 1.47	35.5 ± 2.08 aaa	27.9 ± 1.99 *	74.7 ± 2.60 aaa, bbb	68.5 ± 6.33 aaa, bb
CD8 naive	47.9 ± 1.05	57.5 ± 1.26 ***	47.1 ± 1.74	59.2 ± 1.55 ***	17.9 ± 2.18 aaa, bbb	29.8 ± 6.02 aaa, bbb
CD8 TCM	40.8 ± 1.31	31.0 ± 1.02 ***	42.6 ± 1.57	31.2 ± 1.48 ***	59.4 ± 3.69 aaa, bbb	44.5 ± 2.15 ** aaa, bbb
CD8 TEM	7.1 ± 0.69	7.3 ± 0.59	9.4 ± 0.57 a	7.6 ± 0.42 *	22.4 ± 2.89 aaa, bbb	24.4 ± 4.17 aaa, bbb
Lymph node						
CD4 naive	15.2 ± 0.97	35.7 ± 1.72 ***	16.6 ± 0.66	31.4 ± 1.78 ***	10.6 ± 1.33 a, b	24.5 ± 3.37 ** aa
CD4 TCM	72.1 ± 1.80	48.7 ± 1.95 ***	63.0 ± 4.68 a	54.3 ± 1.70 * a	52.9 ± 2.39 aaa	37.6 ± 3.25 ** aa, bbb
CD4 TEM	11.5 ± 0.99	13.4 ± 1.29	18.7 ± 4.17 a	13.3 ± 0.88	36.2 ± 3.01 aaa, bb	37.1 ± 5.15 aaa, bbb
CD8 naive	57.6 ± 1.19	66.4 ± 1.21 ***	59.7 ± 1.31	65.1 ± 1.51	39.5 ± 2.72 aaa, bbb	40.2 ± 4.64 aaa, bbb
CD8 TCM	37.3 ± 1.25	25.4 ± 0.84 ***	34.5 ± 1.44	28.0 ± 1.73 *	54.1 ± 2.21 aa, bb	47.5 ± 4.29 aaa, bbb
CD8 TEM	2.6 ± 0.21	2.8 ± 0.21	3.5 ± 0.27 a	3.0 ± 0.25	5.9 ± 0.81 aaa, b	9.2 ± 1.66 aaa, bbb
Blood						
CD4 naive	15.8 ± 0.88	27.1 ± 4.20 **	19.3 ± 1.93	31.9 ± 2.87 **	18.7 ± 6.06	30.6 ± 4.45
CD4 TCM	76.7 ± 1.72	36.6 ± 5.31 ***	67.3 ± 2.22 aa	49.9 ± 4.06 **	51.9 ± 5.02 aa, b	40.9 ± 4.03
CD4 TEM	6.6 ± 0.90	27.8 ± 7.45 ***	12.1 ± 1.79 aa	14.0 ± 2.83	34.9 ± 6.08 aaa, bb	28.3 ± 8.25
CD8 naive	53.4 ± 2.86	31.7 ± 6.19 **	48.6 ± 3.18	44.9 ± 4.03	32.5 ± 5.99 aa, b	38.8 ± 6.74
CD8 TCM	42.6 ± 3.00	42.8 ± 1.87	40.5 ± 2.03	41.52 ± 2.39	49.0 ± 5.05	50.5 ± 4.66
CD8 TEM	2.6 ± 0.46	17.4 ± 5.08 ***	8.4 ± 1.81	8.34 ± 1.71	20.8 ± 6.55 aaa, bbb	10.5 ± 2.94

Data (mean ± SEM) are representative of one[1], two[2] or three[3] independent experiments.
Unpaired t-test or Mann-Whitney test was used according to the Gaussian distribution of each set of data.
KO mice compared to age-matched WT: *** $p < 0.001$, ** $p < 0.01$, * $p < 0.05$.
Comparison of 6mo or 18mo vs 3mo (a) and 18mo vs 6mo (b) within the same strain: aaa, bbb: $p < 0.001$; aa, bb: $p < 0.01$; a, b: $p < 0.05$

4.2.4 Conclusions

This second part of the work aimed in investigating the impact of aging upon immune system of *Ghrh*$^{-/-}$ mice. If we assumed that somatopause was responsible for immunosenescence as some authors hypothesized, we could expect that congenital somatotrope deficiency of the *Ghrh*$^{-/-}$ mice would then accelerate immune aging.

Here we observed that *Ghrh*$^{-/-}$ mice present a slight premature thymic atrophy as demonstrated by the decrease in thymic relative weight and absolute and relative

cellularity at 6mo compared to 3mo in KO mice while, in WT mice, this decrease could only be seen at 18mo. However, the final extent of thymus involution was quite similar between normal and mutant mice.

Analysis of thymus phenotype revealed a decrease in the proportion of DN subset in young and middle-aged *Ghrh*$^{-/-}$ mice, compensated by an increase in DP cells at 3mo and CD8 SP cells at 6mo. At 18mo, mutant mice exhibited normal distribution of thymocytes, similar to that observed in normal mice. In addition, mutant mice presented a higher percentage of thymic Treg cells, which increased with age, while the proportion seemed stable in WT mice[iv]. Moreover, the observed differences in proportions of thymocyte subsets were of only 1 to 2%. Reliability and pertinence of such small differences is questionable.

TREC analysis revealed a difference in the effect of aging on thymopoiesis between normal and mutant mice. In aged WT mice, thymopoiesis was altered after the DN stages, with lower intrathymic proliferation and less naïve cells output than in young or middle-aged mice, but no difference in the number of the early dβTRECs. On the opposite, in aged KO mice, a defect in thymopoiesis was reflected by a lower number of dβTRECs, which was compensated by an increase of intrathymic proliferation, although this was unable to maintain thymic export to level similar to those in young animals. This reduction in dβTREC number could result from a quantitative defect resulting from the decline in the entry of progenitors into the thymus, and/or qualitative defect due to diminution of successful β-chain rearrangements. Both of these mechanisms have been described in mice [206,207].

Finally, age-induced changes in lymphocytes distribution in peripheral lymphoid organs were studied in mutant and *Ghrh*$^{-/-}$ mice. First, it is important to note that analysis and interpretation of so many parameters was a complex task. A statistical test with a *p-value* of 0.05 means that there was 5% risk to wrongly affirm that the difference observed is not random. So here, where multiple parameters are analyzed, there was

[iv] However, only 5 of the 9 analyzed thymi were exploitable in this group of 18mo-oldWT, due to experimental problems. Therefore, we could have missed a similar increase in thymic Treg cells of normal mice.

one chance out of 20 to obtain irrelevant statistical significance. Therefore, careful and critical interpretation should be applied. Here, only consistent repeated results were taken into consideration. A first conclusion drawn from analysis of spleen, lymph nodes and blood was that the differences observed between normal and *Ghrh*$^{-/-}$ mice at 3mo (*i.e.* lower B-cell and higher T-cell frequencies and higher proportion of naïve T cells and diminution of memory pool in KO *vs* WT mice) were maintained throughout live. Altogether, analysis did not reveal a strong differential effect of aging on peripheral lymphocytes between *Ghrh*$^{-/-}$ and normal mice. Both maintained relatively constant proportion of B and T cells and, as expected, they experienced a shift in the pool of naïve to memory T cells, within which mostly TEM were increased. Frequency of CD4 T cells decreased in the blood and LN of normal and mutant mice, but an inverted increase of CD8 frequency was observed only in WT organs. This resulted in a decreased CD4/CD8 ratio in the two compartments of the two types of aged mice, although the intensity of this decrease was more important in WT mice.

Taken together, those results highlighted a slight premature thymic involution and some differential mechanisms triggering thymopoiesis defect, but no difference was observed in peripheral immune aging. Those differences were not enough striking to declare that premature immune aging or aggravation of immunosenescence occurred in GH-deficient mice.

4.3 GH supplementation

Several studies demonstrated that GH treatment is able to restore the disturbed immune parameters found in GH-deficient mice [110,111,160,176,184], to increase thymopoiesis in normal mice [161,168], or to rejuvenate the immune system of aged rodents [112,201–203]. In order to verify if a short-term GH treatment could restore the slight differences observed in *Ghrh*$^{-/-}$ mouse (B-cell number and thymopoiesis) model, 3mo-old mice were supplemented during 6 weeks with a physiological dose of recombinant human GH or DPBS as control. Three-month old WT mice were also supplemented in order to detect a possible beneficial effect of GH treatment in non-deficient animals. Finally, aged mutant and normal mice were treated to investigate the ability of GH to improve the aging immune system.

4.3.1 Metabolic effects of GH treatment

The efficiency of GH treatment was easily controlled by studying its metabolic effects. First, weight and glycaemia of GH or control injected mice were recorded each week to control effects of GH upon growth and glucose metabolism. Results showed that daily GH treatment induced a weight gain for both young and aged WT and KO mice, even though the effect was far more important in congenitally deficient mice with a ~45% increase for 3mo and ~15% for 18mo compared to ~11 and ~7% respectively for WT mice (**Figure 4.18 A**). Moreover, GH supplementation significantly increased spleen and thymus weight in KO ($p<0.001$) but not WT mice (**Figure 4.18 B**). Basal glycaemia was lower in GH-deficient than in normal mice. It did not vary during GH treatment in WT mice, while blood glucose increased in mutant mice but remained within normal value (**Figure 4.18 A**). Finally, the expected GH stimulation of IGF-1 was controlled in the liver. Treatment induced a significant increase of *Igf1* expression in the liver of aged and young KO mice, but was ineffective in WT mice, suggesting the existence of regulatory mechanisms that ensured a constant IGF-1 level (**Figure 4.18 C**). Taken together, those results validated the metabolic efficacy of the GH supplementation in young and aged WT and mutant mice, although the effects were far more important in GH-deficient mice.

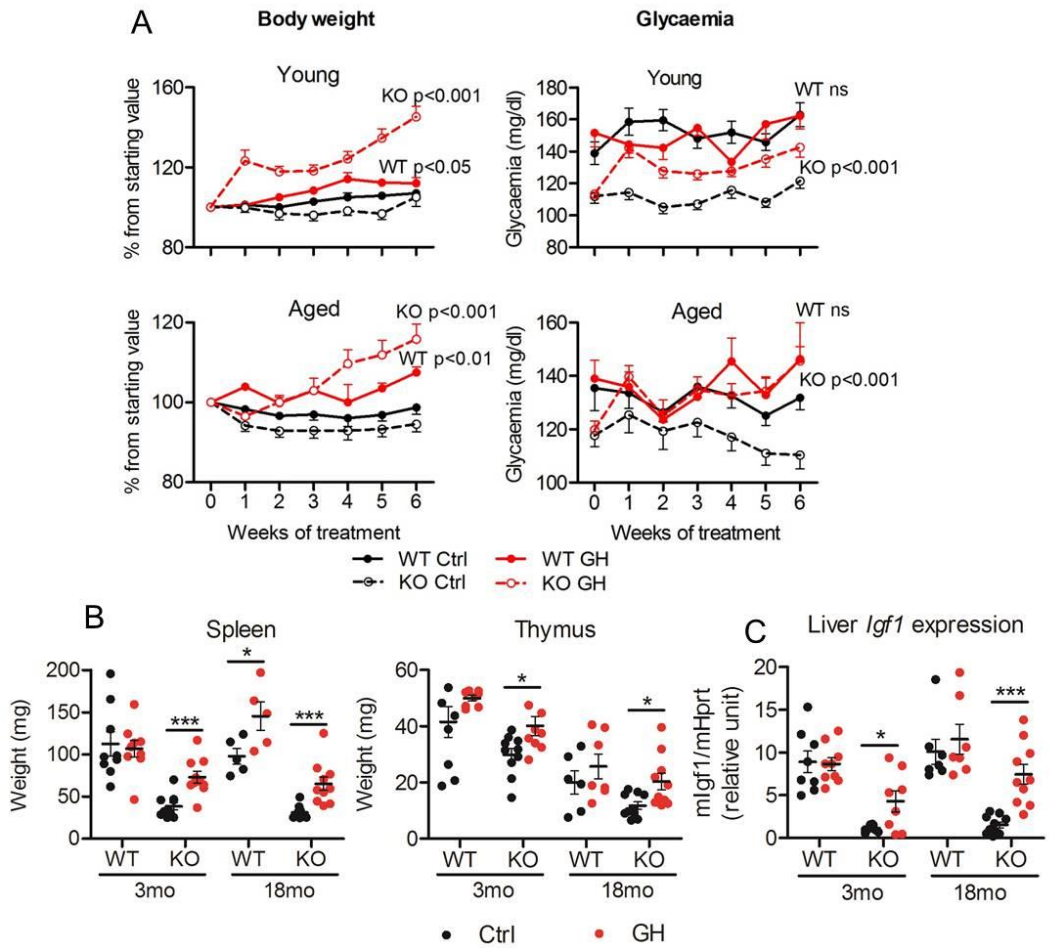

Figure 4.18 – Metabolic effects of short-term GH supplementation. Young (3mo) and aged (18mo) WT and KO mice were daily injected with GH or control DPBS (Ctrl). (**A**) Week-to-week variations of weight expressed in percentage of starting value (weight at d0) and glycaemia (mg/dl). (**B**) Spleen and thymus weight after 6 weeks of treatment. (**C**) Relative expression of *Igf1* to *Hprt* in the liver. Data (mean ± SEM) are representative of 2 independent experiments (*n*=7-10 per group). Two-way ANOVA test (time and treatment, *p-value* are shown for Ctrl *vs* GH; for **A**) or unpaired t-test (for **B** and **C**) were used for statistical analysis. *** $p < 0.001$, ** $p < 0.01$, * $p < 0.05$, ns = non-significant.

4.3.2 Thymus phenotype and function after short-term GH treatment

Immunological effects of GH supplementation were first studied in the thymus. As shown in **Figure 4.19**, frequency of the four thymocytes subpopulations after six weeks of GH treatment did not significantly differ from control injected mice, whatever the age and the phenotype of the mice. Intrathymic Treg cells did not show variations between control and treated mice, except a slight diminution in WT at 3mo (3.4 ± 0.15 in ctrl *vs* 2.66 ± 0.13 in GH groups). In order to follow TREC number variations during GH supplementation, TRECs were measured in PBMC sampled every second week. Basal values were analyzed two weeks before the first GH injection. Globally, results in **Figure 4.20** showed no effects of GH treatment on TREC content in PBMCs. Two-way

ANOVA test revealed a significant difference between control and GH treated groups for sjTRECs in 3mo-old WT mice and dβTRECs in 18mo-old KO mice, but there were no significant interactions between time and treatment, suggesting that GH effect was not the same at each time-point and was probably fortuitous. Moreover, Bonferroni post-tests that compared control and treated group at each time point were non-significant. Therefore, those two significant results were not considered as pertinent.

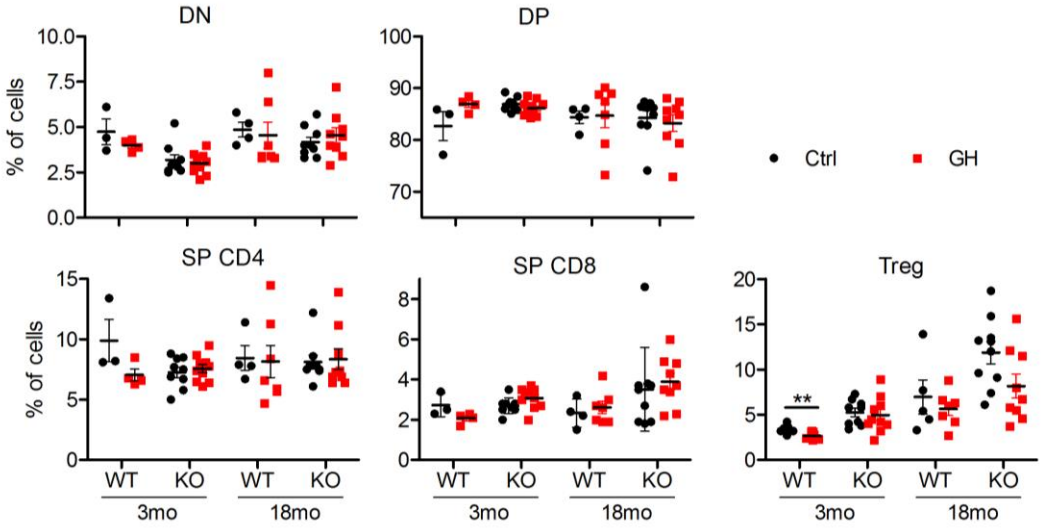

Figure 4.19 – Impact of GH supplementation on thymocyte distribution. Frequency of DN, DP, SP C D4 and SP CD8 thymocytes and intrathymic Treg cells in 3- and 18-mo old WT (*n*=3-7) and KO (*n*=9-10) mice after 6 weeks of daily GH or control DPBS-injection (Ctrl). Data (mean ± SEM) are representative of 2 independent experiments. Unpaired t-test or Mann Whitney test were used for statistical analysis, according to the Gaussian distribution of each group. ** $p < 0.01$.

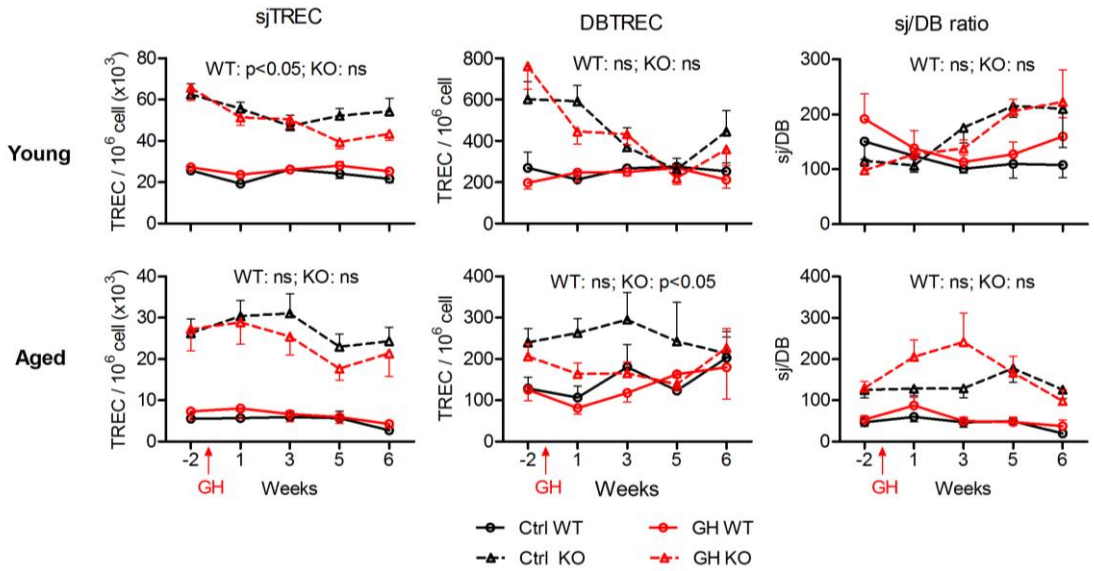

Figure 4.20 – Impact of GH supplementation on TREC frequency. Number of sjTRECs, dβTRECs and the sj/Dβ ratio in PBMCs of young (3mo) and aged (18mo) WT (*n*=9-10) and KO (*n*=10) mice during 6 weeks of daily GH or control DPBS-injection (Ctrl). Data (mean ± SEM) are representative of 2 independent experiments. Two-way ANOVA test (time and treatment) was used for statistical analyses (*p-value* are shown for Ctrl *vs* GH; ns = non-significant).

4.3.3 Peripheral lymphocyte variations during GH treatment

Finally the impact of GH supplementation was analyzed in periphery. A blood sample was taken (every second week) to follow by flow cytometry the variations of peripheral lymphocytes (gating strategy **Figure 4.8**). Some results are shown in **Figure 4.21**. Proportion of B and T cells varied across time. One-way ANOVA test revealed significant difference between control and GH injected groups in both WT and KO mice. Nevertheless, for an unknown reason, these proportions were already different at d0, before the first GH injection. Therefore, the statistical difference was probably due to this basal difference in B- and T-cell proportions between control and treated groups rather than to a true effect of GH treatment. However, no effect of treatment was observed regarding naïve CD4 and CD8 T cells. No variations were either found in CD4, CD8, TCM, TEM or Treg proportions (data not shown). Similar results were obtained in aged mice, as well as in spleen and lymph nodes analyzed after 6 weeks of treatment (data not shown).

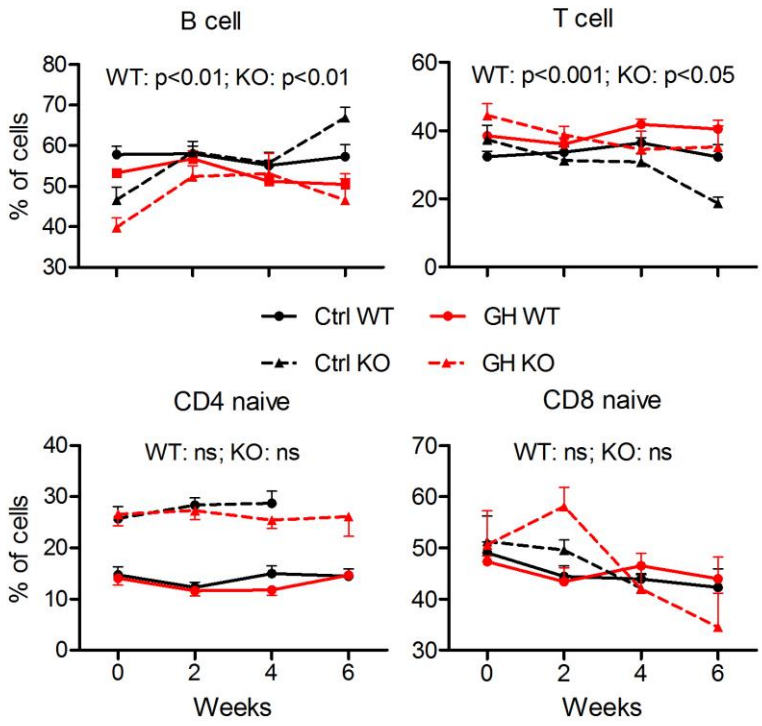

Figure 4.21 – Impact of GH supplementation on blood lymphocytes. Variations of the frequency of B cells, T cells, naïve CD4 and CD8 T cells in the blood of 3mo-old WT (*n*=9-10) and KO (*n*=10) mice during 6 weeks of daily GH or control DPBS injection (Ctrl). Data (mean ± SEM) are representative of 2 independent experiments. Two-way ANOVA test (time and treatment) was used for statistical analyses (*p-value* are shown for Ctrl *vs* GH; ns = non-significant).

4.3.4 Conclusions

This experiment was conducted to evaluate the ability of GH to restore normal immune parameters in *Ghrh*$^{-/-}$ mice, including TREC numbers, B- and T-cell frequency and the proportion of naïve T-cell pool. The potent immunostimulatory properties of GH supplementation were also investigated in normal and GH-deficient young and aged mice. Mice were injected daily with a physiological dose of recombinant human GH (Genotonorm, 1mg/kg), which was sufficient to induce metabolic effects such as growth, glucose release and IGF-1 expression in the liver. The effect was more spectacular in a GH-deficient context, even though treatment failed to restore values of normal mice. In WT mice, the treatment was unable to alter glycaemia or liver *Igf1* expression and induced only a moderate weight gain, probably because of regulatory mechanisms that maintained constant levels of GH and IGF-1 by down-regulating GHRH production (see **Figure 1.1**). Despite clear evidence of its efficiency, GH supplementation had no effect on thymic and immunological parameters. Treatment was unable to restore normal parameters in *Ghrh*$^{-/-}$ mice and had no immunostimulatory properties, except the increase of thymus and spleen weights. Moreover, aging was not a sensitizing factor to GH treatment, since no additional effects were observed in aged mice either.

4.4 DXM-induced stress

At this stage, results obtained in *Ghrh*$^{-/-}$ mice in basal conditions revealed only a small impact of somatotrope deficiency upon immune system development and aging. Moreover, short-term GH treatment was ineffective to induce changes in immune and thymic parameters. This is in accordance with the stress hypothesis, according to which somatotrope hormones could play a role only in case of stress to counteract stress-induced immunosuppressors [186]. Therefore, organisms that lack such hormones would be unable to correctly deal with stressful events and to maintain immune system homeostasis. In an attempt to explore this hypothesis in the *Ghrh*$^{-/-}$ mouse model, stress was mimicked in 3mo-old mice through challenge with DXM, a synthetic GC known to cause reversible thymic atrophy by inducing massive thymocyte apoptosis. A longitudinal follow-up of thymic volume by MRI allowed assessment of thymic atrophy and recovery in mutant and normal mice. In addition, thymopoiesis was investigated by flow cytometry analysis of thymocyte sub-populations and TREC quantification.

4.4.1 Thymic volume follow-up by MRI

MRI has been shown to be a powerful non-invasive quantitative technique to follow DXM-induced thymic atrophy [196,197]. Thymus is detectable without contrast agent because of its signal intensity different from surrounding tissues (**Figure 4.22 A**, yellow line). MRI sessions were performed in collaboration with Dr Guillaume Becker and Pr Alain Plenevaux from the Cyclotron Research center. Mice were scanned at d0 before the single injection of DXM 20mg/kg and at days 2, 5, 10 and 14 thereafter in order to cover the thymus atrophy, expected to occur at d2 post-injection, and subsequent recovery starting from d5 and complete at d14. As shown in the pictures **4.22 A**, thymus integrity seemed fully recovered in WT mice 2 weeks post-injection, while sections appeared smaller at d14 than at d0 for KO mice. As thymus volume was smaller in mutant mice than in WT, data were normalized in percentage of starting value (volume at d0) and are shown in **Figure 4.22 B**. Both WT and KO mice displayed a diminution of their thymic volumes at d2, followed by progressive recovery. Two-way ANOVA test revealed that variations of thymic volumes after DXM-injection differed between WT and KO mice (effects of strain $p<0.01$; time $p<0.001$; interaction $p<0.05$). Indeed,

Bonferroni post-tests showed a significant lower recovery of mutant thymus at d10 and 14 (respectively 66.1 ± 1.04% and 66.4 ± 6.48% of starting volume) compared to WT mice (107.5 ± 10.58% and 126.7 ± 15.2%). Evolution of thymic volumes in control injected groups was similar between both strains, revealing no effect of control injection or experimental procedure upon thymic volumes.

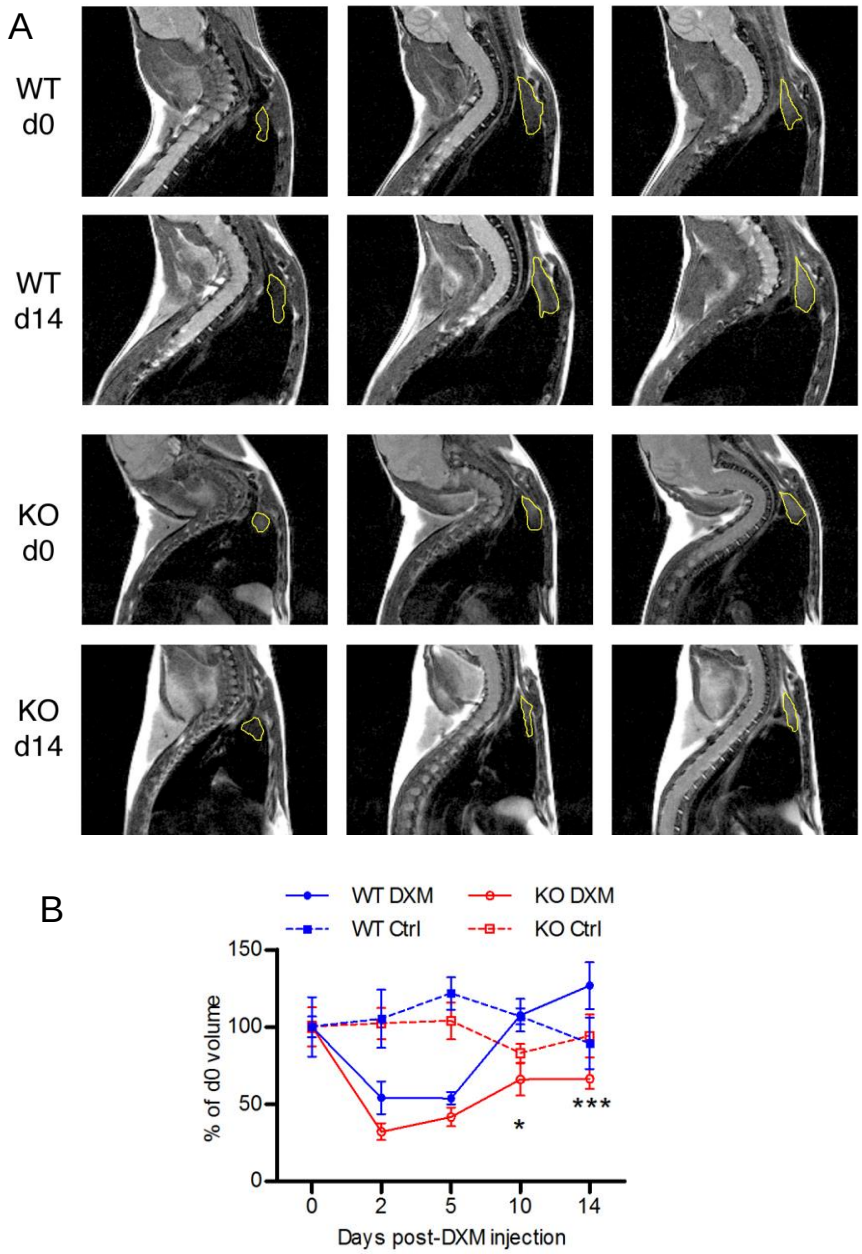

Figure 4.22 – MRI follow-up of thymic volume after DXM injection. (**A**) Representatives MRI slices showing thymus (ROI, yellow) of WT and KO mice at d0 and d14 after a single DXM injection. Lines show three successive slices around the maximal ROI. (**B**) Evolution of thymic volumes normalized in % of d0 value is shown for WT and KO mice treated with DXM (*n*=6 per group) or control solution (Ctrl, *n*=4 per group). Data (mean ± SEM) are representative of 2 independent experiments. Two-way ANOVA test (time and strain) with Bonferroni post-test (WT *vs* KO) were used for statistical analyses. *** $p < 0.001$, * $p < 0.05$.

4.4.2 Thymus weight and cellularity

In order to complete and reinforce results obtained by longitudinal follow-up, groups of mice were injected with DXM and killed at each time-point. Thymus were weighted and numbers of cells in cell suspensions were counted in Neubauer chamber. As represented in **Figure 4.23**, thymic weights and cellularities were significantly decreased at d2 and d5 post-DXM injection compared to basal d0 measures (without DXM injection), in both WT and KO mice. As soon as d10, thymus returned to basal values (left panel). Since thymic weight and number of cells were different between normal and mutant mice, data was normalized in percentage of d0 values, in order to be able to compare WT and KO atrophy and recovery after DXM-injection (right panel). Variations of thymic weight were similar in both strains. On the opposite, recovery of thymic cellularity differed between WT and KO groups (two-way ANOVA: strain $p<0.05$; time $p<0.001$; interaction non-significant), with a significant difference at d15 (171.8 ± 34.8% in WT *vs* 87.7 ± 12.32% in KO).

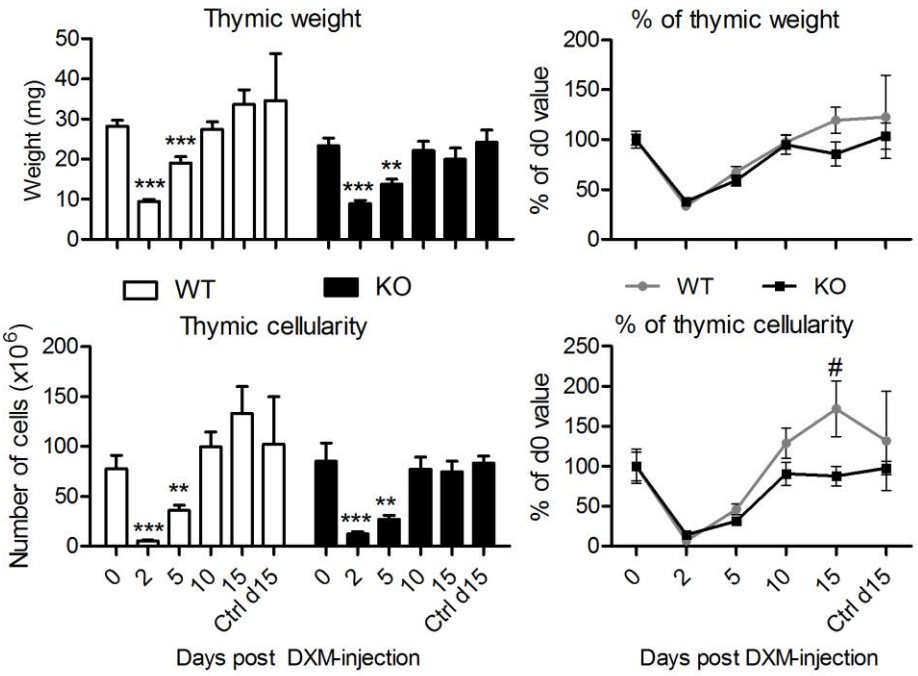

Figure 4.23 – Evolution of thymus weight and cellularity after DXM injection. Absolute thymus weight and cellularity (left panel) and weight and cellularity normalized in % of d0 value (right panel) in WT and KO mice at d0, 2, 5, 10 and 15 post DXM injection (*n*=8-12 per group) and d15 post control injection (*n*=4). Data (mean ± SEM) are representative of 3 independent experiments. Left panel: unpaired t-test or Mann Whitney test were used for statistical analysis, according to the Gaussian distribution of each group (comparison to d0: *** $p < 0.001$, ** $p < 0.01$ * $p < 0.05$). Right panel: two-way ANOVA test (time and strain) with Bonferroni post-test (WT *vs* KO: # $p < 0.05$) were used for statistical analyses.

Altogether, those results indicated that the thymus of normal and *Ghrh*$^{-/-}$ mice returned to normal weight and cellularity by d10 post DXM injection, but recovery of cells was slightly greater in WT animals.

4.4.3 Flow cytometry analysis of thymocyte sub-populations

DXM strongly disturbs thymopoiesis by inducing severe thymocyte apoptosis. To follow this effect, flow cytometry analyses of thymocyte subpopulations were performed at basal level (d0) and at days 2, 5, 10 and 15 post DXM injection. The number of each cell subset was counted with the FACS Verse method (see 4.1.4 spleen phenotype). Results showed again that both WT and KO mice recovered normal distribution and number of thymocytes at d10 post-DXM injection (**Figure 4.24 and 4.25**). However, the impact of DXM treatment strongly differed at d2 post-injection. Indeed, DP population almost completely disappeared (2.2±0.62%) in WT thymus, resulting in increased proportion of the three others subpopulations while, in KO mice, the DP percentage remained important (37.4±4.03%) and equivalent to SP CD4 cells (35.6±2.41%, **Figure 4.24 A**). Analysis of cell number in each subset revealed that this difference in proportion was exclusively due to DP cells ($0.2x10^6 \pm 62.6x10^4$ cells in WT *vs* $2.7x10^6 \pm 39.7x10^4$ cells in KO mice) while other subset presented similar cell number in WT and KO groups (**Figure 4.24 B**). Comparison of the impact of DXM and recovery between WT and KO mice by normalization of thymocytes frequency to basal value confirmed a differential effect at d2, where WT animals exhibited an ~97% drop in DP frequency and an approximately 8-fold increase in SP CD4 and SP CD8 frequencies while changes in KO mice were far more moderate (only 2-fold difference, **Figure 4.25**). Recovery at d5 also significantly differed between WT and KO animals (**Figure 4.25**). It seemed that WT mice returned to normal values of DN, DP and SP CD8 percentages faster than KO mice. DXM treatment increased Treg cell proportions in the thymus of both mice, but with a higher effect in KO mice (**Figure 4.25**).

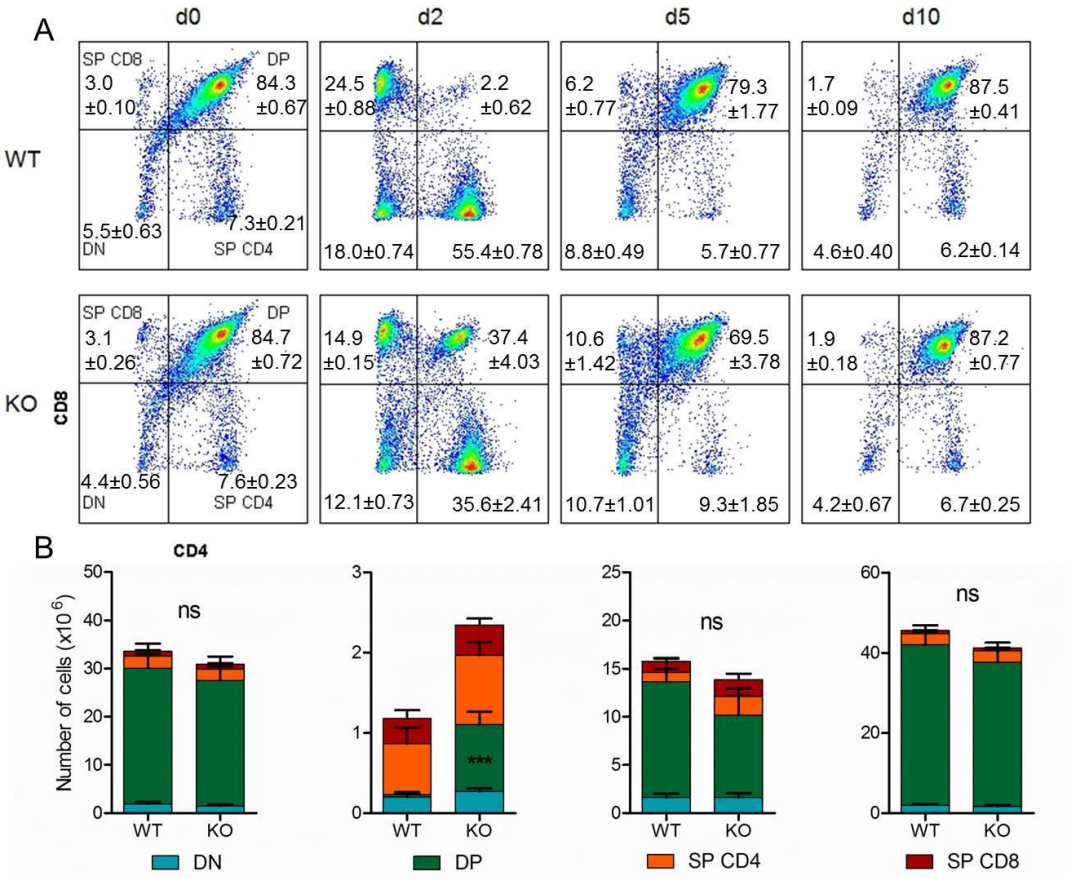

Figure 4.24 – Evolution of thymocyte frequency and number after DXM injection. (**A**) Representative dot plot of flow cytometry analysis of thymus (pre-gated on Thy1.2$^+$ cells) of WT and KO mice after DXM injection. Means ± SEM are shown for each subset. (**B**) Number of DN, DP, SP CD4 and SP CD8 cells at d0, 2, 5 and 10 after DXM injection. Data (mean ± SEM) are representative of 3 independent experiments (*n*=8-12). Unpaired t-test or Mann Whitney test were used for statistical analysis, according to the Gaussian distribution of each group (comparison WT *vs* KO: *** $p < 0.001$, ns: non-significant).

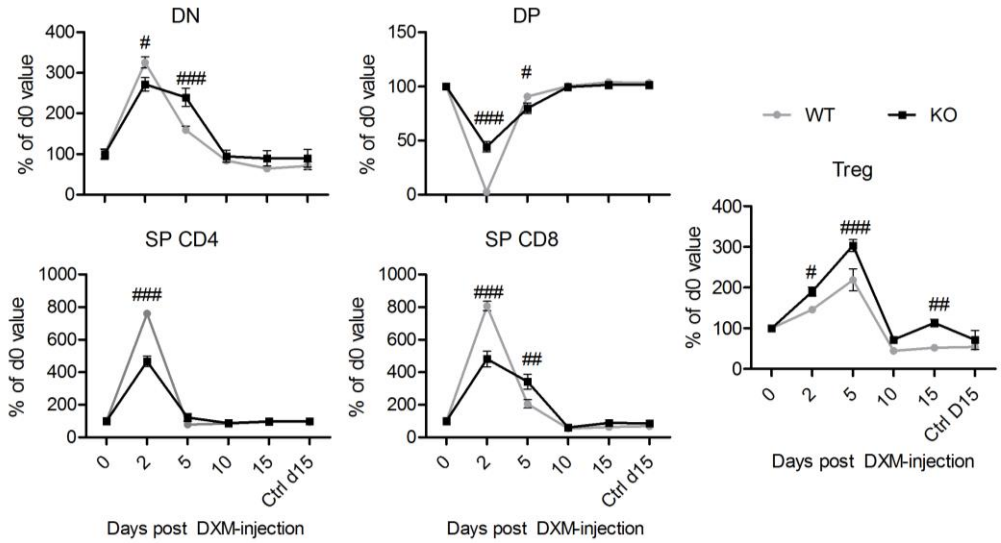

Figure 4.25 – Variations of thymocyte subpopulations distribution after DXM injection. Distribution of DN, DP, SP CD4, SP CD8 and Treg cell subsets normalized in % of d0 value in WT and KO mice at d0, 2, 5, 10 and 15 post DXM injection (*n*=8-12 per group) and d15 post control injection (*n*=4). Data (mean ± SEM) are representative of 3 independent experiments. Two-way ANOVA test (time and strain) with Bonferroni post-test (WT *vs* KO: ### $p < 0.001$, ## $p < 0.01$ # $p < 0.05$) were used for statistical analyses.

4.4.4 TREC quantification

Another way to investigate the effects of DXM on thymopoiesis was to analyze TRECs in thymic cell suspensions. Intrathymic TRECs were quantified as described in section 3.4. Unfortunately, results were hardly interpretable because of the differences in frequency of DN, DP and SP thymocytes induced by DXM treatment. Indeed, with this method, TRECs were expressed in function of total thymocytes. As DβTRECs are produced in DN cells and sjTRECs in DP cells, the number of each TREC in the thymus is strongly dependent on the proportion of each subset. For example, since DN frequency was higher at d2 than in d0 in WT mice (**Figure 4.24 A**), it resulted in a 2-fold increase in DβTREC number (data not shown). It would therefore be interesting to quantify TRECs in sorted thymocytes to avoid this bias of subset frequency. Hence, TREC quantification will not be taken into account in this experiment.

4.4.5 Conclusions

In this part, a metabolic stress was induced in mice by injection of DXM and ability of mice to respond to this stress was studied in the thymus. Indeed, this synthetic GC induces massive thymic atrophy by apoptosis of thymocytes, but normal thymus function and histology is restored within two weeks. This thymus reduction and recovery was followed by longitudinal study of of thymic volumes by MRI or in a cross-sectional measurement of thymus weight and cellularity. Unfortunately, those techniques reported here contradictory results. With the first one, *Ghrh*$^{-/-}$ mice recovered less than normal mice, with a mean thymic volume of 66% of initial value two weeks after DXM injection while WT mice showed an even increased volume. But tissue weight measurement did not confirm this delayed recovery since both mutant and normal mice presented normal weight and cellularity as soon as d10 post-DXM treatment. This discrepancy of results could reflect a difference in cell density of mutant thymus. If cells were more spaced within the thymus area, this could lead to some increased volume without affecting the absolute weight as the quantity of matter is equal. However, we cannot exclude technical imprecisions in measurement of thymus volumes by MRI. Despite that Brooks and colleagues validated MRI as a non-invasive method to follow thymus involution with high statistical power and less animals needed [196], our own

experience was less convincing. Images were not always clear and thymus was sometimes hardly distinguishable from surrounding tissues, especially in dwarf mice for which the stereotaxic holder was not adapted to their smaller size, making it difficult to correctly position the mouse for MRI acquisition. Therefore, a reasonable doubt can be assumed regarding the accuracy of MRI-measurement of thymic volumes.

This idea is reinforced by flow cytometry analysis of thymopoiesis. Frequencies of the four thymic subpopulations were markedly disturbed at d2 post DXM-injection, but they returned to normal by d10 in both normal and mutant mice. Nevertheless, the effect of DXM at d2 differed between both mice. DP cells almost completely disappeared in WT mice, while a significant DP population was visible in *Ghrh*$^{-/-}$ thymus. DP thymocytes are known to be the most sensitive to GC-induced apoptosis [208]. Two non-mutually exclusive possibilities could explain this difference in DP number: either *Ghrh*$^{-/-}$ DP cells are more resistant to DXM-induced apoptosis, or the recovery in mutant mice occurs faster and better so that they already showed more than 30% of DP cells at d2. This last theory is consistent with the hypothesis of increased influx of ETPs in mutant thymus as evocated in section 4.1.7.

Finally, flow cytometry analysis also revealed a slight delay in mutant recovery at d5. Indeed, WT mice showed frequencies of DN, DP and SP CD8 closer to normal values than mutant mice.

Altogether, those results did not allow validating or invalidating the stress hypothesis. Mutant mice seemed more resistant to DXM effects on thymopoiesis at d2, but they also presented a slight delay in recovery of thymocyte distribution and possibly of thymus volume. Further investigations with other type of stress will be of interest, like LPS or infectious stress.

5 Discussion and conclusions

While an abundant literature describes the effects of GH upon the immune system, its real implication in immune physiology remains unclear and controversial. Most of the previous work was done in mouse models with multiple pituitary deficiencies (GH, prolactin and thyrotropic hormone), making it difficult to identify the precise role of each hormone. In my thesis, I investigated a model with a unique specific deficiency of the somatotrope GHRH/GH/IGF1 axis due to *Ghrh* deletion, in an attempt to elucidate the physiological role of somatotropic hormones in immune system development and function. I did not find any obvious immunodeficiency, thymic defect or premature aging in *Ghrh*$^{-/-}$ mice. Moreover, GH treatment had no immunological effects whatever the phenotype and the age of the mice. Altogether, those results suggest that the somatotrope axis is not crucial for normal immune system development and maintenance. This is in accordance with the stress hypothesis. Nevertheless, the DXM experiment was unhelpful in figuring out the necessity of somatotrope hormones to manage GC-mediated stress since *Ghrh*$^{-/-}$ mice exhibited either enhanced, delayed or comparable response to DXM-treatment.

5.1 Critical reviewing of results homogeneity across experiments

This work includes four distinct experimental parts (basal characterization, aging, GH supplementation and DXM), within which the same parameters were analyzed in WT and *Ghrh*$^{-/-}$ mice. **Table 5.1** summarizes the results obtained in KO mice compared to WT controls for parameters shared by the four experiments (*i.e.* thymus and spleen weight and cellularity, thymus phenotype, TREC and peripheral lymphocyte frequency). Some results were not consistent across experiments: statistical differences observed in one group were not reproduced or even the opposite result was found in other experiments. In addition to the normal biological variations in living animals, this heterogeneity of results could be explained in part by experimental bias that could have occurred despite our effort to minimize time-to-time variations. Indeed, this work was spread over 5 years. During this long period, technical and analytical skills of manipulators had evolved, product lots were different, devices were getting older or replaced, and housing conditions of mice colonies may have varied. This could induce small differences

from one experiment to another. In addition, it is important to keep in mind that statistical analyses could also lead to wrong interpretations. With the criteria applied here, 5% of the statistical differences between WT and KO mice might be presumably due to coincidence rather than to the *Ghrh* mutation.

Given these restrictions, only results that were found repeated across several experiments are considered as true and reliable and will be taken into account to build the firmest conclusions (in bold in **Table 5.1**). This includes the following differences found in *Ghrh*$^{-/-}$ compared to non-deficient animals:

- Reduced absolute weight for spleen and thymus.
- Reduced relative weight for spleen (relative spleen weight is equal between WT and KO group in backcrossed animals, but Salvatori's team also found reduced relative spleen weight [49] so this result seems reliable).
- Decreased absolute spleen cellularity but equal relative spleen and thymus cellularity.
- Tendency to reduced frequency of DN cells in the thymus.
- Higher number of sjTREC.
- Lower B and higher T frequencies in peripheral lymphoid organs.
- Increased pool of naïve T cells and reduction in memory T cells.

Table 5.1. Comparison of results in KO compared to WT mice in different experiments

KO *vs* WT	Original strain (DXM d0)	Backcrossed groups	Aging (3mo, 6mo, 18mo)[2]	GH supplementation[1] (3mo, 18mo)[2]
Thymus weight	↙ **absolute** ; ↗ relative	↙ **absolute** ; ↗ relative	↙ **absolute** 3-6mo ; ↗ relative 18mo ↙ 6mo = 3mo	↙ **absolute** ; = relative
Spleen weight	↙ **absolute** ; ↙ relative	↙ **absolute** ; = relative	↙ **absolute** ; ↙ relative	↙ **absolute** ; ↙ relative
Thymus cellularity	= absolute ; **= relative**	= absolute ; = **relative**	↙ absolute ; **= relative**	N.D.
Spleen cellularity	↙ **absolute** ; **= relative**	↙ **absolute** ; **= relative**	↙ **absolute** ; **= relative** (3-6mo) ↗ 18mo	N.D.
Thymus phenotype	No differences (except tendency ↙ **DN**)	↗ DP ; ↙ SP CD4 ; tendency ↙ **DN**	↙ **DN** 3-6mo ; ↗ DP 3mo ; ↗ SP CD8 6mo ; ↗ Treg 3-18mo	↙ **DN** 3mo ; ↗ DP 3mo ; ↙ SP CD4 3mo ; ↗ Treg 3-18mo
TREC	N.D.	↗**sj** ; = Dβ ; = ratio	↗**sj** ; ↗ Dβ ; ↙ ratio 3mo = 6mo ↗ 18mo	↗**sj** ; ↗ Dβ ; = ratio 3mo ↗ 18mo
Peripheral B-T (%)	↙ **B ; ↗ T**	↙ **B ; ↗ T**	↙ **B ; ↗ T**	↙ **B ; ↗ T** blood and LN but = spleen
Peripheral CD4-CD8 (%)	= CD4 ; = CD8	= CD4 ; = CD8	= CD4 except ↗ in LN and blood 18mo ; = CD8 except ↙ in LN, blood 3-18mo and spleen 18mo	= CD4 in spleen, ↗ in LN and blood ; = CD8 in spleen and LN, ↙ in blood
Peripheral naïve-memory T cells (%)	↗**naive** ; ↙ TCM ; = TEM	↗**naive** ; ↙ TCM CD8 ; ↙ TEM	↗ **naive** ; ↙ TCM (except = CD4 TCM spleen 6-18mo and = CD8 TCM blood) ; = TEM (except ↙ in spleen 6mo and ↗ blood 3mo)	↗ **naive** ; ↙ TCM (except = CD4 TCM spleen 3-18mo, blood 18mo, LN 18mo) ; = TEM (except ↙ in spleen 3-18mo and ↙ CD4 TEM in blood 18mo and LN 18mo)
Peripheral Treg (%)	**= Treg**	**= Treg**	**= Treg** except ↗ in spleen 3mo	**= Treg** except ↗ in spleen 3mo and ↙ blood 18mo

In **bold** are results found similar in all experiments. ND: not determined

[1] Results from all mice before GH injection if data available or only DPBS group otherwise

[2] If not specifically stated, similar difference occurs at all ages and in all organs analyzed

5.2 Reassessment of the impact of the somatotrope axis upon adaptive immunity

The first objective of my thesis was to evaluate the role of the somatotrope GHRH/GH/IGF-1 axis upon immune system development. If GHRH, GH or IGF-1 were crucial for immune system physiology, we could expect that the severe somatotrope deficiency of the *Ghrh*$^{-/-}$ mouse will result in significant immunodeficiency, especially in the thymus, as this was shown in Snell-Bagg and Ames-Dwarf mice [109,111,159,160]. My thesis reveals that *Ghrh*$^{-/-}$ mice are not thymo-deficient. Thymus weight and cellularity are similar to normal animals when corrected to the smaller size of *Ghrh*$^{-/-}$ mice and the distribution of the four thymocyte subsets is unaltered, with the exception of a slight decrease in DN frequency. On the opposite, *Ghrh*$^{-/-}$ mice show an improved thymopoiesis compared to normal mice, as demonstrated by the higher number of sjTRECs and the increased proportion of naïve cells. It was shown that naïve cells in mice derived mostly from thymic output and not from peripheral proliferation as in humans, even in older animals [209]. Therefore, the higher pool of naïve cells in *Ghrh*$^{-/-}$ mice truly reflects enhanced thymopoiesis, probably due to increased influx of progenitors into the thymus, faster commitment of DN to DP stages and/or decreased apoptosis of thymocytes. This sounds surprising since GH and IGF-1 had been shown to have exactly the same effects: they increase thymopoiesis [162,163,165] and improve homing to the thymus [162,168,169]. How the deficiency in those hormones could lead to similar effects than what they are supposed to induce is intriguing. It probably involves compensation by other neuroendocrine hormones. Indeed, PRL and thyroid hormones have also been shown to improve intrathymic T-cell development [210–213].

Similarly, no deficiency in peripheral mature T lymphocytes was found. Instead, T-cell frequency was enhanced while B-cell frequency was reduced in peripheral lymphoid organs of *Ghrh*$^{-/-}$ mice. Similar observations were previously obtained in Snell-Bagg and lit/lit mouse models, where cellularity and phenotype of the thymus was normal but mice exhibited reduced splenic B cells [177,184]. In addition, those authors found normal B lymphopoiesis in bone marrow of GHRHR-deficient lit/lit mice, suggesting that the somatotrope axis is involved in the maintenance of the peripheral B-cell pool but not in their development [177]. *Ghrh*$^{-/-}$ mice also exhibit functional B lymphopoiesis and

their bone marrow contains more B-committed $B220^+$ cells than normal mice. This is in contradiction with a previous study showing that GH promotes commitment of marrow stem cells to the B lineage [181]. Another study revealed that IGF-1 triggers the expression of μ-heavy chain by pro-B cells, leading to differentiation into pre-B cell [179]. However, in *Ghrh*$^{-/-}$ mice, progression of pro-B to pre-B cells seems also increased as suggested by the lower proportion of pre-pro-B and pro-B subsets and higher frequency of pre-B cells. A possible explanation of those discordant results is that in those two studies, GH and IGF-1 effects upon B lymphopoiesis were tested *in vitro* and could not reflect the normal *in vivo* situation. In any case, the decrease in peripheral B-cell frequency observed in *Ghrh*$^{-/-}$ mice is a strictly peripheral event that does not originate in the bone marrow. Moreover, it is not due either to a reduced B-cell proliferation, since Ki67 labeling revealed a higher proliferation rate of B-cell in *Ghrh*$^{-/-}$ spleen. This lets the possibility of an increase in B-cell apoptosis. GH has been shown to prevent mature B-cell apoptosis in B-cell lines, by increasing Bcl-2 and reducing caspase-3 intracellular levels [214]. Finally, investigations in *Ghrh*$^{-/-}$ mice do not allow figuring out if B-cell number is really decreased in periphery or if the proportion is reduced because of an increase in T-cell production.

The second part of my thesis consisted of evaluating immune aging in *Ghrh*$^{-/-}$ mice. The current hypothesis suggests that immunosenescence is triggered by the decrease in neuroendocrine hormones, especially GH and IGF-1. The hallmark of immunosenescence is thymus involution. First studies in dwarf mice revealed premature thymic atrophy [109,159,160]. In those studies, mice lifespan did not exceed 60 days, therefore suggesting that the mice were not in healthy conditions since GH deficiency normally leads to increased lifespan [51]. Premature immune aging was not reproduced in other studies in dwarf mice or in other mouse models like lit/lit, *Igf1*$^{-/-}$ or thyreotrope-deficient mice [177,184,205]. A group even found delayed immune aging in Snell-Bagg mice [54]. Study in *Ghrh*$^{-/-}$ mice show that thymic involution seems to occur between 3- and 6-mo of age in mutant mice while it starts after 6mo in non-deficient mice. In addition, TREC quantification reveals possible differential mechanism involved in the loss of efficiency of thymopoiesis, with an alteration that seems to occur after DN stage in normal mice while defect in *Ghrh*$^{-/-}$ mice affects earlier stages. Nevertheless, both normal and mutant

mice exhibited a decreased thymic output at 18 but not 6mo of age. Similarly, the replacement of naïve T cells by memory cells and the increase in CD4/CD8 ratio occurs between 6 and 18mo in both types of mice. In humans, CD4/CD8 ratio tends to decrease with age [215], but the opposite trend was observed in mice [216,217]. Taken together, those results reveal only slight impact of the somatotrope deficiency on immune aging, arguing that somatopause is not the main factor that induces immunosenescence.

Numerous studies showed that GH treatment in mice could improve several immune parameters, including thymus and spleen weight and cellularity, thymopoiesis or lymphocyte numbers [110,111,160,161,169,175,176]. Especially in aged rodents, GH treatment has been shown to be able to rejuvenate involuted thymus [112,201–203]. However, our own experiments reveal that GH treatment has no effect on immunological parameters of young or aged C57BL/6J and *Ghrh*$^{-/-}$ mice, despite evidences of metabolic activity induced by GH injections. Indeed, at physiological dose of 1mg/kg daily-injected, total body and spleen and thymus weight were increased and liver production of IGF-1 was stimulated, although without reaching WT values in *Ghrh*$^{-/-}$ mice, as previously observed [49]. Nevertheless, thymus function and peripheral lymphocyte frequencies remained similar to control injected animals, even in old animals. This is not in contradiction with previous studies. Most of them demonstrate that GH treatment increases size and cellularity of lymphoid organs and enhances cell proliferation, which is probably what happens in *Ghrh*$^{-/-}$ mice although we do not have data about cellularity and cell proliferation after GH treatment. But frequency of thymocytes or peripheral lymphocytes, when analyzed, was generally not influenced by GH treatment [201,202]. Only one report describes reactivation of thymopoiesis with increase in DP and decrease in DN cells following implantation in aged rats of GH3 cells, which produce GH and PRL [203]. However, the proportion of DP and DN cells in young rats were quite aberrant in this study (20% and 30% respectively). Thus, it seems that GH treatment exerts a promoting effect indifferently on all cell types of the immune system and even more globally on the whole body scale. Nonetheless, it is still perplexing that the differences induced by the somatotrope deficiency observed in *Ghrh*$^{-/-}$ mice, like decreased B-cell proportion and increased naïve T cells and TREC number, are not corrected when mice are supplemented with GH. It might be because the dose injected

was not sufficient to have some impact on those parameters despite its evident metabolic efficiency. Most of the studies showing immune restoration in dwarf mice used doses that were 100-times higher than in the present work [110,111,176]. Another possibility is that defects in *Ghrh*$^{-/-}$ mice are acquired during B and T cells ontogeny and are independent of the peripheral GH environment. In that case, only long-term or post-natal GH supplementation could restore the B-T ratio and naïve-memory proportion. Finally, we cannot exclude that the differences exhibited by *Ghrh*$^{-/-}$ mice are not due to GH or IGF-1 but directly to GHRH deficiency. If true, GHRH treatment should be able to restore normal parameters in *Ghrh*$^{-/-}$ mice.

Altogether, results obtained in *Ghrh*$^{-/-}$ mice in basal conditions reveal only a weak impact of the somatotrope deficiency on immune system development and aging, suggesting that integrity of the somatotrope axis is not required for those processes in normal conditions. This is in agreement with the stress hypothesis according which somatotrope hormones are important regulators of immune homeostasis in case of stress by counteracting negative effects of stress mediators, like GC [186]. In this work, DXM was used to mimic stress in *Ghrh*$^{-/-}$ mice, and thymic atrophy and recovery was followed. It appears that *Ghrh*$^{-/-}$ mice present a better resistance and faster recovery of DP thymocytes 2 days post-DXM treatment, but recovery was slightly delayed at d5 compared to non-deficient mice. Previous studies demonstrated that PRL prevents DXM-induced *in vitro* apoptosis of thymocytes, while GH was less efficient [218]. It would be interesting to measure PRL levels in *Ghrh*$^{-/-}$ mice. Maybe the activity of the lactotrope axis is enhanced to compensate the somatotrope deficiency? Higher PRL concentrations would explain the better resistance of DP thymocytes to DXM-induced apoptosis. On the opposite, IGF-1 administration in rats has no anti-apoptotic effects but increases the DP recovery at day 5 post-DXM injection [219]. The lack of IGF-1 in *Ghrh*$^{-/-}$ mice might explain the delayed DP recovery as seen at d5. Nevertheless, altogether those results do not allow validating or invalidating the stress hypothesis. Further investigations with other types of stress are needed. My colleague Khalil Farhat is currently testing the resistance of *Ghrh*$^{-/-}$ mice to *Streptococcus pneumoniae* (*S.pneum*) infection and vaccination. Preliminary results are very interesting. Indeed, *Ghrh*$^{-/-}$ mice show acute pulmonary infection after intranasal *S.pneum* instillation, as assessed by pulmonary

bacterial load (**Figure 5.1**), accompanied by septicemia, while non-deficient WT or HZ animals are able to eliminate the infection within 24h. In addition to the reduced resistance to *S.pneum* infection, response to *S.pneum* vaccination is also impaired in *Ghrh*$^{-/-}$ mice, as demonstrated by the lower production of specific IgM compared to non-deficient mice [220]. Quite interestingly, lymphocyte infiltration in the lungs presents a lower proportion of B cells in *Ghrh*$^{-/-}$ mice compared to WT, similar to that found in lymphoid organs in basal conditions (**Figure 5.2**).

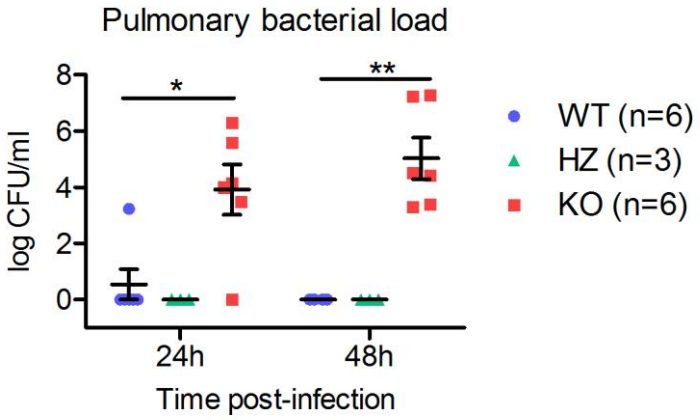

Figure 5.1 – Bacterial load in lungs after *Streptococcus pneumoniae* infection. The presence of bacteria in lung homogenates of backcrossed (WTb, HZb, KOb) mice was determined by CFU assay 24h and 48h post intra-nasal infection. Data (mean ± SEM) are representative of 2 independent experiments. Unpaired t-test was used for statistical analysis. *n*=8 per group. *** $p < 0.001$, * $p < 0.05$.

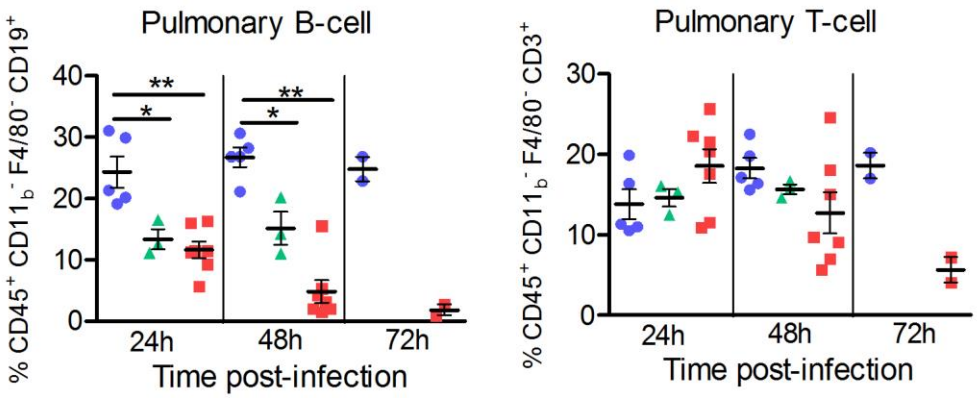

Figure 5.2 – Lymphocyte infiltrates in lungs after *Streptococcus pneumoniae* infection. Percentage of B- and T-cell in lungs of backcrossed (WTb, HZb, KOb) mice was determined by flow cytometry analysis. Data (mean ± SEM) are representative of 2 independent experiments. Mann-Whitney test was used for statistical analysis. *n*=2-7 per group. ** $p < 0.01$, * $p < 0.05$.

5.3 Toward a new approach: somatotrope axis and innate immunity

In light of the recent results obtained by my colleague Khalil Farhat regarding *S.pneum* infection in *Ghrh*$^{-/-}$ mice, we are suggesting a new theory: **somatotrope hormones could be required for innate immunity development and function.** Indeed, at the time where normal mice eliminated *S.pneum* infection, cellular and humoral responses are not yet activated. Bacterial elimination seems therefore triggered by innate cells. The dramatic loss of control of *S.pneum* infection in *Ghrh*$^{-/-}$ mice could result from a defect in innate immunity. This hypothesis will be the subject of K.Farhat's further investigations. To our knowledge, the impact of somatotrope deficiency upon innate immune system has never been studied. However, as described in section 1.4.2, innate cells are potential targets for GH and IGF-1. They promote their survival, activation and function (killing and phagocytosis). Somatotrope deficiency might result in: 1) developmental defect in the generation of innate cells; 2) inability of innate cell to recognize and/or be activated by foreign antigens and/or 3) reduced killing, phagocytic and antigen-presenting functions.

Interestingly, this hypothesis could explain several of the surprising results obtained during basal characterization of the *Ghrh*$^{-/-}$ mouse model. First, if somatotrope hormones are required during myeloid cell development, their absence could induce a reduction in the number of myeloid progenitors in the bone marrow, leading to increased proportion of others progenitors, including B220^{+} B-committed cells as observed in *Ghrh*$^{-/-}$ mice. Secondly, the involvement of the somatotrope axis in innate cell activation and function may affect not only innate but also adaptive responses. Indeed, adaptive immunity requires proper activation signals provided by innate APCs. In a context of a somatotrope deficiency, functional defect in innate immunity could lead to reduced killing activity and poor early control of infections, but also to impaired phagocytosis and presentation to adaptive cells, resulting in lower B- and T-cell activation. This could explain the poor vaccine response observed by K.Farhat in *Ghrh*$^{-/-}$ mice. It is also a possible explanation for the GH-dependent decreased susceptibility of these mice to induction of EAE [193]. This experimental model of multiple sclerosis is induced by injection of MOG antigen. If the antigen is not properly processed and presented by CPA, auto-reactive lymphocytes will not be activated and mice will develop

less severe symptoms. The defect in antigen presentation and lymphocyte activation could also explain the increased *in vitro* response observed for *Ghrh*$^{-/-}$ B and T cells. Indeed, lymphocytes may have adapted to the lack of activation by lowering the activation threshold required for cell activation. This is called the 'tuning', a concept according which lymphocytes may reversely adapt their activation threshold in function of the ambient signals, including APC contacts [221]. A lower activation threshold leads to higher/faster activation than in normal mice in response to the same stimulatory signal. Nevertheless, this compensatory mechanism in lymphocytes seems not sufficient to restore a normal *in vivo* response to vaccination or MOG antigen.

In conclusion, this works brings new evidence of the non-essential role played by the GHRH/GH/IGF-1 axis on adaptive immune system development and maintenance. Instead, it argues in favor of an effect upon innate immunity and opens the way for further investigations of this hypothesis and the role of the somatotrope axis in supporting immune system during infectious stress. This could lead to new interesting findings about the physiological role of the somatotrope axis in immunity and help to set up new therapeutic strategies to improve immune response in contexts of immunodeficiency, like acute infection or aging.

6 References

1 Weigent DA, Blalock JE. Associations between the neuroendocrine and immune systems. *J Leukoc Biol* 1995;**58**:137–50.

2 Gunawardane K, Krarup Hansen T, Sandahl Christiansen J, Lunde Jorgensen JO. Normal Physiology of Growth Hormone in Adults. In: De Groot LJ, Beck-Peccoz P, Chrousos G, Dungan K, Grossman A, Hershman JM, *et al.*, eds. . South Dartmouth (MA) 2000.

3 Murray PG, Higham CE, Clayton PE. 60 YEARS OF NEUROENDOCRINOLOGY: The hypothalamo-GH axis: the past 60 years. *J Endocrinol* 2015;**226**:T123-40.

4 Guillemin R, Brazeau P, Bohlen P, Esch F, Ling N, Wehrenberg WB. Growth hormone-releasing factor from a human pancreatic tumor that caused acromegaly. *Science* 1982;**218**:585–7.

5 Rivier J, Spiess J, Thorner M, Vale W. Characterization of a growth hormone-releasing factor from a human pancreatic islet tumour. *Nature* 1982;**300**:276–8.

6 Lin-Su K, Wajnrajch MP. Growth Hormone Releasing Hormone (GHRH) and the GHRH Receptor. *Rev Endocr Metab Disord* 2002;**3**:313–23.

7 Hattori N. Expression, regulation and biological actions of growth hormone (GH) and ghrelin in the immune system. *Growth Horm IGF Res* 2009;**19**:187–97.

8 Shimon I, Taylor JE, Dong JZ, Bitonte RA, Kim S, Morgan B, *et al.* Somatostatin receptor subtype specificity in human fetal pituitary cultures. Differential role of SSTR2 and SSTR5 for growth hormone, thyroid-stimulating hormone, and prolactin regulation. *J Clin Invest* 1997;**99**:789–98.

9 Tentler JJ, Hadcock JR, Gutierrez-Hartmann A. Somatostatin acts by inhibiting the cyclic 3',5'-adenosine monophosphate (cAMP)/protein kinase A pathway, cAMP response element-binding protein (CREB) phosphorylation, and CREB transcription potency. *Mol Endocrinol* 1997;**11**:859–66.

10 Kojima M, Hosoda H, Date Y, Nakazato M, Matsuo H, Kangawa K. Ghrelin is a growth-hormone-releasing acylated peptide from stomach. *Nature* 1999;**402**:656–60.

11 Yang J, Brown MS, Liang G, Grishin N V, Goldstein JL. Identification of the acyltransferase that octanoylates ghrelin, an appetite-stimulating peptide hormone. *Cell* 2008;**132**:387–96.

12 Gutierrez JA, Solenberg PJ, Perkins DR, Willency JA, Knierman MD, Jin Z, *et al.* Ghrelin octanoylation mediated by an orphan lipid transferase. *Proc Natl Acad Sci U S A* 2008;**105**:6320–5.

13 Muller TD, Nogueiras R, Andermann ML, Andrews ZB, Anker SD, Argente J, *et al.* Ghrelin. *Mol Metab* 2015;**4**:437–60.

14 Guan XM, Yu H, Palyha OC, McKee KK, Feighner SD, Sirinathsinghji DJ, *et al.* Distribution of mRNA encoding the growth hormone secretagogue receptor in brain and peripheral tissues. *Brain Res Mol Brain Res* 1997;**48**:23–9.

15 Gnanapavan S, Kola B, Bustin SA, Morris DG, McGee P, Fairclough P, *et al.* The tissue distribution of the mRNA of ghrelin and subtypes of its receptor, GHS-R, in humans. *J Clin Endocrinol Metab* 2002;**87**:2988.

16 Khatib N, Gaidhane S, Gaidhane AM, Khatib M, Simkhada P, Gode D, *et al.* Ghrelin: ghrelin as a regulatory Peptide in growth hormone secretion. *J Clin Diagn Res* 2014;**8**:MC13-7.

17 Herington AC, Ymer S, Stevenson J. Identification and characterization of specific binding proteins for growth hormone in normal human sera. *J Clin Invest*;**77**:1817–23.

18 Baumbach WR, Horner DL, Logan JS. The growth hormone-binding protein in rat serum is an alternatively spliced form of the rat growth hormone receptor. *Genes Dev* 1989;**3**:1199–205.

19 Edens A, Southard JN, Talamantes F. Mouse growth hormone-binding protein and growth hormone receptor transcripts are produced from a single gene by alternative splicing. *Endocrinology* 1994;**135**:2802–5.

20 Zhang Y, Jiang J, Black RA, Baumann G, Frank SJ. Tumor necrosis factor-alpha converting enzyme (TACE) is a growth hormone binding protein (GHBP) sheddase: the metalloprotease TACE/ADAM-17 is critical for (PMA-induced) GH receptor proteolysis and GHBP generation. *Endocrinology* 2000;**141**:4342–8.

21 Schilbach K, Bidlingmaier M. Growth hormone binding protein - physiological and analytical aspects. *Best Pract Res Clin Endocrinol Metab* 2015;**29**:671–83.

22 Castrillo JL, Theill LE, Karin M. Function of the homeodomain protein GHF1 in pituitary cell proliferation. *Science* 1991;**253**:197–9.

23 Li S, Crenshaw EB 3rd, Rawson EJ, Simmons DM, Swanson LW, Rosenfeld MG. Dwarf locus mutants lacking three pituitary cell types result from mutations in the POU-domain gene pit-1. *Nature* 1990;**347**:528–33.

24 Sornson MW, Wu W, Dasen JS, Flynn SE, Norman DJ, O'Connell SM, *et al.* Pituitary lineage determination by the Prophet of Pit-1 homeodomain factor defective in Ames dwarfism. *Nature* 1996;**384**:327–33.

25 Waters MJ. The growth hormone receptor. *Growth Horm IGF Res* 2016;**28**:6–10.

26 Brown RJ, Adams JJ, Pelekanos RA, Wan Y, McKinstry WJ, Palethorpe K, *et al.* Model for growth hormone receptor activation based on subunit rotation within a receptor dimer. *Nat Struct Mol Biol* 2005;**12**:814–21.

27 Waters MJ, Brooks AJ. JAK2 activation by growth hormone and other cytokines. *Biochem J* 2015;**466**:1–11.

28 Smit LS, Vanderkuur JA, Stimage A, Han Y, Luo G, Yu-Lee LY, *et al.* Growth hormone-induced tyrosyl phosphorylation and deoxyribonucleic acid binding activity of Stat5A and Stat5B. *Endocrinology* 1997;**138**:3426–34.

29 Gronowski AM, Zhong Z, Wen Z, Thomas MJ, Darnell JEJ, Rotwein P. In vivo growth hormone treatment rapidly stimulates the tyrosine phosphorylation and activation of Stat3. *Mol Endocrinol* 1995;**9**:171–7.

30 Moutoussamy S, Kelly PA, Finidori J. Growth-hormone-receptor and cytokine-receptor-family signaling. *Eur J Biochem* 1998;**255**:1–11.

31 Hwa V, Oh Y, Rosenfeld RG. The insulin-like growth factor-binding protein (IGFBP) superfamily. *Endocr Rev* 1999;**20**:761–87.

32 SALMON WDJ, DAUGHADAY WH. A hormonally controlled serum factor which stimulates sulfate incorporation by cartilage in vitro. *J Lab Clin Med* 1957;**49**:825–36.

33 Jones JI, Clemmons DR. Insulin-like growth factors and their binding proteins: biological actions. *Endocr Rev* 1995;**16**:3–34.

34 Blakesley VA, Scrimgeour A, Esposito D, Le Roith D. Signaling via the insulin-like growth factor-I receptor: does it differ from insulin receptor signaling? *Cytokine Growth Factor Rev* 1996;**7**:153–9.

35 Nielsen FC. The molecular and cellular biology of insulin-like growth factor II. *Prog Growth Factor Res* 1992;**4**:257–90.

36 Laron Z, Pertzelan A, Mannheimer S. Genetic pituitary dwarfism with high serum concentation of growth hormone--a new inborn error of metabolism? *Isr J Med Sci* 1966;**2**:152–5.

37 Laron Z. An update on Laron syndrome. *Arch Dis Child* 1993;**68**:345–6.

38 Laron Z. Insulin-like growth factor 1 (IGF-1): a growth hormone. *Mol Pathol* 2001;**54**:311–6.

39 Snell GD. DWARF, A NEW MENDELIAN RECESSIVE CHARACTER OF THE HOUSE MOUSE. *Proc Natl Acad Sci U S A* 1929;**15**:733–4.

40 Schaible R, Gowen JW. A new dwarf mouse. *Genetics* 1961;**46**:896.

41 Eicher EM, Beamer WG. Inherited ateliotic dwarfism in mice. Characteristics of the mutation, little, on chromosome 6. *J Hered* 1976;**67**:87–91.

42 Godfrey P, Rahal JO, Beamer WG, Copeland NG, Jenkins NA, Mayo KE. GHRH receptor of little mice contains a missense mutation in the extracellular domain that disrupts receptor function. *Nat Genet* 1993;**4**:227–32.

43 Donahue LR, Beamer WG. Growth hormone deficiency in 'little' mice results in aberrant body composition, reduced insulin-like growth factor-I and insulin-like growth factor-binding protein-3 (IGFBP-3), but does not affect IGFBP-2, -1 or -4. *J*

Endocrinol 1993;**136**:91–104.

44 Zhou Y, Xu BC, Maheshwari HG, He L, Reed M, Lozykowski M, *et al.* A mammalian model for Laron syndrome produced by targeted disruption of the mouse growth hormone receptor/binding protein gene (the Laron mouse). *Proc Natl Acad Sci U S A* 1997;**94**:13215–20.

45 Coschigano KT, Holland AN, Riders ME, List EO, Flyvbjerg A, Kopchick JJ. Deletion, but not antagonism, of the mouse growth hormone receptor results in severely decreased body weights, insulin, and insulin-like growth factor I levels and increased life span. *Endocrinology* 2003;**144**:3799–810.

46 Powell-Braxton L, Hollingshead P, Warburton C, Dowd M, Pitts-Meek S, Dalton D, *et al.* IGF-I is required for normal embryonic growth in mice. *Genes Dev* 1993;**7**:2609–17.

47 Alba M, Salvatori R. A mouse with targeted ablation of the growth hormone-releasing hormone gene: A new model of isolated growth hormone deficiency. *Endocrinology* 2004;**145**:4134–43.

48 Alba M, Schally A V., Salvatori R. Partial reversibility of growth hormone (GH) deficiency in the GH-releasing hormone (GHRH) knockout mouse by postnatal treatment with a GHRH analog. *Endocrinology* 2005;**146**:1506–13.

49 Alba M, Fintini D, Salvatori R. Effects of recombinant mouse growth hormone treatment on growth and body composition in GHRH knock out mice. *Growth Horm IGF Res* 2005;**15**:275–82.

50 Bartke A, Sun LY, Longo V. Somatotropic signaling: trade-offs between growth, reproductive development, and longevity. *Physiol Rev* 2013;**93**:571–98.

51 Bartke A, List EO, Kopchick JJ. The somatotropic axis and aging: Benefits of endocrine defects. *Growth Horm IGF Res* 2016;**27**:41–5.

52 Brown-Borg HM. The somatotropic axis and longevity in mice. *Am J Physiol Endocrinol Metab* 2015;**309**:E503-10.

53 Brown-Borg HM, Borg KE, Meliska CJ, Bartke A. Dwarf mice and the ageing process. Nature. 1996;**384**:33.

54 Flurkey K, Papaconstantinou J, Miller RA, Harrison DE. Lifespan extension and delayed immune and collagen aging in mutant mice with defects in growth hormone production. *Proc Natl Acad Sci U S A* 2001;**98**:6736–41.

55 Panici JA, Harper JM, Miller RA, Bartke A, Spong A, Masternak MM. Early life growth hormone treatment shortens longevity and decreases cellular stress resistance in long-lived mutant mice. *FASEB J Off Publ Fed Am Soc Exp Biol* 2010;**24**:5073–9.

56 Sun LY, Spong A, Swindell WR, Fang Y, Hill C, Huber JA, *et al.* Growth hormone-releasing hormone disruption extends lifespan and regulates response to caloric

restriction in mice. *Elife* 2013;**2**:e01098.

57 Holzenberger M, Dupont J, Ducos B, Leneuve P, Geloen A, Even PC, *et al.* IGF-1 receptor regulates lifespan and resistance to oxidative stress in mice. *Nature* 2003;**421**:182–7.

58 Svensson J, Sjogren K, Faldt J, Andersson N, Isaksson O, Jansson J-O, *et al.* Liver-derived IGF-I regulates mean life span in mice. *PLoS One* 2011;**6**:e22640.

59 Moser M, Leo O. Key concepts in immunology. *Vaccine* 2010;**28 Suppl 3**:C2-13.

60 Rivera A, Siracusa MC, Yap GS, Gause WC. Innate cell communication kick-starts pathogen-specific immunity. *Nat Immunol* 2016;**17**:356–63.

61 Riera Romo M, Perez-Martinez D, Castillo Ferrer C. Innate immunity in vertebrates: an overview. *Immunology* 2016;**148**:125–39.

62 Walker JA, Barlow JL, McKenzie ANJ. Innate lymphoid cells - how did we miss them? *Nat Rev Immunol* 2013;**13**:75–87.

63 Vivier E, Raulet DH, Moretta A, Caligiuri MA, Zitvogel L, Lanier LL, *et al.* Innate or adaptive immunity? The example of natural killer cells. *Science* 2011;**331**:44–9.

64 Hirahara K, Nakayama T. CD4+ T-cell subsets in inflammatory diseases: beyond the Th1/Th2 paradigm. *Int Immunol* 2016;**28**:163–71.

65 Murphy KM, Stockinger B. Effector T cell plasticity: flexibility in the face of changing circumstances. *Nat Immunol* 2010;**11**:674–80.

66 Jordan MS, Boesteanu A, Reed AJ, Petrone AL, Holenbeck AE, Lerman MA, *et al.* Thymic selection of CD4+CD25+ regulatory T cells induced by an agonist self-peptide. *Nat Immunol* 2001;**2**:301–6.

67 Fontenot JD, Gavin MA, Rudensky AY. Foxp3 programs the development and function of CD4+CD25+ regulatory T cells. *Nat Immunol* 2003;**4**:330–6.

68 Rothenberg E V. Transcriptional control of early T and B cell developmental choices. *Annu Rev Immunol* 2014;**32**:283–321.

69 Rolink AG, Massa S, Balciunaite G, Ceredig R. Early lymphocyte development in bone marrow and thymus. *Swiss Med Wkly* 2006;**136**:679–83.

70 Perera J, Huang H. The development and function of thymic B cells. *Cell Mol Life Sci* 2015;**72**:2657–63.

71 Ichii M, Oritani K, Kanakura Y. Early B lymphocyte development: Similarities and differences in human and mouse. *World J Stem Cells* 2014;**6**:421–31.

72 Hardy RR, Hayakawa K. B cell development pathways. *Annu Rev Immunol* 2001;**19**:595–621.

73 Meffre E, Casellas R, Nussenzweig MC. Antibody regulation of B cell development. *Nat Immunol* 2000;**1**:379–85.

74 Clark MR, Mandal M, Ochiai K, Singh H. Orchestrating B cell lymphopoiesis through interplay of IL-7 receptor and pre-B cell receptor signalling. *Nat Rev Immunol* 2014;**14**:69–80.

75 Panaroni C, Wu JY. Interactions between B lymphocytes and the osteoblast lineage in bone marrow. *Calcif Tissue Int* 2013;**93**:261–8.

76 Ceredig R, Rolink AG. The key role of IL-7 in lymphopoiesis. *Semin Immunol* 2012;**24**:159–64.

77 Corfe SA, Paige CJ. The many roles of IL-7 in B cell development; mediator of survival, proliferation and differentiation. *Semin Immunol* 2012;**24**:198–208.

78 Labrie JE 3rd, Borghesi L, Gerstein RM. Bone marrow microenvironmental changes in aged mice compromise V(D)J recombinase activity and B cell generation. *Semin Immunol* 2005;**17**:347–55.

79 Peschon JJ, Morrissey PJ, Grabstein KH, Ramsdell FJ, Maraskovsky E, Gliniak BC, *et al.* Early lymphocyte expansion is severely impaired in interleukin 7 receptor-deficient mice. *J Exp Med* 1994;**180**:1955–60.

80 Prieyl JA, LeBien TW. Interleukin 7 independent development of human B cells. *Proc Natl Acad Sci U S A* 1996;**93**:10348–53.

81 Miller JF. The golden anniversary of the thymus. *Nat Rev Immunol* 2011;**11**:489–95.

82 Geenen V, Bodart G, Henry S, Michaux H, Dardenne O, Charlet-Renard C, *et al.* Programming of neuroendocrine self in the thymus and its defect in the development of neuroendocrine autoimmunity. Front. Neurosci. 2013.

83 MacDonald HR, Wilson A. The role of the T-cell receptor (TCR) in alpha beta/gamma delta lineage commitment: clues from intracellular TCR staining. *Immunol Rev* 1998;**165**:87–94.

84 Shibata K. Close link between development and function of gamma-delta T cells. *Microbiol Immunol* 2012;**56**:217–27.

85 Bhandoola A, von Boehmer H, Petrie HT, Zuniga-Pflucker JC. Commitment and developmental potential of extrathymic and intrathymic T cell precursors: plenty to choose from. *Immunity* 2007;**26**:678–89.

86 von Boehmer H. The developmental biology of T lymphocytes. *Annu Rev Immunol* 1988;**6**:309–26.

87 Ciofani M, Zuniga-Pflucker JC. The thymus as an inductive site for T lymphopoiesis. *Annu Rev Cell Dev Biol* 2007;**23**:463–93.

88 Zuniga-Pflucker JC, Lenardo MJ. Regulation of thymocyte development from immature progenitors. *Curr Opin Immunol* 1996;**8**:215–24.

89 Singer A, Adoro S, Park J-H. Lineage fate and intense debate: myths, models and

mechanisms of CD4- versus CD8-lineage choice. *Nat Rev Immunol* 2008;**8**:788–801.

90 Taniuchi I. Views on helper/cytotoxic lineage choice from a bottom-up approach. *Immunol Rev* 2016;**271**:98–113.

91 Klein L, Kyewski B, Allen PM, Hogquist KA. Positive and negative selection of the T cell repertoire: what thymocytes see (and don't see). *Nat Rev Immunol* 2014;**14**:377–91.

92 Hsieh C-S, Lee H-M, Lio C-WJ. Selection of regulatory T cells in the thymus. *Nat Rev Immunol* 2012;**12**:157–67.

93 Weissler KA, Caton AJ. The role of T-cell receptor recognition of peptide:MHC complexes in the formation and activity of Foxp3(+) regulatory T cells. *Immunol Rev* 2014;**259**:11–22.

94 Taghon T, Waegemans E, Van de Walle I. Notch signaling during human T cell development. *Curr Top Microbiol Immunol* 2012;**360**:75–97.

95 Rodewald HR, Kretzschmar K, Swat W, Takeda S. Intrathymically expressed c-kit ligand (stem cell factor) is a major factor driving expansion of very immature thymocytes in vivo. *Immunity* 1995;**3**:313–9.

96 Muegge K, Vila MP, Durum SK. Interleukin-7: a cofactor for V(D)J rearrangement of the T cell receptor beta gene. *Science (80-)* 1993;**261**:93–5.

97 Takahama Y. Journey through the thymus: stromal guides for T-cell development and selection. *Nat Rev Immunol* 2006;**6**:127–35.

98 Bunting MD, Comerford I, McColl SR. Finding their niche: chemokines directing cell migration in the thymus. *Immunol Cell Biol* 2011;**89**:185–96.

99 Zuklys S, Handel A, Zhanybekova S, Govani F, Keller M, Maio S, *et al.* Foxn1 regulates key target genes essential for T cell development in postnatal thymic epithelial cells. *Nat Immunol* 2016;**17**:1206–15.

100 Palmer DB. The effect of age on thymic function. Front. Immunol. 2013;**4**. doi:10.3389/fimmu.2013.00316

101 Haynes BF, Sempowski GD, Wells AF, Hale LP. The human thymus during aging. *Immunol Res* 2000;**22**:253–61.

102 Taub DD, Longo DL. Insights into thymic aging and regeneration. *Immunol Rev* 2005;**205**:72–93.

103 Naylor K, Li G, Vallejo AN, Lee W-W, Koetz K, Bryl E, *et al.* The influence of age on T cell generation and TCR diversity. *J Immunol* 2005;**174**:7446–52.

104 Schatz DG, Ji Y. Recombination centres and the orchestration of V(D)J recombination. *Nat Rev Immunol* 2011;**11**:251–63.

105 Kinds TJ, Osborne BA, Goldsby RA. *Kuby Immunology*. 6th editio. W.H. Freeman 2007.

106 Geenen V, Poulin J-F, Dion ML, Martens H, Castermans E, Hansenne I, *et al.* Quantification of T cell receptor rearrangement excision circles to estimate thymic function: an important new tool for endocrine-immune physiology. *J Endocrinol* 2003;**176**:305–11.

107 Dion M-L, Sekaly R-P, Cheynier R. Estimating thymic function through quantification of T-cell receptor excision circles. *Methods Mol Biol* 2007;**380**:197–213.

108 Smith PE. The effect of hypophysectomy upon the involution of the thymus in the rat. *Anat Rec* 1930;**47**:119–29.

109 Baroni C. Thymus, peripheral lymphoid tissues and immunological responsiveness of the pituitary dwarf mouse. *Experientia* 1967;**23**:282–3.

110 Baroni CD, Fabris N, Bertoli G. Effects of hormones on development and function of lymphoid tissues. Synergistic action of thyroxin and somatotropic hormone in pituitary dwarf mice. *Immunology* 1969;**17**:303–14.

111 Pierpaoli W, Baroni C, Fabris N, Sorkin E. Hormones and immunological capacity. II. Reconstitution of antibody production in hormonally deficient mice by somatotropic hormone, thyrotropic hormone and thyroxin. *Immunology* 1969;**16**:217–30.

112 Kelley KW, Brief S, Westly HJ, Novakofski J, Bechtel PJ, Simon J, *et al.* GH3 pituitary adenoma cells can reverse thymic aging in rats. *Proc Natl Acad Sci U S A* 1986;**83**:5663–7.

113 Lesniak MA, Roth J. Regulation of receptor concentration by homologous hormone. Effect of human growth hormone on its receptor in IM-9 lymphocytes. *J Biol Chem* 1976;**251**:3720–9.

114 Gagnerault MC, Postel-Vinay MC, Dardenne M. Expression of growth hormone receptors in murine lymphoid cells analyzed by flow cytofluorometry. *Endocrinology* 1996;**137**:1719–26.

115 de Mello-Coelho V, Gagnerault MC, Souberbielle JC, Strasburger CJ, Savino W, Dardenne M, *et al.* Growth hormone and its receptor are expressed in human thymic cells. *Endocrinology* 1998;**139**:3837–42.

116 Hattori N, Saito T, Yagyu T, Jiang BH, Kitagawa K, Inagaki C. GH, GH receptor, GH secretagogue receptor, and ghrelin expression in human T cells, B cells, and neutrophils. *J Clin Endocrinol Metab* 2001;**86**:4284–91.

117 Maggiano N, Piantelli M, Ricci R, Larocca LM, Capelli A, Ranelletti FO. Detection of growth hormone-producing cells in human thymus by immunohistochemistry and non-radioactive in situ hybridization. *J Histochem Cytochem* 1994;**42**:1349–54.

118 Sabharwal P, Varma S. Growth hormone synthesized and secreted by human thymocytes acts via insulin-like growth factor I as an autocrine and paracrine growth factor. *J Clin Endocrinol Metab* 1996;**81**:2663–9.

119 Weigent DA, Blalock JE. Expression of growth hormone by lymphocytes. *Int Rev Immunol* 1989;**4**:193–211.

120 Hansson HA, Nilsson A, Isgaard J, Billig H, Isaksson O, Skottner A, *et al.* Immunohistochemical localization of insulin-like growth factor I in the adult rat. *Histochemistry* 1988;**89**:403–10.

121 Verland S, Gammeltoft S. Functional receptors for insulin-like growth factors I and II in rat thymocytes and mouse thymoma cells. *Mol Cell Endocrinol* 1989;**67**:207–16.

122 Kooijman R, Willems M, De Haas CJ, Rijkers GT, Schuurmans AL, Van Buul-Offers SC, *et al.* Expression of type I insulin-like growth factor receptors on human peripheral blood mononuclear cells. *Endocrinology* 1992;**131**:2244–50.

123 Kooijman R, Lauf JJ, Kappers AC, Rijkers GT. Insulin-like growth factor induces phosphorylation of immunoreactive insulin receptor substrate and its association with phosphatidylinositol-3 kinase in human thymocytes. *J Exp Med* 1995;**182**:593–7.

124 Kooijman R, Scholtens LE, Rijkers GT, Zegers BJ. Type I insulin-like growth factor receptor expression in different developmental stages of human thymocytes. *J Endocrinol* 1995;**147**:203–9.

125 de Mello Coelho V, Villa-Verde DM, Farias-de-Oliveira DA, de Brito JM, Dardenne M, Savino W. Functional insulin-like growth factor-1/insulin-like growth factor-1 receptor-mediated circuit in human and murine thymic epithelial cells. *Neuroendocrinology* 2002;**75**:139–50.

126 Kecha O, Martens H, Franchimont N, Achour I, Hazee-Hagelstein MT, Charlet-Renard C, *et al.* Characterization of the insulin-like growth factor axis in the human thymus. *J Neuroendocrinol* 1999;**11**:435–40.

127 Kecha O, Brilot F, Martens H, Franchimont N, Renard C, Greimers R, *et al.* Involvement of insulin-like growth factors in early T cell development: a study using fetal thymic organ cultures. *Endocrinology* 2000;**141**:1209–17.

128 Yamada M, Hato F, Kinoshita Y, Tominaga K, Tsuji Y. The indirect participation of growth hormone in the thymocyte proliferation system. *Cell Mol Biol* 1994;**40**:111–21.

129 Timsit J, Savino W, Safieh B, Chanson P, Gagnerault MC, Bach JF, *et al.* Growth hormone and insulin-like growth factor-I stimulate hormonal function and proliferation of thymic epithelial cells. *J Clin Endocrinol Metab* 1992;**75**:183–8.

130 Bodart G, Goffinet L, Morrhaye G, Farhat K, de Saint-Hubert M, Debacq-Chainiaux F, *et al.* Somatotrope GHRH/GH/IGF-1 axis at the crossroads between

immunosenescence and frailty. *Ann N Y Acad Sci* 2015;**1351**:61–7.

131 Edwards CK 3rd, Ghiasuddin SM, Schepper JM, Yunger LM, Kelley KW. A newly defined property of somatotropin: priming of macrophages for production of superoxide anion. *Science* 1988;**239**:769–71.

132 Fu YK, Arkins S, Wang BS, Kelley KW. A novel role of growth hormone and insulin-like growth factor-I. Priming neutrophils for superoxide anion secretion. *J Immunol* 1991;**146**:1602–8.

133 Fu YK, Arkins S, Fuh G, Cunningham BC, Wells JA, Fong S, *et al.* Growth hormone augments superoxide anion secretion of human neutrophils by binding to the prolactin receptor. *J Clin Invest* 1992;**89**:451–7.

134 Warwick-Davies J, Lowrie DB, Cole PJ. Growth hormone is a human macrophage activating factor. Priming of human monocytes for enhanced release of H2O2. *J Immunol* 1995;**154**:1909–18.

135 Warwick-Davies J, Lowrie DB, Cole PJ. Growth hormone activation of human monocytes for superoxide production but not tumor necrosis factor production, cell adherence, or action against Mycobacterium tuberculosis. *Infect Immun* 1995;**63**:4312–6.

136 Silva PRB, Machado KS, Da Silva DNL, Moraes JGN, Keisler DH, Chebel RC. Effects of recombinant bovine somatotropin during the periparturient period on innate and adaptive immune responses, systemic inflammation, and metabolism of dairy cows. *J Dairy Sci* 2015;**98**:4449–64.

137 Bjerknes R, Aarskog D. Priming of human polymorphonuclear neutrophilic leukocytes by insulin-like growth factor I: increased phagocytic capacity, complement receptor expression, degranulation, and oxidative burst. *J Clin Endocrinol Metab* 1995;**80**:1948–55.

138 Martinez R, Ubieta K, Herrera F, Forellat A, Morales R, de la Nuez A, *et al.* A novel GH secretagogue, A233, exhibits enhanced growth activity and innate immune system stimulation in teleosts fish. *J Endocrinol* 2012;**214**:409–19.

139 Manfredi R, Tumietto F, Azzaroli L, Zucchini A, Chiodo F, Manfredi G. Growth hormone (GH) and the immune system: impaired phagocytic function in children with idiopathic GH deficiency is corrected by treatment with biosynthetic GH. *J Pediatr Endocrinol* 1994;**7**:245–51.

140 Szynaka E, Petriczko E, Grabarek J, Miklaszewicz A, Domagala W, Walczak M. Effects of recombinant human growth hormone (rhGH) replacement therapy on detailed immunologic parameters in somatotropine--deficient paediatrics patients prior and after 6 months of rhGH treatment. *Neuro Endocrinol Lett* 2010;**31**:553–8.

141 Kotzmann H, Schmidt A, Lercher P, Schuster E, Geyer G, Frisch H, *et al.* One-year growth hormone therapy improves granulocyte function without major effects on nutritional and anthropometric parameters in malnourished hemodialysis

patients. *Nephron Clin Pract* 2003;**93**:C75-82.

142 Fornari MC, Palacios MF, Diez RA, Intebi AD. Decreased chemotaxis of neutrophils in acromegaly and hyperprolactinemia. *Eur J Endocrinol* 1994;**130**:463–8.

143 Wiedermann CJ, Niedermuhlbichler M, Geissler D, Beimpold H, Braunsteiner H. Priming of normal human neutrophils by recombinant human growth hormone. *Br J Haematol* 1991;**78**:19–22.

144 Wiedermann CJ, Reinisch N, Braunsteiner H. Stimulation of monocyte chemotaxis by human growth hormone and its deactivation by somatostatin. *Blood* 1993;**82**:954–60.

145 Wiedermann CJ, Reinisch N, Kahler C, Geisen F, Zilian U, Herold M, *et al.* In vivo activation of circulating monocytes by exogenous growth hormone in man. *Brain Behav Immun* 1992;**6**:387–93.

146 Petersen TK, Smith CW, Jensen AL. Characterization of the priming effect by pituitary canine growth hormone on canine polymorphonuclear neutrophil granulocyte function. *Clin Diagn Lab Immunol* 2000;**7**:226–32.

147 Ryu H, Lee JH, Kim KS, Jeong SM, Kim PH, Chung HT. Regulation of neutrophil adhesion by pituitary growth hormone accompanies tyrosine phosphorylation of Jak2, p125FAK, and paxillin. *J Immunol* 2000;**165**:2116–23.

148 Sneppen SB, Mersebach H, Ullum H, Feldt-Rasmussen U. Immune function during GH treatment in GH-deficient adults: an 18-month randomized, placebo-controlled, double-blinded trial. *Clin Endocrinol (Oxf)* 2002;**57**:787–92.

149 Kiess W, Malozowski S, Gelato M, Butenand O, Doerr H, Crisp B, *et al.* Lymphocyte subset distribution and natural killer activity in growth hormone deficiency before and during short-term treatment with growth hormone releasing hormone. *Clin Immunol Immunopathol* 1988;**48**:85–94.

150 Auernhammer CJ, Feldmeier H, Nass R, Pachmann K, Strasburger CJ. Insulin-like growth factor I is an independent coregulatory modulator of natural killer (NK) cell activity. *Endocrinology* 1996;**137**:5332–6.

151 Shimizu K, Adachi K, Teramoto A. Growth hormone enhances natural killer cell activity against glioma. *J Nippon Med Sch* 2005;**72**:335–40.

152 Matsuda T, Saito H, Inoue T, Fukatsu K, Han I, Furukawa S, *et al.* Growth hormone inhibits apoptosis and up-regulates reactive oxygen intermediates production by human polymorphonuclear neutrophils. *JPEN J Parenter Enteral Nutr* 1998;**22**:368–74.

153 Burgess W, Jesse K, Tang Q, Broussard SR, Dantzer R, Kelley KW. Insulin-like growth factor-I and the cytokines IL-3 and IL-4 promote survival of progenitor myeloid cells by different mechanisms. *J Neuroimmunol* 2003;**135**:82–90.

154 Kooijman R, Coppens A, Hooghe-Peters E. Igf-I inhibits spontaneous apoptosis in

human granulocytes. *Endocrinology* 2002;**143**:1206–12.

155 Renier G, Clement I, Desfaits AC, Lambert A. Direct stimulatory effect of insulin-like growth factor-I on monocyte and macrophage tumor necrosis factor-alpha production. *Endocrinology* 1996;**137**:4611–8.

156 Liu Q, Wang Y, Wang J. Effect of growth hormone on the immune function of dendritic cells. *Chin Med J (Engl)* 2010;**123**:1078–83.

157 Sohmiya M, Kanazawa I, Kato Y. Effect of recombinant human GH on circulating granulocyte colony-stimulating factor and neutrophils in patients with adult GH deficiency. *Eur J Endocrinol* 2005;**152**:211–5.

158 Liu Z, Yu Y, Jiang Y, Li J. Growth hormone increases circulating neutrophil activation and provokes lung microvascular injury in septic peritonitis rats. *J Surg Res* 2002;**105**:195–9.

159 Duquesnoy RJ. Immunodeficiency of the thymus-dependent system of the Ames dwarf mouse. *J Immunol* 1972;**108**:1578–90.

160 Murphy WJ, Durum SK, Longo DL. Role of neuroendocrine hormones in murine T cell development. Growth hormone exerts thymopoietic effects in vivo. *J Immunol* 1992;**149**:3851–7.

161 Smaniotto S, de Mello-Coelho V, Villa-Verde DM, Pleau JM, Postel-Vinay MC, Dardenne M, *et al.* Growth hormone modulates thymocyte development in vivo through a combined action of laminin and CXC chemokine ligand 12. *Endocrinology* 2005;**146**:3005–17.

162 Chu YW, Schmitz S, Choudhury B, Telford W, Kapoor V, Garfield S, *et al.* Exogenous insulin-like growth factor 1 enhances thymopoiesis predominantly through thymic epithelial cell expansion. *Blood* 2008;**112**:2836–46.

163 Morrhaye G, Kermani H, Legros JJ, Baron F, Beguin Y, Moutschen M, *et al.* Impact of growth hormone (GH) deficiency and GH replacement upon thymus function in adult patients. *PLoS One* 2009;**4**:e5668.

164 Napolitano LA, Lo JC, Gotway MB, Mulligan K, Barbour JD, Schmidt D, *et al.* Increased thymic mass and circulating naive CD4 T cells in HIV-1-infected adults treated with growth hormone. *AIDS* 2002;**16**:1103–11.

165 Napolitano LA, Schmidt D, Gotway MB, Ameli N, Filbert EL, Ng MM, *et al.* Growth hormone enhances thymic function in HIV-1-infected adults. *J Clin Invest* 2008;**118**:1085–98.

166 Clark R, Stresser J, McCabe S, Bobbins K, Jardieu P. Insulin-like growth factor-1 stimulation of lymphopoiesis. *J Clin Invest* 1993;**92**:540–8.

167 Postel-Vinay MC, De Mello Coelho V, Gagnerault MC, Dardenne M. Growth hormone stimulates the proliferation of activated mouse T lymphocytes. *Endocrinology* 1997;**138**:1816–20.

168 Murphy WJ, Durum SK, Longo DL. Human growth hormone promotes engraftment of murine or human T cells in severe combined immunodeficient mice. *Proc Natl Acad Sci U S A* 1992;**89**:4481–5.

169 Taub DD, Tsarfaty G, Lloyd AR, Durum SK, Longo DL, Murphy WJ. Growth hormone promotes human T cell adhesion and migration to both human and murine matrix proteins in vitro and directly promotes xenogeneic engraftment. *J Clin Invest* 1994;**94**:293–300.

170 de Mello-Coelho V, Villa-Verde DM, Dardenne M, Savino W. Pituitary hormones modulate cell-cell interactions between thymocytes and thymic epithelial cells. *J Neuroimmunol* 1997;**76**:39–49.

171 Tseng YH, Kessler MA, Schuler LA. Regulation of interleukin (IL)-1alpha, IL-1beta, and IL-6 expression by growth hormone and prolactin in bovine thymic stromal cells. *Mol Cell Endocrinol* 1997;**128**:117–27.

172 Dixit VD, Yang H, Sun Y, Weeraratna AT, Youm YH, Smith RG, *et al.* Ghrelin promotes thymopoiesis during aging. *J Clin Invest* 2007;**117**:2778–90.

173 Koo GC, Huang C, Camacho R, Trainor C, Blake JT, Sirotina-Meisher A, *et al.* Immune enhancing effect of a growth hormone secretagogue. *J Immunol* 2001;**166**:4195–201.

174 Smaniotto S, Mendes-da-Cruz DA, Carvalho-Pinto CE, Araujo LM, Dardenne M, Savino W. Combined role of extracellular matrix and chemokines on peripheral lymphocyte migration in growth hormone transgenic mice. *Brain Behav Immun* 2010;**24**:451–61.

175 Murphy WJ, Durum SK, Anver MR, Longo DL. Immunologic and hematologic effects of neuroendocrine hormones. Studies on DW/J dwarf mice. *J Immunol* 1992;**148**:3799–805.

176 Montecino-Rodriguez E, Clark R, Johnson A, Collins L, Dorshkind K. Defective B cell development in Snell dwarf (dw/dw) mice can be corrected by thyroxine treatment. *J Immunol* 1996;**157**:3334–40.

177 Montecino-Rodriguez E, Clark RG, Powell-Braxton L, Dorshkind K. Primary B cell development is impaired in mice with defects of the pituitary/thyroid axis. *J Immunol* 1997;**159**:2712–9.

178 Jardieu P, Clark R, Mortensen D, Dorshkind K. In vivo administration of insulin-like growth factor-I stimulates primary B lymphopoiesis and enhances lymphocyte recovery after bone marrow transplantation. *J Immunol* 1994;**152**:4320–7.

179 Landreth KS, Narayanan R, Dorshkind K. Insulin-like growth factor-I regulates pro-B cell differentiation. *Blood* 1992;**80**:1207–12.

180 Gibson LF, Piktel D, Landreth KS. Insulin-like growth factor-1 potentiates expansion of interleukin-7-dependent pro-B cells. *Blood* 1993;**82**:3005–11.

181 Sumita K, Hattori N, Inagaki C. Effects of growth hormone on the differentiation of mouse B-lymphoid precursors. *J Pharmacol Sci* 2005;**97**:408–16.

182 Robbins K, McCabe S, Scheiner T, Strasser J, Clark R, Jardieu P. Immunological effects of insulin-like growth factor-I--enhancement of immunoglobulin synthesis. *Clin Exp Immunol* 1994;**95**:337–42.

183 Yoshida A, Ishioka C, Kimata H, Mikawa H. Recombinant human growth hormone stimulates B cell immunoglobulin synthesis and proliferation in serum-free medium. *Acta Endocrinol (Copenh)* 1992;**126**:524–9.

184 Dumont F, Robert F, Bischoff P. T and B lymphocytes in pituitary dwarf Snell-Bagg mice. *Immunology* 1979;**38**:23–31.

185 Foster MP, Jensen ER, Montecino-Rodriguez E, Leathers H, Horseman N, Dorshkind K. Humoral and cell-mediated immunity in mice with genetic deficiencies of prolactin, growth hormone, insulin-like growth factor-I, and thyroid hormone. *Clin Immunol* 2000;**96**:140–9.

186 Dorshkind K, Horseman ND. The roles of prolactin, growth hormone, insulin-like growth factor-I, and thyroid hormones in lymphocyte development and function: insights from genetic models of hormone and hormone receptor deficiency. *Endocr Rev* 2000;**21**:292–312.

187 Berczi I. The stress concept and neuroimmunoregulation in modern biology. *Ann N Y Acad Sci* 1998;**851**:3–12.

188 Dorshkind K, Horseman ND. Anterior pituitary hormones, stress, and immune system homeostasis. *Bioessays* 2001;**23**:288–94.

189 Dorshkind K, Welniak L, Gault RA, Hixon J, Montecino-Rodriguez E, Horseman ND, *et al.* Effects of housing on the thymic deficiency in dwarf mice and its reversal by growth hormone administration. *Clin Immunol* 2003;**109**:197–202.

190 Velkeniers B, Dogusan Z, Naessens F, Hooghe R, Hooghe-Peters EL. Prolactin, growth hormone and the immune system in humans. *Cell Mol Life Sci* 1998;**54**:1102–8.

191 Abbassi V, Bellanti JA. Humoral and cell-mediated immunity in growth hormone-deficient children: effect of therapy with human growth hormone. *Pediatr Res* 1985;**19**:299–301.

192 Campos VC, Barrios MR, Salvatori R, de Almeida RP, de Melo E V, Nascimento ACS, *et al.* Infectious diseases and immunological responses in adult subjects with lifetime untreated, congenital GH deficiency. *Endocrine* 2016;**54**:182–90.

193 Shohreh R, Pardo CA, Guaraldi F, Schally A V., Salvatori R. GH, but Not GHRH, plays a role in the development of experimental autoimmune encephalomyelitis. *Endocrinology* 2011;**152**:3803–10.

194 Dulude G, Cheynier R, Gauchat D, Abdallah A, Kettaf N, Sékaly R-P, *et al.* The

magnitude of thymic output is genetically determined through controlled intrathymic precursor T cell proliferation. *J Immunol* 2008;**181**:7818–24.

195 Kermani H, Goffinet L, Mottet M, Bodart G, Morrhaye G, Dardenne M, *et al.* Expression of the growth hormone (GH)/Insulin-like growth factor (IGF) axis during Balb/c thymus ontogeny and effects of GH upon ex-vivo T-cell differentiation. *Neuroimmunomodulation* 2011;**18**.

196 Brooks KJ, Bunce KT, Haase M V, White A, Changani KK, Bate ST, *et al.* MRI quantification in vivo of corticosteroid induced thymus involution in mice: correlation with ex vivo measurements. *Steroids* 2005;**70**:267–72.

197 Beckmann N, Gentsch C, Baumann D, Bruttel K, Vassout A, Schoeffter P, *et al.* Non-invasive, quantitative assessment of the anatomical phenotype of corticotropin-releasing factor-overexpressing mice by MRI. *NMR Biomed* 2001;**14**:210–6.

198 Gruver AL, Hudson LL, Sempowski GD. Immunosenescence of ageing. *J Pathol* 2007;**211**:144–56.

199 Hakim FT, Gress RE. Immunosenescence: deficits in adaptive immunity in the elderly. *Tissue Antigens* 2007;**70**:179–89.

200 Lamberts SW, van den Beld AW, van der Lely AJ. The endocrinology of aging. *Science* 1997;**278**:419–24.

201 French RA, Broussard SR, Meier WA, Minshall C, Arkins S, Zachary JF, *et al.* Age-associated loss of bone marrow hematopoietic cells is reversed by GH and accompanies thymic reconstitution. *Endocrinology* 2002;**143**:690–9.

202 Goya RG, Gagnerault MC, De Moraes MC, Savino W, Dardenne M. In vivo effects of growth hormone on thymus function in aging mice. *Brain Behav Immun* 1992;**6**:341–54.

203 Li YM, Brunke DL, Dantzer R, Kelley KW. Pituitary epithelial cell implants reverse the accumulation of CD4-CD8- lymphocytes in thymus glands of aged rats. *Endocrinology* 1992;**130**:2703–9.

204 Montecino-Rodriguez E, Clark R, Dorshkind K. Effects of insulin-like growth factor administration and bone marrow transplantation on thymopoiesis in aged mice. *Endocrinology* 1998;**139**:4120–6.

205 Min H, Montecino-Rodriguez E, Dorshkind K. Reassessing the role of growth hormone and sex steroids in thymic involution. *Clin Immunol* 2006;**118**:117–23.

206 Min H, Montecino-Rodriguez E, Dorshkind K. Reduction in the developmental potential of intrathymic T cell progenitors with age. *J Immunol* 2004;**173**:245–50.

207 Aspinall R. Age-associated thymic atrophy in the mouse is due to a deficiency affecting rearrangement of the TCR during intrathymic T cell development. *J Immunol* 1997;**158**:3037–45.

208 Ashwell JD, Lu FW, Vacchio MS. Glucocorticoids in T cell development and function*. *Annu Rev Immunol* 2000;**18**:309–45.

209 den Braber I, Mugwagwa T, Vrisekoop N, Westera L, Mogling R, de Boer AB, *et al.* Maintenance of peripheral naive T cells is sustained by thymus output in mice but not humans. *Immunity* 2012;**36**:288–97.

210 Gagnerault MC, Touraine P, Savino W, Kelly PA, Dardenne M. Expression of prolactin receptors in murine lymphoid cells in normal and autoimmune situations. *J Immunol* 1993;**150**:5673–81.

211 De Mello-Coelho V, Savino W, Postel-Vinay MC, Dardenne M. Role of prolactin and growth hormone on thymus physiology. *Dev Immunol* 1998;**6**:317–23.

212 Gaufo GO, Diamond MC. Prolactin increases CD4/CD8 cell ratio in thymus-grafted congenitally athymic nude mice. *Proc Natl Acad Sci U S A* 1996;**93**:4165–9.

213 van der Weerd K, van Hagen PM, Schrijver B, Heuvelmans SJWM, Hofland LJ, Swagemakers SMA, *et al.* Thyrotropin acts as a T-cell developmental factor in mice and humans. *Thyroid* 2014;**24**:1051–61.

214 Mitsunaka H, Dobashi H, Sato M, Tanaka T, Kitanaka A, Yamaoka G, *et al.* Growth hormone prevents Fas-induced apoptosis in lymphocytes through modulation of Bcl-2 and caspase-3. *Neuroimmunomodulation* 2001;**9**:256–62.

215 Wikby A, Maxson P, Olsson J, Johansson B, Ferguson FG. Changes in CD8 and CD4 lymphocyte subsets, T cell proliferation responses and non-survival in the very old: the Swedish longitudinal OCTO-immune study. *Mech Ageing Dev* 1998;**102**:187–98.

216 Miller RA. Age-related changes in T cell surface markers: a longitudinal analysis in genetically heterogeneous mice. *Mech Ageing Dev* 1997;**96**:181–96.

217 Hale JS, Boursalian TE, Turk GL, Fink PJ. Thymic output in aged mice. *Proc Natl Acad Sci U S A* 2006;**103**:8447–52.

218 Biswas R, Roy T, Chattopadhyay U. Prolactin induced reversal of glucocorticoid mediated apoptosis of immature cortical thymocytes is abrogated by induction of tumor. *J Neuroimmunol* 2006;**171**:120–34.

219 Hinton PS, Peterson CA, Dahly EM, Ney DM. IGF-I alters lymphocyte survival and regeneration in thymus and spleen after dexamethasone treatment. *Am J Physiol* 1998;**274**:R912-20.

220 Farhat K, Bodart G, Renard J de C, Desmet C, Moutschen M, Baron F, *et al.* Severe deficiency of the somatotrope GHRH/GH/IGF1 axis induces a dramatic susceptibility to Streptococcus pneumoniae infection. Poster presented at the 50th congress of the SFI, Paris http://hdl.handle.net/2268/203101

221 Grossman Z, Paul WE. Dynamic tuning of lymphocytes: physiological basis, mechanisms, and function. *Annu Rev Immunol* 2015;**33**:677–713.

7 Appendices

1. Bodart G, Farhat K, Charlet-Renard C, Salvatori R, Geenen V, Martens HJ. The somatotrope Growth Hormone-Releasing Hormone/Growth Hormone/Insulin-like Growth Factor-1 Axis in immunoregulation and immunosenescence. *Front Horm Res.* 2017;**48**:147-159.

2. Bodart G, Goffinet L, Morrhaye G, Farhat K, de Saint-Hubert M, Debacq-Chainiaux F, Swine C, Geenen V, Martens HJ. Somatotrope GHRH/GH/IGF-1 axis at the crossroads between immunosenescence and frailty. *Ann N Y Acad Sci* 2015;**1351**:61–67.

3. Geenen V, Bodart G, Henry S, Michaux H, Dardenne O, Charlet-Renard C, Martens H, Hober D. Programming of neuroendocrine self in the thymus and its defect in the development of neuroendocrine autoimmunity. *Front. Neurosci.* 2013;**7**.

4. Kermani H, Goffinet L, Mottet M, Bodart G, Morrhaye G, Dardenne O, Renard C, Overbergh L, Baron F, Beguin Y, Geenen V, Martens HJ. Expression of the growth hormone (GH)/Insulin-like growth factor (IGF) axis during Balb/c thymus ontogeny and effects of GH upon ex-vivo T-cell differentiation. *Neuroimmunomodulation* 2012;**19**:137-147.